ORNL/TM-2016/195

Status of Chronic Oxidation Studies of Graphite

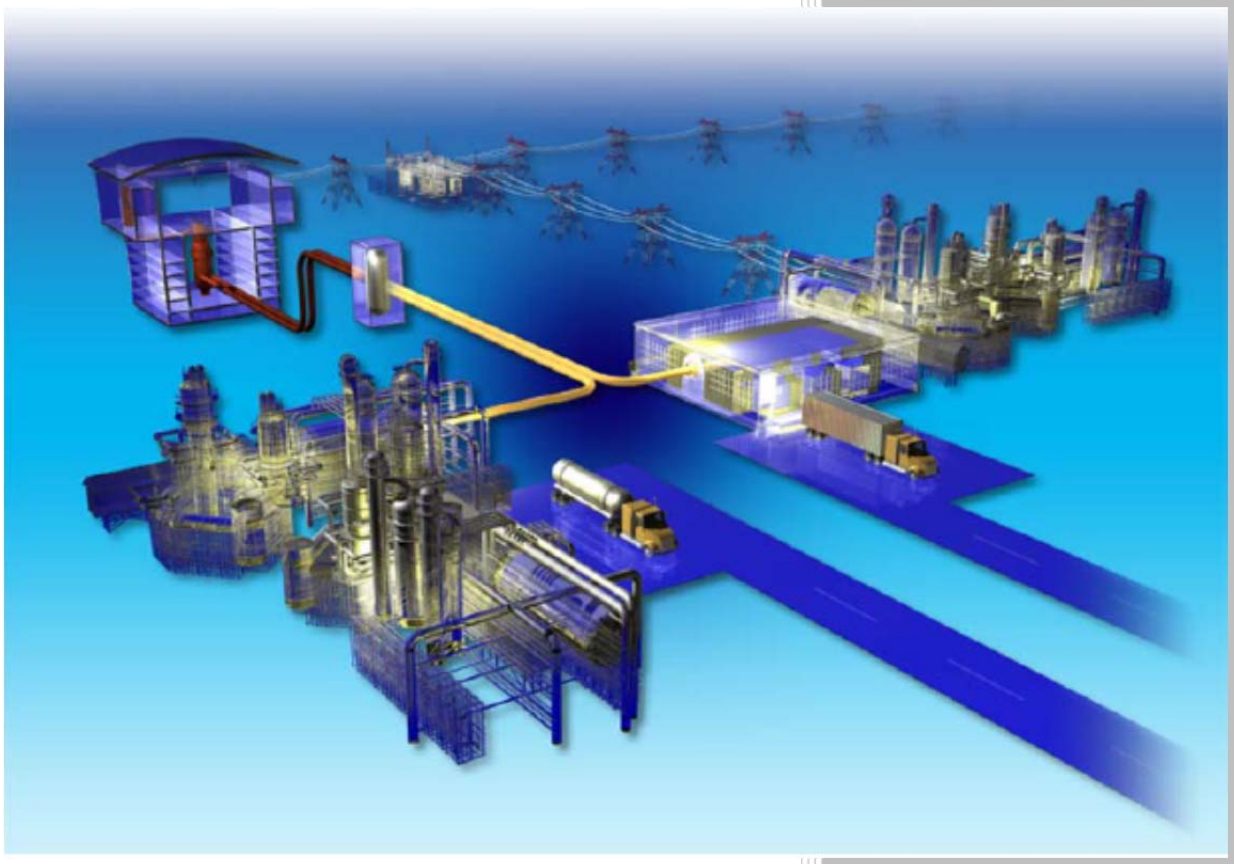

Cristian I Contescu
Robert W Mee

Approved for public release.
Distribution is unlimited.

May 2016

OAK RIDGE NATIONAL LABORATORY
MANAGED BY UT-BATTELLE FOR THE US DEPARTMENT OF ENERGY

DOCUMENT AVAILABILITY

Reports produced after January 1, 1996, are generally available free via US Department of Energy (DOE) SciTech Connect.

Website http://www.osti.gov/scitech/

Reports produced before January 1, 1996, may be purchased by members of the public from the following source:

National Technical Information Service
5285 Port Royal Road
Springfield, VA 22161
Telephone 703-605-6000 (1-800-553-6847)
TDD 703-487-4639
Fax 703-605-6900
E-mail info@ntis.gov
Website http://www.ntis.gov/help/ordermethods.aspx

Reports are available to DOE employees, DOE contractors, Energy Technology Data Exchange representatives, and International Nuclear Information System representatives from the following source:

Office of Scientific and Technical Information
PO Box 62
Oak Ridge, TN 37831
Telephone 865-576-8401
Fax 865-576-5728
E-mail reports@osti.gov
Website http://www.osti.gov/contact.html

This report was prepared as an account of work sponsored by an agency of the United States Government. Neither the United States Government nor any agency thereof, nor any of their employees, makes any warranty, express or implied, or assumes any legal liability or responsibility for the accuracy, completeness, or usefulness of any information, apparatus, product, or process disclosed, or represents that its use would not infringe privately owned rights. Reference herein to any specific commercial product, process, or service by trade name, trademark, manufacturer, or otherwise, does not necessarily constitute or imply its endorsement, recommendation, or favoring by the United States Government or any agency thereof. The views and opinions of authors expressed herein do not necessarily state or reflect those of the United States Government or any agency thereof.

ORNL/TM-2016/195

Materials Science and Technology Division

STATUS OF CHRONIC OXIDATION STUDIES OF GRAPHITE

Cristian I Contescu [1] and Robert W Mee [2]

[1] Oak Ridge National Laboratory

[2] University of Tennessee at Knoxville

May 2016

Prepared by
OAK RIDGE NATIONAL LABORATORY
Oak Ridge, Tennessee 37831-6283
managed by
UT-BATTELLE, LLC
for the
US DEPARTMENT OF ENERGY
under contract DE-AC05-00OR22725

This page was intentionally left blank

CONTENTS

Page

LIST OF FIGURES v
LIST OF TABLES vii
ACRONYMS ix

ABSTRACT 1

1. INTRODUCTION 3

2. GENERAL INFORMATION AND UPDATE ON EXPERIMENTAL RESUTLS……. …….5
   2.1. GRAPHITE GRADES AND MEASUREMENTS PERFORMED 5
   2.2. KINETIC MEASUREMENTS RESULTS…… .6

3. THE LANGMUIR-HINSHELWOOD MODEL……...9
   3.1. PREMISSES AND CLASICAL APPLICATIONS…….9
   3.2. LIMITATIONS OF THE LANGMUIR-HINSHELWOOD MODEL…… 11
   3.3. STOCHASTIC MODEL - AN ALTERNATIVE TO DETERMINISTIC LH MODEL……..12

4. NEW KINETIC MODEL FOR GRAPHITE OXIDATION BY MOISTURE……...15
   4.1. WATER SURFACE COMPLEXES AND REACTION ROUTES……..15
   4.2. COOPERATIVE BEHAVIOR IN REACTION KINETICS…….17
   4.3. ENHANCED KINETIC MODEL FOR GRAPHITE OXIDATION……19
      4.3.1. Site Cooperativity and Apparent Reaction Order…….19
      4.3.2. Enhanced LH Model with Boltzmann Activation of Surface Sites…… ..... ….21
      4.3.3. Testing the Boltzmann-enhanced LH Model 22

5. RESULTS ……24
   5.1. GRAPHITE IG-110……..... .24
   5.2. GRAPHITE NBG-17 28
   5.3. GRAPHITE PCEA..... 32
   5.4. GRAPHITE H-451..... 35
   5.5 COMPARISON OF THE TWO MODELS……...……35

6. DISCUSSION……..37

7. SUMMARY AND CONCLUSION……39

REFERENCES ……41

ANNEXES: PHYSICAL MEASUREMENTS AND TEST CONDITIONS……..44
   ANNEX 1 - Physical measurements on graphite IG-110 specimens before and after tests…..…..45
   ANNEX 2 - Log of experimental results - graphite IG-110…….. …...47
   ANNEX 3 - Physical measurements on graphite NBG-17 specimens before and after tests …….53
   ANNEX 4 - Log of experimental results - graphite NBG-17……..55
   ANNEX 5 - Physical measurements on graphite PCEA specimens before and after tests….....63
   ANNEX 6 - Log of experimental results - graphite PCEA ……....66

This page was intentionally left blank

LIST OF FIGURES

Figure **Page**

1 Comparison of oxidation by moisture rate data for graphite grades PCEA, NBG-17 and IG-110 characterized at ORNL (2012-2016) and for historic grade H-451…….. 7

2 Behavior of the global oxidation rate predicted for solids with a Gauss distribution of surface sites' desorption energies…….. 13

3 Energy diagram steps of dissociative chemisorption of H_2O on a vacancy site on graphite basal plane…… 15

4 Schematic diagram of surface complexes formed by chemisorption of water at exposed zig-zag and armchair sites on graphene, and of their subsequent transformations during graphite gasification….16

5 Schematic diagram of surface complexes formed by adsorption of water on hydrogen saturated and oxygen-containing zig-zag sites on graphene edges, and of their subsequent transformations during graphite gasification …….. 17

6 Left: Comparison between hyperbolic and sigmoidal dependence of reaction rate versus ligand concentration indicating, respectively, lack of cooperativity (blue hyperbola line) and positive cooperativity (red sigmoid curve). Right: By varying the Hill parameter sigmoid curves are able to describe a multitude of positive cooperative phenomena…….. 19

7 Temperature dependence of apparent reaction order calculated directly from experimental data compared with model predictions based on best fit LH parameters……. 20

8 Experimental evidence of site cooperativity effects: Oxidation rates measured according to Method 1 (random P_{H2O} variation from multiple specimens) follow an increasing trend with $P_{H2O,}$ albeit scattered, while rates measured according to Method 2 (continuous P_{H2O} decrease on the same specimen) are higher and show a trend reversed to that expected……. 24

9 Oxidation rates measured for graphite IG-110 and the trends predicted by LH model with 6 parameters…… 25

10 Comparison between rates measured for oxidation of IG-110 graphite and rates predicted by the LH model…….. 26

11 Oxidation rates measured for graphite IG-110 and the trends predicted by the Boltzmann-enhanced LH model (10 parameters). …….. 27

12 Comparison between rates measured for oxidation of IG-110 graphite and the rates predicted by the Boltzmann-enhanced LH model……28

13 Fit of LH model to oxidation data for graphite NBG-17 at P_{H2} = 0 and P_{H2} = 26 Pa……29

14 Fit of Boltzmann-enhanced LH model to oxidation data collected for graphite NBG-17 at P_{H2} = 0 and P_{H2} = 26 Pa……..30

15 Goodness of fit comparison between the LH model and the Boltzmann-enhanced LH model applied to graphite NBG-17oxidation by moisture…….. 31

16 Fit of PCEA oxidation data using the LH model (top panel) and the Boltzmann-enhanced LH model (bottom panel)……. 33

17 Goodness of fit comparison between LH model and Boltzmann-enhanced LH model applied to graphite PCEA oxidation by moisture…… 34

18 Goodness of fit comparison between LH and Boltzmann-enhanced LH models applied to graphite H-451 oxidation by moisture……35

19 Visualization of electronic states localized at edge carbon atoms of graphene with different number of hydrogen atoms…….. 36

LIST OF TABLES

Table **Page**

1 Best fit LH parameters for graphite IG-110 26

2 Best fit parameters for graphite IG-110 using the Boltzmann-enhanced LH model 27

3 Best fit LH parameters for graphite NBG-17 31

4 Best fit parameters for graphite IG-110 using the Boltzmann-enhanced LH model 31

5 Best fit LH parameters for graphite PCEA 31

6 Best fit parameters for graphite PCEA using the Boltzmann-enhanced LH model 31

7 Best fit LH parameters for graphite H-451 (“low water” variant) 36

8 Best fit parameters for graphite H-451 using the Boltzmann-enhanced LH model 36

9 Comparison of scattered regression plots between observed and model-predicted rates 36

This page was intentionally left blank

ACRONYMS

ASTM	American Society for Testing and Materials
BLH	Boltzmann-Langmuir-Hinshelwood (kinetic model)
DFT	density functional theory (method)
GA	General Atomics (company)
HTGR	High Temperature Gas-cooled Reactor
LH	Langmuir-Hinshelwood (kinetic model)
MLE	maximum likelihood estimation (method)
MS	mass spectrometer / mass spectrometry
ORNL	Oak Ridge National Laboratory
TPD	temperature-programmed desorption
TPO	temperature-programmed oxidation
STM	scanning tunneling microscopy

This page was intentionally left blank

ABSTRACT

Graphite will undergo extremely slow, but continuous, oxidation by traces of moisture that will be present, albeit at very low levels, in the helium coolant of an HTGR. This chronic oxidation may cause degradation of mechanical strength and of other properties of graphite components if a porous oxidation layer penetrates deep enough in the bulk of graphite components during the lifetime of the reactor. The current research on graphite chronic oxidation is motivated by the acute need to understand the behavior of each graphite grade during prolonged exposure to chemical attack by moisture at high temperature. The goal is to provide the elements needed to develop predictive models for long-time oxidation behavior of graphite components in the cooling helium of HTGR. The tasks derived from this goal are: (1) Oxidation rate measurements in order to determine and validate a comprehensive kinetic model suitable for prediction of intrinsic oxidation rates as a function of temperature and oxidant gas composition; (2) Characterization of effective diffusivity of water vapor in the graphite pore system in order to account for the in-pore transport of moisture; and (3) Development and validation of a predictive model for the penetration depth of the oxidized layer, in order to assess the risk of oxidation-caused damage of particular graphite grades after prolonged exposure to the environment of helium coolant in an HTGR.

The most important – and most time consuming – of these tasks is the measurement of oxidation rates in accelerated oxidation tests (but still under kinetic control) and the development of a reliable kinetic model. This report summarizes the status of chronic oxidation studies on graphite, and then focuses on model development activities, progress of kinetic measurements, validation of results, and improvement of the kinetic models. Analysis of current and past results obtained with three nuclear graphite grades showed that the classical Langmuir-Hinshelwood model cannot reproduce all data collected so far.

Starting from here we propose a modification of the LH model to include temperature activation of the graphite surface, modeled as a Boltzmann activation function. The Boltzmann-enhanced Langmuir-Hinshelwood model (BLH) was tested successfully on three grades of graphite. The model is a robust, comprehensive mathematical function that allows better fitting of experimental results spanning a wide range of temperatures and partial pressures of water vapor and hydrogen. However, the model did not improve much the fitting of old data on graphite H-451 oxidation by water.

This page was intentionally left blank

1. INTRODUCTION

High purity isotropic graphite is used as a neutron moderator and structural element in High Temperature Gas-Cooled Reactors (HTGRs). Although stable at the operating temperatures of HTGRs (about 700 – 900 ^{o}C) in a reducing environment, graphite is susceptible to oxidation by traces of oxygen, water, and carbon dioxide if these gases are present in the high temperature gas environment. Even though the chemical composition of the helium coolant is strictly controlled, water (moisture) is the most difficult gas species to remove. Depending on specific designs, the admissible water vapor partial pressure in HTGR varies between about 5 Pa (Fort St. Vrain, USA, 1976-1979) and 0.04 Pa (PBMR project, South Africa), with most practical values grouped around 1.1 – 1.4 Pa (Peach Bottom, USA, 1967-1974; HTR-10, China, 2003) at total helium pressures of 7 – 9 MPa [1,2,3,4,5,6]. Over the predicted lifetime of several decades, it is inevitable that extremely slow, but continuous (chronic) oxidation of graphite by traces of water will occur at these high temperatures. The reaction products are hydrogen and carbon dioxide:

$$C_{\text{graphite}} + H_2O_{\text{vapor}} = CO_{\text{gas}} + H_{2\ \text{gas}} \qquad \text{(I)}$$

The main concern about oxidation by moisture is not about accumulation of CO (a toxic gas) and H_2 (flammable and explosive in mixtures with air) in the reactor. The amounts will be small and the coolant gas composition is controlled. The real concern is that chronic oxidation of graphite may slowly but surely corrode the fuel elements and other structural components in the core, weakening their mechanical strength and jeopardizing the reactor integrity. Early analyses of the possible effect of chronic oxidation were carried out at General Atomics (GA) Company. In the 1970's they performed accelerated oxidation tests of graphite grade H-451, which at the time was the U. S. graphite candidate for HTGRs. The report by Velasquez, Hightower and Burnette [7] contains carefully measured slow oxidation rates in presence of moisture and hydrogen. The results were analyzed according to the Langmuir-Hinshelwood (LH) model for graphite oxidation by moisture. The numerical values of all kinetic parameters obtained by fitting the LH model to the experimental observations were provided. Building on these results, Richards [8] performed a finite element analysis of moisture transport in porous graphite and consumption in the oxidation reaction. He concluded that chronic oxidation of graphite under normal operating conditions in HTGR will not affect safety operation. According to this analysis, oxidation by moisture will occur only in a thin layer (about 1-2 mm) at the surface of graphite components provided the steam concentration in helium at a total design pressure of 63 atm is kept below 0.1 ppm (less than 6.4 Pa partial pressure).

The problem with this analysis is that the kinetic data used as input were those from the GA report on graphite H-451, while the measurements of oxidized layer thickness used for model validation were performed with graphite 2020. Later it became clear that the graphite microstructure is a very strong differentiator between grades of nuclear graphite; and that structural properties have a strong influence on oxidation behavior of various grades [9,10]. Moreover, graphite H-451 is no longer available, and little is known about the oxidation by moisture of the newer grades regarded as possible candidates for HTGR in the United States.

The need to understand their behavior during operation of gas-cooled reactors motivated the initiation of a new research direction at Oak Ridge National Laboratory (ORNL) in 2012 – systematic investigation of chronic oxidation by moisture of new grades of graphite selected as HTGR candidates. This report summarizes the achievements and the current status of this multi-year research effort. It makes reference to already published studies [11,12,13,14] and contains updates on the latest results. The main goal is to emphasize the experimental progress so far and the challenges encountered with data analysis. A second

goal is to underscore, as often as possible, our current understanding of the relationship between graphite microstructure and oxidation behavior. Along these lines, this report will highlight current knowledge gaps and will point to those areas where better understanding is required to further the model development of graphite chronic oxidation. Based on information from quantum chemical calculations and stochastic models for graphite gasification kinetics, this report concludes that the classical Langmuir-Hinshelwood model has limited applicability over broad ranges of experimental conditions, and advances an enhanced kinetic model which better fits available kinetic results for several grades of nuclear graphite.

2. GENERAL INFORMATION AND UPDATE ON EXPERIMENTAL RESULTS

2.1 GRAPHITE GRADES AND MEASUREMENTS PERFORMED

Chronic oxidation by traces of moisture and hydrogen in helium was studied at ORNL for the following three graphite grades:

- PCEA - medium grain nuclear graphite obtained from petroleum needle coke by an extrusion process developed by GrafTech International, USA [15];
- NBG-17 - medium grain nuclear graphite developed by SGL Carbon (Germany / France) and obtained by vibrational molding from a coal-tar pitch coke [16];
- IG-110 – fine grain nuclear graphite manufactured by Toyo Tanso (Japan) from highly crystalline petroleum coke using isostatic pressing.

Three types of measurements were performed:

- **Oxidation kinetics measurements in accelerated oxidation tests**. The goal of this task is to determine the graphite-specific kinetic parameters in the oxidation rate equation over a broad range of temperature and gas composition conditions. The measurements were completed for graphite grades PCEA, NBG-17 and IG-110 [11,12,13]. A high sensitivity thermogravimetric system was employed for the experimental work. It allows control of temperature, flow rate, and composition of the oxidant gas. Typically, a series of weight loss rates were measured for each graphite grade in isothermal conditions with duration varying from 3 hours (more often) to 12 hours (in some instances). The specimens were machined as cylinders, 4 mm diameter and 20 mm long. The small diameter was selected in order to minimize as much as possible the diffusional limitations and to maximize the surface/volume ratio. Measurements were made at temperatures between 800 and 1100 ^{o}C and total pressure equal to the atmospheric pressure. All data were reduced at standard conditions, taking into account the actual pressure in the reaction tube. A 1.5 L/min flow rate of ultrahigh purity helium was used which corresponds to 7.5 cm/s linear velocity in the reaction tube. The gas composition was adjusted to contain partial pressures of water vapor between 3 and 1000 Pa, occasionally with added partial pressures of hydrogen between 10 and 300 Pa. The final weight loss of individual specimens was in general less than 0.5 %, and only occasionally reached 1.5 % in the most aggressive oxidation conditions. At these low oxidation levels the correction for the "burn-off factor" that accounts for the variation of oxidation rates with the degree of oxidation was not necessary (assuming the microstructure did not change over this small range).

- **Water vapor effective diffusivity in graphite.** The goal of this task is to determine the effective diffusion coefficient for water, which is a property of the pore system in each graphite grade. The ratio $\beta = D_{eff} / D_{gas}$ between the effective diffusivity measured for the porous material (D_{eff}) and the bulk diffusivity in free gas (D_{gas}) defines the structural parameter β characteristic to each graphite grade. This parameter accounts for the increased diffusional resistance to water vapor transport in the pore system, and depends on graphite microstructure, mainly on pore sizes, connectivity and tortuosity. These measurements were performed so far for grades PCEA and NBG-17 only [14] by an outside contractor (Porous Materials Inc., Ithaca, NY) according to procedure in ASTM F229 [17] adapted for graphite materials. Graphite samples were machined as thin (3 mm) rectangular slabs and placed between two parallel flows of helium gas. The humidity difference between the two flows was held constant and the total pressure difference was varied. The water diffusion rate at

zero pressure difference and known water concentration gradient was calculated from mass balance calculations using four-point measurements of pressure, humidity, flow rate, and temperature at gas inlet and outlet on each side of the graphite specimen. The results show that water diffusivity is slower in graphite NBG-17 than in PCEA, in agreement with the structural differences [14].

- **Density profile of the oxidized layer.** Measurements for graphite PCEA are complete, and those for graphite NBG-17 are currently in progress. The goal is to correlate the density profile in the oxidized layer with information from oxidation kinetics and water diffusivity, and thus to demonstrate the validity of a predictive model for chronic oxidation [18]. The predictive model is based on the mass balance equation for combined transport and reaction in the pore system. The ultimate objective is to determine the effect of temperature and total pressure on the maximum depth of the oxidized layer that will develop on the surfaces of graphite components during lifetime exposure to humidity traces in normal operating conditions. Work is currently in progress for further validation of the model with at least one more graphite grade (NBG-17).

The remainder of this report will discuss in detail recent results on modeling and interpretation of oxidation rate measurements for several grades of nuclear graphite. Modeling oxidation kinetics is of prime importance in comparison with oxidation layer profile and diffusivity characterization. A robust, comprehensive kinetic model, able to describe experimental results on a broad range of conditions, should be the solid ground for further development of predictive models of chronic graphite oxidation. The starting point of this analysis is recent experimental results (2015-2016) on oxidation by moisture of graphite IG-110. These data were very difficult to model using the classical Langmuir-Hinshelwood (LH) kinetics. Looking back to results for other grades of graphite, it became obvious that the LH model cannot consistently reproduce all experimental data available for the grades investigated so far: not only for IG-110, but also for PCEA (2013-2014) and NBG-17 (2014-2015). This finding made it necessary to critically review the applicability of the LH model for graphite oxidation kinetics. Based on this analysis, we propose an improved model that enhances the capabilities of the classical LH model. The enhanced model accounts for surface stoichiometry variations through a variable kinetic order coefficient, which is modeled by a Boltzmann distribution function and accounts for the temperature-dependent activation of surface sites on graphite. It will be shown in conclusion how this enhanced model is more successful in reproducing the experimental results obtained not only for graphite IG-110, but also for grades NBG-17 and PCEA, for which the respective experimental results were re-analyzed with the new model.

2.2. KINETIC MEASUREMENTS RESULTS

Figure 1 shows examples of kinetic measurement results for graphite grades PCEA, NBG-17, and IG-110. The double logarithmic scale was used to represent large variations of oxidation rates over broad ranges of water vapor partial pressures. Symbols represent measured oxidation rates and continuous lines show predicted rates based on best non-linear fitting according to the classical LH model. Each color indicates oxidation rates observed and predicted at constant temperature. Only data measured in mixtures of H_2O/He are shown in these figures. Similar measurements were made in mixtures of (H_2O + H_2)/He (not shown here). The graph for graphite H-451 was built by digitizing the graphs of experimental oxidation rates reported in the 1978 report from General Atomics [7].

The four graphs of Fig. 1 show common trends and significant differences between the four graphite grades.

First, the oxidation rates increase with the partial pressure of water vapor, P_{H2O}, but the rate of increase depends on temperature and, at constant temperature, on the actual range of P_{H2O}.

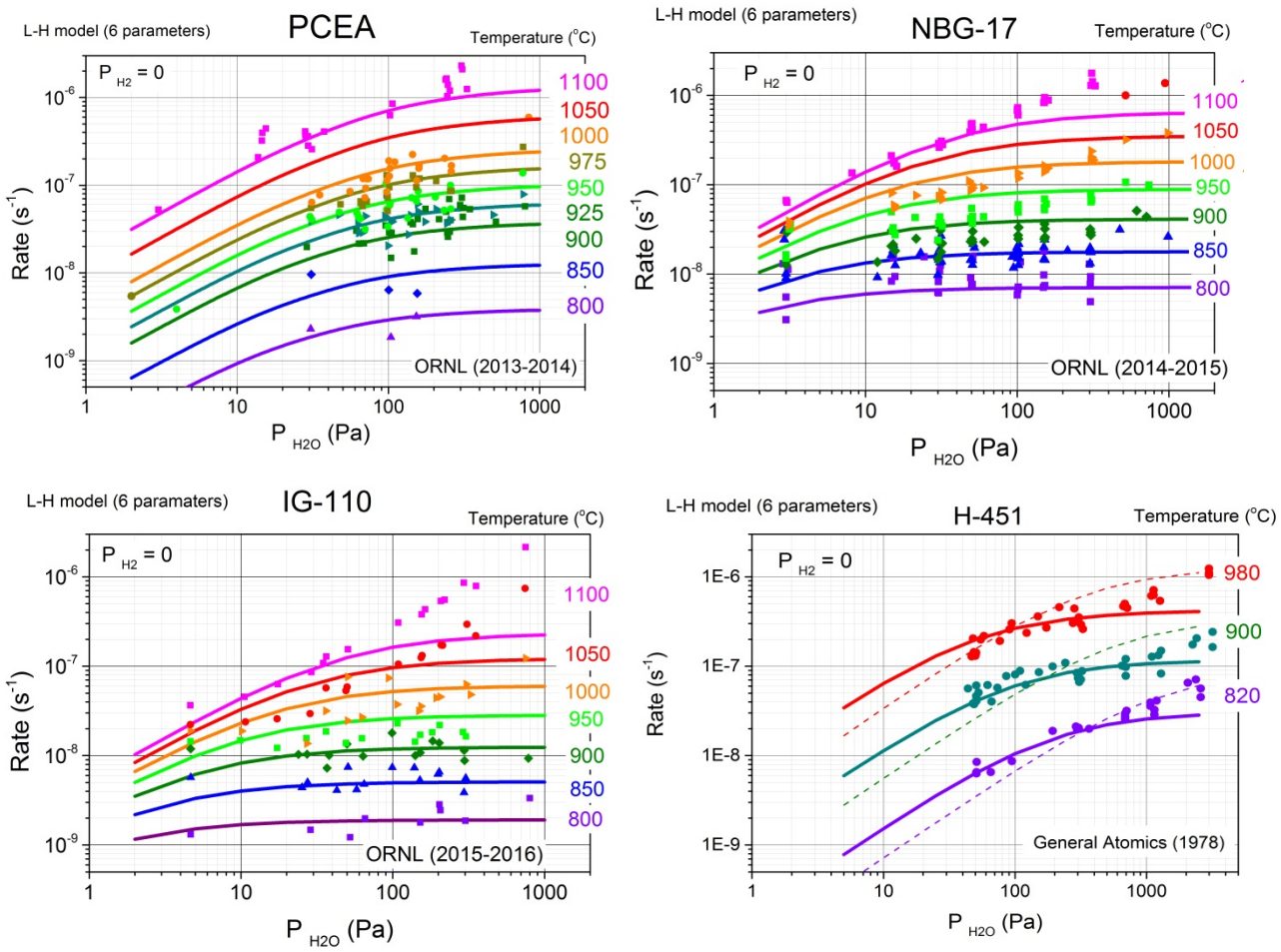

Figure 1: Comparison of oxidation by moisture rate data for graphite grades PCEA, NBG-17 and IG-110 characterized at ORNL (2012-2016) and for historic grade H-451. Data points for grade H-451 were obtained by digitizing the graphs in the GA report [7] and the models compared are "low water" for $P_{H2O} < 300$ Pa (solid lines) and "combined model" at $P_{H2O} < 3000$ Pa (dotted lines).

Second, all experimental values at constant temperature are more or less scattered, yet still show a trend which agrees in general with the isothermal trends predicted by models. Two sources of scattering were identified: material variability and experimental errors during measurements. The error caused by material variability was about twice as large as the measurement errors [11,12]. Data scattering was observed also in the classical report on graphite H-451 [7].

Third, each graphite grade exhibits different behavior in oxidation by moisture. When all data available for three graphites are compared on the same scale with the data reported for the historic grade H-451, as in Figure 1, differences are easily seen. It appears that the new grades of graphite show slower oxidation rates than grade H-451 at the same temperature. It can also be observed that graphite IG-110 shows slower oxidation rates than graphite NBG-17 at low temperatures.

Fourth, predictions based on the best fit of kinetic parameters in the LH model deviate from experimental oxidation rates. These deviations are observed systematically at high temperatures (above about 950 – 1000 °C) and high water vapor pressures (above about 100 Pa). Deviations are larger for grades IG-110 and NBG-17 than for graphite PCEA. Deviations were also reported in the GA study on

graphite H-451, and are clearly seen in the plots drawn with digitized data extracted from the GA report [7]. Faced with the dilemma that oxidation rate data of graphite H-451 cannot be represented by a single set of kinetic parameters, the authors of the GA report proposed that two different sets of parameters should be used for the so-called "low water" range ($P_{H2O} < 300$ Pa) and "high water" range ($300 < P_{H2O} < 3000$ Pa). Realizing that splitting the P_{H2O} range is not practical, they designed an empirical set of parameters to be used in the "combined" range that covers all pressures investigated ($0 < P_{H2O} < 3000$ Pa). Figure 1 shows only the "low water" and the "combined" model for graphite H-451.

Figure 1 demonstrates that the LH model cannot consistently reproduce all oxidation rate data measured over broad ranges of temperature and water vapor pressure. It is to be observed, in all fairness, that not all previous studies on kinetics of graphite oxidation reported that the classical LH model may have limited applicability. The limitations may have not been observed in the early studies (1950's and 1960's) that have advanced the LH model because they contained only a limited number of experimental data points. Later, other reports identified some limitations and attributed them to particular properties of their graphite (or carbon materials in general).

3. THE LANGMUIR-HINSHELWOOD MODEL

3.1 PREMISES AND CLASSICAL APPLICATIONS

In the literature on graphite oxidation it was long time assumed that oxidation by H_2O (reaction I) has similar kinetic behavior as oxidation by CO_2 (reaction II):

$$C_{\text{graphite}} + CO_{2\ \text{gas}} = 2\ CO_{\text{gas}} \qquad \text{(II)}$$

Both processes can be formally described by the same general rate equation, where indices $_{ox}$ and $_{prod}$ refer to the oxidant agent (H_2O or CO_2) and oxidation products (H_2 or CO):

$$Rate = \frac{k_1(P_{ox})^m}{1+k_2(P_{prod})^n+k_3P_{ox}} \qquad (1)$$

and the exponents *m* and *n* are the respective reaction orders for the oxidant and the oxidation product. This non-linear equation agrees with the observations that oxidation is accelerated by the increase of oxidant partial pressure, P_{ox}, and it is slowed down by an excess of the reaction product, P_{prod}. The temperature dependence is formally introduced by assuming that all rate constants k_i (i = 1, 2, 3) in Eq. (1) obey the classical Arrhenius relationship:

$$k_i = A_i \exp\left(-\frac{E_i}{RT}\right) \qquad (2)$$

The particular form of Eq. (1) for oxidation by water vapor is given in Eq. (3). This form was used previously in numerous studies, including the above-referenced GA report [7]:

$$Rate(P_{H2O}, P_{H2}, T) = \frac{k_1P_{H2O}}{1+k_2(P_{H2})^n+k_3P_{H2O}} \qquad (3)$$

At the microscopic level, graphite gasification is the result of a series of processes that include gas adsorption, surface diffusion, reactions at active surface sites, and desorption of oxidation products. For reactions occurring in the pore space, two additional steps include oxidant (H_2O) diffusion from gas phase and diffusion of the oxidation products (CO and H_2) back to the gas phase. However, the exact sequence of elementary reaction steps that yield the overall kinetic equation (3) is not known. At least two different reaction schemes were proposed for graphite oxidation by water, which both lead to the rate equation (3). Gadsby et. al. [19] proposed that inhibition by hydrogen is caused by molecularly adsorbed H_2 blocking surface sites according to the following chain of elementary reaction steps:

$$\begin{aligned} &C_f + H_2O_{\ (g)} \underset{j_1}{\overset{i_1}{\leftrightarrows}} C(H_2O) \\ &C(H_2O) \xrightarrow{j_3} CO_{\ (g)} + H_{2\ (g)} \\ &C_f + H_{2\ (g)} \underset{j_2}{\overset{i_2}{\leftrightarrows}} C(H_2) \end{aligned} \qquad \text{(III)}$$

Giberson and Walker [20] proposed a different mechanism, where surface blockage is caused by chemisorption of atomic hydrogen on reactive surface sites:

$$C_f + H_2O \xrightarrow{i_1} C(O) + H_2$$

$$C_f + \tfrac{1}{2} H_2 \underset{j_2}{\overset{i_2}{\leftrightarrow}} C(H)$$
$$C(O) \xrightarrow{i_3} CO + C_f \qquad \text{(IV)}$$

In the above schemes, C_f is a free carbon surface site and $C(H_2O)$, $C(H_2)$, C(O) and C(H) are surface sites with adsorbed H_2O, H_2, O, and H, respectively. Both reaction schemes correspond formally to the global rate equation (3), but the significance of rate constants is different. In the Gadsby mechanism, $k_1 = (i_1 j_3)/(j_1+j_3)$; $k_2 = i_2/j_2$; $k_3 = i_1/(j_1+j_3)$ and $m = 1$. In the Giberson and Walker mechanism, $k_1 = i_1$; $k_2 = i_2/j_2$; $k_3 = i_1/j_3$ and $m = 0.5$. In these schemes, the arrows represent fast (irreversible) elementary steps (→) or equilibrium processes (←→) and scripts *i* and *j* associated with the arrows are rate constants of forward and backward transformations.

A totally different mechanism was proposed by Long and Sykes [21] who assumed that H_2O molecules dissociate on carbon surface into H* and OH* radicals that are adsorbed at adjacent carbon atoms. This step is followed by hydroxyl dissociation and desorption of molecular H_2:

$$2\,C_f + H_2O \underset{j_1}{\overset{i_1}{\leftrightarrow}} C(H) + C(OH)$$
$$C(H) + C(OH) \xrightarrow{i_1^*} C(H_2) + C(O)$$
$$C(H_2) \underset{j_2}{\overset{i_2}{\leftrightarrow}} C_f + H_2 \qquad \text{(V)}$$
$$C(O) \xrightarrow{i_3} CO$$

In this mechanism the definition of rate constants k_i in global Eq. (3) are even more complicated: $k_1 = i_1 i_1^* / (i_1^* + j_1)$; $k_2 = i_2/j_2$; $k_3 = (i_1 i_1^*)(1/i_1^* + 1/j_2 + 1/i_3) / (i_1^* + j_1)$ and $n = 1$. The experimental data used in support were collected at steam pressures between 1.3 and 100 kPa and temperatures between 680 and 800 °C.

These examples show that the rate constants k_i in Eq. (3) are in fact mechanism-dependent composite constants, i.e. they are mathematically defined by combinations of rate constants for several elementary reaction steps. The specific combinations depend on which elementary reaction scheme is accepted. This question does not have a clear answer. The rate constants of elementary steps are supposed to obey the Arrhenius temperature dependence

$$i = a\, exp\left(-\frac{\epsilon}{RT}\right) \qquad (4)$$

where the pre-exponent *a* is a frequency factor related to the number of molecular events occurring per unit of time (e.g. successful collisions between reacting species leading to reactions). The exponential is derived from the Boltzmann distribution of molecules with the energy above a specific energy threshold, ε, which is required for successful completion of one molecular reaction. It is generally assumed that the energy barrier of elementary reaction steps is a positive number (positive activation energy).

These assumptions are not necessarily true for the composite constants k_i of the global reaction rate, Eq. (3). Not only that their significance is so much obscured by the existence of several possible reaction mechanisms, but their mathematical definition – the ratio of two exponentials (in the simplest case) – allows for any sign, positive or negative, of the number under the exponential sign (depending on the difference of energy barriers between elementary steps). Because of that fact, the kinetic parameters A_i and E_i in the global rate equation (3) should be regarded as apparent constants (mechanism-dependent) that should not necessarily carry clear significations at the level of molecular processes. Although the majority of chemical reactions have positive activation energy, examples can be found in the graphite oxidation literature of negative apparent activation energies obtained from the best fit of the LH model,

Eq. (3), to experimental data [22]. Other reports [23] chose not to explicitly mention the negative activation energy result, but that is obvious at a closer inspection of data. Examples of negative activation energies were encountered mostly in studies relying on a large enough number of experimental data points [11,12,13].

The arguments provided above lead to the recognition that the LH model has limited applicability for graphite oxidation kinetics. We have previously reported that the best fit of the LH model to experimental data for oxidation by moisture of graphite PCEA and NBG-17 led to negative activation energies [11,12,13]. Even more difficult was to fit recently measured data on graphite IG-110. The best LH fit for all these graphites shows deviations at high temperatures and high P_{H2O}, where the measured rates are in general higher than what the LH fit would predict. These deviations were shown in Fig. 1.

3.2. LIMITATIONS OF THE LANGMUIR-HINSHELWOOD MODEL

The limitations of the LH model when used in the graphite oxidation context reside in its very basic assumptions. The underlying premise of all reactions schemes presented above (and of others [24,25,26,27,28] that will not be discussed here) is that the solid graphite surface contains a finite number of non-interacting, equivalent reaction sites, which can be occupied with equal probability by any surface species (either oxidant or reaction product) such as H_2O, H_2, CO, H^*, OH^* etc. In other words, the surface was assumed to be energetically and structurally homogeneous, elementary reaction steps were supposed to occur independently of each other, and the extent of reactive surface was supposed to be a small fraction of the total available surface (such that the lateral interactions could be neglected). These assumptions, even though necessary in the early stages of theory development, are no longer supported by the current understanding of nuclear graphite structure and properties.

Another criticism of the LH models (when applied to oxidation by water) follows from the character of oxidation rate dependence on water vapor pressure. The slope of ln(*Rate*) versus ln(P_{H2O}) curves is the apparent reaction order for water, based on the empirical linear equation

$$Rate = k\, {P_{H2O}}^{m} \qquad \text{or} \qquad \ln(Rate) = \ln k + m \ln(P_{H2O}) \qquad (4)$$

According to the classical LH equation (3), an increase in P_{H2O} will cause a proportional increase in rate as long as $1 >> k_3 P_{H2O}$ and the retardation effect of H_2 can be neglected ($P_{H2} \approx 0$). However, as P_{H2O} continues to increase, the proportional effect of P_{H2O} at the numerator gradually diminishes in comparison with the gradually increasing contribution of $k_3 P_{H2O}$ term in the denominator. Consequently, the apparent reaction order in the LH model is expected to vary from near one at low P_{H2O} to near zero at high P_{H2O}. Measurements made in a narrow range of P_{H2O} did not conflict with this prediction but some reports of kinetic measurements over broader ranges of P_{H2O} and temperature indicate a variation contrary to the LH prediction: the apparent kinetic order was close to zero at low temperatures, and increased towards unity at higher temperatures and high P_{H2O} [26,31].

Other studies invalidated the LH assumption on the energetic equivalence and reaction independence of surface sites. Binford and Eyring [31] observed that the character of oxidation rate dependence on P_{H2O}, Eq. (4), changes with the temperature. They proposed that two oxidation processes occur simultaneously on graphite surface: one with zero order with respect to P_{H2O} and one with first order. This implies that two types of active sites exist on "imperfect graphite lattice" and their relative number varies with the oxidation temperature [31]. Similar observations were made in carbon gasification by CO_2 [32]. Magne et al. [33] found by thermodesorption and mass spectroscopy that water chemisorbed on carbon above 200 ^oC forms a surface complex that decomposes on increase of temperature in CO and H_2 simultaneously. They hypothesized the presence of two types of surface sites: labile sites that react first and stable sites that participate in steady state oxidation reactions. Other authors suggested that the adsorption strength of carbon monoxide, water or hydrogen on carbon changes with temperature, and so it does the mechanism of surface site blocking by these species [34,35]. Olander et al. [36] studied the

formation and evolution of the surface complex formed by adsorption of water on pure graphite. Their results show that H_2O adsorb dissociatively into H^* and HO^* radicals bounded at neighboring carbon atoms. Then the surface complex undergoes rearrangements in an activated process (170 kJ/mol) by which one H atom migrates from C-OH to C-H to form a pair of >C=O and $>CH_2$. This is followed by desorption of H_2 and CO. Moreover, Binford and Eyring [31] found that graphite specimens that had reacted for a while at high temperature (1300 ^oC) showed abnormally high oxidation rates after lowering the temperature (900 ^oC). This apparent lack of reversibility shows that some complex interactions occur between surface species, in disagreement with the basic hypothesis of the LH model.

The role of the graphite microstructure was later added to the discussion. Miura and Morimoto [37] found that water chemisorption on natural graphite starts from 25 ^oC. Chemisorption occurs differently at crystal edge carbon atoms with zig-zag and armchair configuration. Lusier et al. [36] suggested that surface sites active in carbon gasification by steam may have a continuous distribution of properties: (a) zig-zag sites that adsorb H strongly and irreversibly; (2) armchair sites that preferentially adsorb H and participate in oxygen-exchange reactions; (3) stable sites that form strong >C=O groups; (4) unstable sites (most reactive) where weakly bound oxide forms and desorbs as CO, while H adsorbs in limited amounts, if at all.

Obviously the LH model premises about the equivalence and independence of reactive surface sites do not hold for graphite materials. The microstructure is an important factor for surface reactivity, which is not accounted for in the LH model.

3.3 STOCHASTIC MODELS - AN ALTERNATIVE TO DETERMINISTIC LH MODEL

Based on what is known today about the microstructure of graphite materials, it should be easy to argue that mechanistic oxidation models like those presented in schemes (III) – (V) above are inadequate to fully describe the complexity of gasification reactions. The rate equation (3) of the LH model was derived by combining the Langmuirean assumptions enumerated above with the steady-state approximation. The latter is an approximation commonly used in descriptive chemical kinetics according to which the forward and backward reactions have equal rate at steady state conditions. Although formally correct, many of previous models were statistically deficient. As Fig. 1 shows, LH model predictions using a single set of “best fit” parameters fail to correctly reproduce a large number of experimental data points over a broad range of conditions. We have the choice to either restrict the range of variables (water pressure, temperature) for which one can define a statistically significant set of LH model parameters, or to accept that several sets of parameters are valid over various ranges of experimental conditions.

A third option is finding a proper mathematical form of the kinetic equation, such that it is able to reproduce correctly the temperature dependence (apparent activation energies) and concentration dependence (apparent reaction order) for steady state oxidation by moisture of particular grades of graphite, over a broad range of conditions. The measurements should be conducted in kinetic regime and be free of transport limitations (as much as possible), and therefore the result should represent intrinsic properties of graphite grades of interest.

It goes without questioning that the carbon (or graphite) surface is covered by a copious number of surface complexes formed after exposure to oxygen, carbon dioxide, water, etc. The issues that still do not have an answer are the same, irrespective whether oxidation is caused by air (oxygen), water (moisture) or carbon dioxide:

- Which (and when) surface complexes are active in gasification reactions?
- What factors determine whether active surface complexes act as just spectators or even as inhibitors of gasification?
- How many surface sites (carbon atoms) are affected by the gasification reaction induced by one single H_2O molecules?

The fact remains that surface complexes formed under common circumstances (temperature, gas exposure, etc) have a wide range of structures and reactivity. If this fact is neglected, then all attempts to formulate rational chemical kinetics mechanisms using deterministic premises are empirical and have limited capacity to capture the global process. It was argued in the recent literature [39] that a stochastic (probabilistic) description of surface reactions may be more successful. A series of recent papers by Haynes [40,41,42] and Hurt [43,44] investigate the possibility that carbon gasification reactivity in air (oxygen) reflects the nanoscale diversity of local surface topography, atomic configurations, and bonding energies of surface complexes. As argued by Hurt and Haynes [44] heterogeneity may be intrinsic, related to local structures, or may be induced, a reflection of chemical changes occurring between neighboring surface sites. The result of surface heterogeneity is that the desorption energy of surface complexes is better described by a distribution function, $f(E_{des})$ than by a unique value. The focus on the desorption energy is significant because gasification (oxidation) occurs through desorption of surface complexes. Then, the total rate of global gasification reaction can be written as

$$R_{total} = \int f(E_{des}) R(E_{des}) \mathrm{d}E_{des} \qquad (5)$$

where $R(E_{des})$ is the local gasification rate, which can be approximated by the LH model. The distribution function $f(E_{des})$ can conveniently by modeled by a Gauss distribution characterized by its center E_{des}^{o} and standard deviation $\sigma_{E\text{-}des}$. El-Genk et al. [45] used Gaussian-like distributions of adsorption and desorption energies of oxygen complexes to model the kinetics of oxidation by air of several graphite grades. Hurt and Hayes [44] demonstrate that, with these assumptions, the pressure dependence of the reaction rate depends on the breadth of the Gauss distribution. This is shown in Figure 2, reproduced from their work. The case with $\sigma_{E\text{-}des} = 0$ corresponds to a homogeneous surface (energetically and structurally), as in the basic LH model. In this case the plot of ln(*Rate*) vs. ln(P_{ox}), Eq. (4), starts with high slope at low pressure and bends to zero slope at high pressure. This is the typical LH behavior, where the apparent reaction order *m* is close to unity at low pressure (adsorption control) and trends towards zero at high pressure (saturation of surface sites, desorption control). However, if surface nonuniformity is introduced in the model ($\sigma_{E\text{-}des} \neq 0$), the ln(*Rate*) vs. ln(P_{ox}) plots bend less, as shown by simulations by the same authors [44] reproduced in Fig. 2. The larger the breath $\sigma_{E\text{-}des}$ of the Gauss distribution (or the more heterogeneous the distribution of surface complexes is) the less bending is observed and the higher remains the apparent reaction order. Recall, the latter was introduced by Eq. (4) above as the slope of the log-log variation of oxidation rate versus oxidant pressure:

$$m = \frac{d\ln(Rate)}{d\ln(P_{ox})} = \frac{1}{1+\frac{k_{ads}P_{ox}}{k_{des}}} \qquad (6)$$

The right term in Eq, (6) is valid for the most general and simplest form of the LH kinetic model, in absence of hydrogen retardation (P_{H2} = 0). The two kinetic constants k_{ads} and k_{des} correspond to the rate of oxidant adsorption and gasification product desorption.

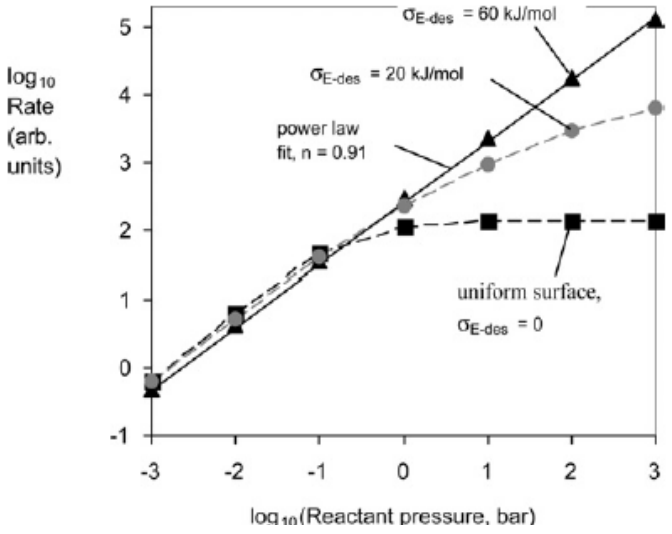

Figure 2: Behavior of the global oxidation rate predicted for solids with a Gauss distribution of surface sites' desorption energies (from ref. [44]).

As Fig. 2 shows, the "persistent power law" identified by Hurt and Haynes [44] for carbon gasification in air can be explained by the energetic and structural heterogeneity of real surfaces. Application of this model required prior knowledge of desorption energy distribution function for surface complexes for the graphite grade of interest. The $f(E_{des})$ function can be determined experimentally using the method of temperature-programmed desorption (TPD) of surface species on each graphite grade [46,47,48,49].

The equipment available at ORNL is suitable for such measurements, because the thermogravimetric balance (TAG) is connected to a mass spectrometer (MS). In the future it is worth pursuing this route, but for the moment we do not have experimental information on desorption energy distribution of surface complexes formed by exposure to moisture. Therefore, a different route for development of a global model for graphite oxidation by moisture was chosen.

We need first to look at the structure, energetics and reactivity on surface complexes formed by interaction of water with graphite surfaces. Recent literature information obtained by computational chemistry methods shall be used.

4. NEW KINETIC MODEL FOR GRAPHITE OXIDATION BY MOISTURE

4.1 WATER SURFACE COMPLEXES AND REACTION ROUTES

The structure, energetics and reactivity of surface complexes formed by interaction of water with graphite surfaces can be modeled by using powerful molecular simulation methods based on quantum density functional theory (DFT). In essence, DFT calculations confirm that dissociative chemisorption is the first step of graphite gasification by water, as proposed by Long and Sykes [21] from experimental observations. Perfect graphite is essentially hydrophobic, and water experiences very weak, delocalized physisorption. However, if atomic vacancies are present on the flat basal plane, physisorption interactions are stronger [50] and as a result a carbon atom is slightly pulled out towards the H atom of an water molecule [51]. From this strong physisorption state (18 kJ/mol) dissociative chemisorption of water occurs after overcoming a barrier of 72-84 kJ/mol. A second path of lesser energy barrier (45 kJ/mol) is available for gas-phase molecules that avoid the physisorption state and go directly to the dissociative chemisorption state. After one more intermediate state the chemisorbed –OH breaks into O and H atoms bonded to separate C atoms. The total exothermicity of the final state is 306 kJ/mol. The energy diagram in Fig. 3 shows the molecular transformations and the structures of intermediate states [51]. The second dissociation path (not shown in the diagram) is more probable at high temperatures. Note that a direct transition from gas phase to the completely dissociated and separated state has negative activation energy.

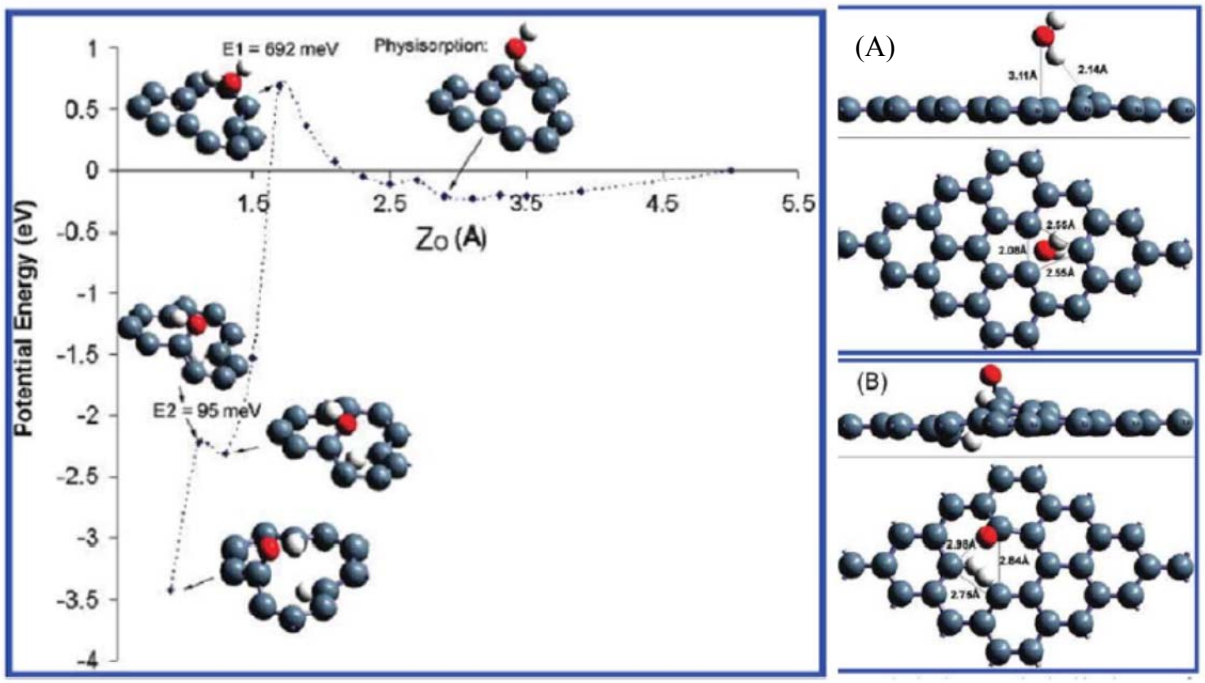

Figure 3: Energy diagram steps of dissociative chemisorption of H_2O on a vacancy site of graphite basal plane. The structures in the right panels represent strong physisorbed state (A) and the chemisorbed state (B) with totally dissociated H_2O molecule (O – red; C – navy blue; H – grey). Adapted from [51].

More significant, and much more complex, are the processes occurring at graphite edges. In essence dissociative chemisorption of water remains the first step. Espinal et al. [52] used DFT calculations to

investigate the water reactions with clean, oxidized and hydrogenated carbon surfaces. They confirmed that H_2O chemisorption on clean zig-zag and armchair sites is highly exothermic and forms stable surface intermediate complexes containing oxygen bonded in hydroxyls, semiquinones, and cyclic ethers groups. The zig-zag configuration is energetically more reactive than the armchair configuration. Figure 4 shows the transformations chain of most probable surface complexes formed at zig-zag and armchair sites on graphene sheets. The vertical position of structural formula reflects the stability of various complexes with respect to the initial state, but the drawing is not at scale. The evolution of these complexes towards the final products of gasification, namely CO and H_2, was also investigated. Several paths are possible, but all are endothermic (and will be favored by high temperatures). The main point to observe from these schemes is that the release of CO and H_2 after adsorption of one single water molecule involves participation of several surface sites (carbon atoms) on either zig-zag or armchair edges, and results in drastic reconfiguration of the carbon skeleton (replacement of an aromatic 6-atoms ring by a 5-member cycle). These observations will be used later.

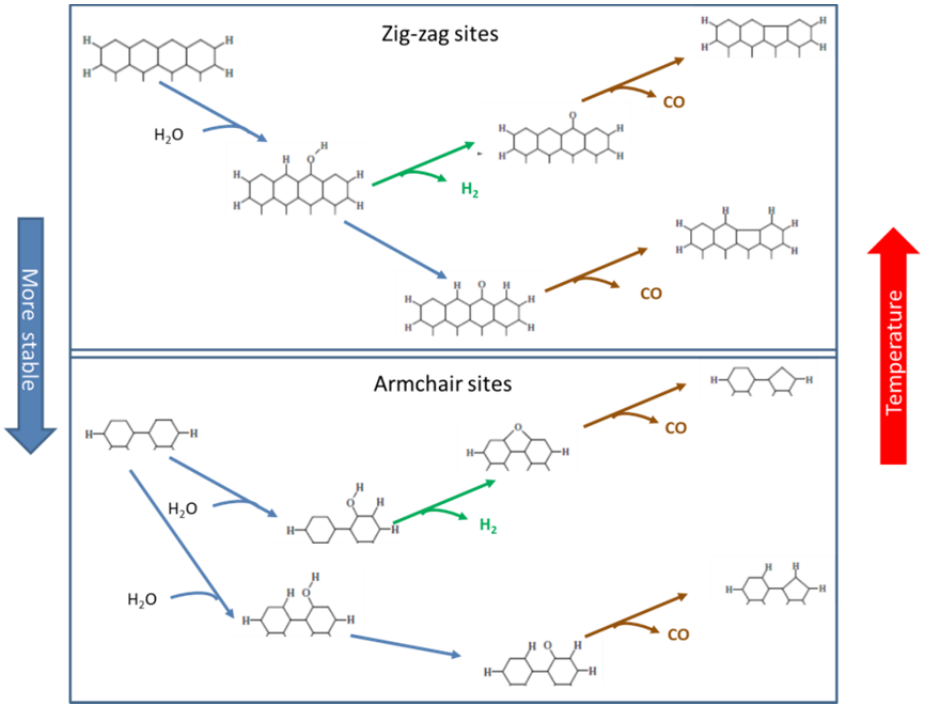

Figure 4: Schematic diagram of surface complexes formed by chemisorption of water at exposed zig-zag and armchair sites on graphene, and of their subsequent transformations during graphite gasification. Adapted from [52].

Espinal et al. [52] calculated the overall energetics of water reactions on clean graphite surface. They found that the global process for the reactions shown in Fig. 4 is exothermic when CO desorption occurs after the dissociation of H_2O either on zig-zag or armchair sites. When hydrogen evolution was also considered, the global process of H_2 evolution and CO desorption is exothermic for zig-zag sites (Fig. 4, top panel) but endothermic for armchair sites (Fig. 4, bottom panel). In reality, the number of exposed active sites on "clean" graphite is small unless they were formed by prior high temperature treatment and pyrolysis steps. Of most significant importance are the reactions occurring on hydrogen-saturated or pre-oxidized surfaces. These reactions are summarized in Figure 5.

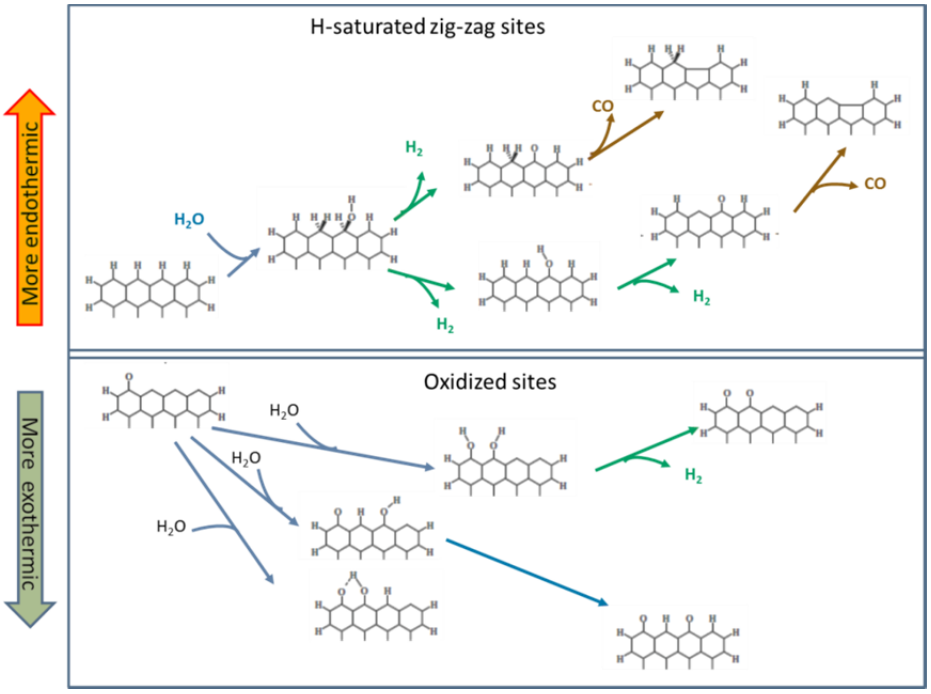

Figure 5: Schematic diagram of surface complexes formed by adsorption of water on hydrogen saturated and oxygen-containing zig-zag sites on graphene edges, and of their subsequent transformations during graphite gasification. Adapted from [52]

The bottom panel in this figure shows that water adsorption and dissociation on a pre-oxidized surface is even more exothermic than on the clean surface. This suggests that oxidized surfaces can be more reactive towards water than clean surfaces, possible because oxygen containing groups can form hydrogen bonds with H_2O molecules that would lower the energy barrier to dissociative chemisorption [52]. We found out that this feature explains some of our recent observations (to be discussed later). On the other hand, dissociation of water on a hydrogen-saturated surface is endothermic (as often observed in experiments) and requires more energy than the reaction of water with clean surface. The top panel of Fig. 5 shows the diagram of these reactions. The retardation by hydrogen of gasification by water is explained by the fact that H_2 molecules compete with H_2O for the same active sites [52].

4.2 COOPERATIVE BEHAVIOR IN REACTION KINETICS

The main conclusion from the above discussion is that reaction of water with graphite is a complex process, that can occur on numerous routes (of which only a few were listed above) which involve a multitude of surface sites. After each reaction step, be it chemisorption and dissociation of H_2O, surface spillover of H atoms, release of H_2 or desorption of CO, the configuration of surface sites changes, carbon bonds are broken, and new bonds are formed. These changes are not localized to single carbon atoms. Because of the π electrons delocalization in graphite, chemical transformations occurring at one carbon site modify the chemical environment of the neighboring carbon atoms. These processes are too complex

to be treated individually, yet they need to be considered for a more accurate model development. An important aspect of the new model should be inclusion of cooperative behavior between active sites on carbon, and the correlation between separate chemical events.

Cooperative behavior is a fundamental property of molecular interactions and binding phenomena in biological systems [53]. Many polymers and proteins exhibit cooperativity, whereby their ligands bind in a non-independent, interacting way. After binding an oxygen molecule on hemoglobin, the probability of binding a second molecule increases. This is a well-known example of positive cooperativity. Conversely, polyelectrolyte polymers binding ligands by electrostatic interactions see their binding probability decrease after binding the first ligands. This is an example of negative cooperativity. According to some scholars [53,54] there is a close analogy between collective behaviors in chemical kinetics, biochemistry, cybernetics, neuron interactions and other interdisciplinary fields. The property of cooperativity links descriptions of chemical systems at the individual atom (or molecule) level with the macroscopic behavior observed in real systems, either macromolecules, organisms, microbes, etc. The common property in these systems is the occurrence of "active sites". As the occupancy of these sites increases the interaction between sites can lead to increased affinity for further binding (positive cooperativity) or to retardation of further binding (negative cooperativity).

Chemical kinetics of elementary step reactions is derived from the mass action law that postulates that the reaction rates of elementary processes are proportional with the reactant concentrations raised to a power defined by stoichiometry coefficients. The global rate equation is derived by combining these simple rules with the steady state hypothesis, according to which the forward and reverse reactions occur with equal rate. This is how the global kinetic equations for graphite oxidation, Eqs. (1) – (3), where derived in the LH model. An equation of similar form describes the dependence of enzymatic reaction rates on the concentration of substrates in enzyme catalysis; it is known as the Michaelis-Menten equation for non-cooperative enzymatic reactions [55]:

$$v = \frac{v_{max}[S]}{K_M + [S]} \tag{7}$$

where [S] is the substrate (ligand) concentration and K_M is a combined rate constant. This equation is formally equivalent with the rate equations for graphite oxidation based on the LH model, such as Eq. (3), in the particular case of no product inhibition (P_{H2} = 0). The rate response to ligand concentration variations is described by a hyperbola (Fig. 6). A similar variation is predicted by the LH model for the relationship between oxidation rate and oxidant concentration.

Enzymatic kinetics has numerous examples of cooperative effects, where Eq. (7) fails to reproduce the data. In these cases, the variation of rate versus changes in substrate concentration is a sigmoidal curve (Fig. 6). This type of variation is described by the following empirical equation proposed by Hill:

$$v = \frac{v_{max}[S]^m}{K_d + [S]^m} \tag{8}$$

where K_d is a dissociation constant and m formally represents the number of binding sites available per enzyme unit (the Hill parameter):

$$E + m\ S \longleftrightarrow ES_m \tag{VI}$$

Recalling the chemical kinetics theory definition introduced by Eq. (4) above, one can also regard m from scheme (VI) as the apparent reaction order in Eq. (8). Fitting the Hill equation to real data rarely gives integer m values, as expected if m was the stoichiometric coefficient in an elementary reaction step. The Hill equation may not be an accurate description of elementary step mechanisms, but it is very useful in describing cooperative enzymatic systems because variations of m provide a needed flexibility [55].

Figure 6 compares rate of enzymatic reactions versus concentration relationship typical for lack of cooperativity (hyperbola) and for positive cooperativity (sigmoid curves) with various *m* values.

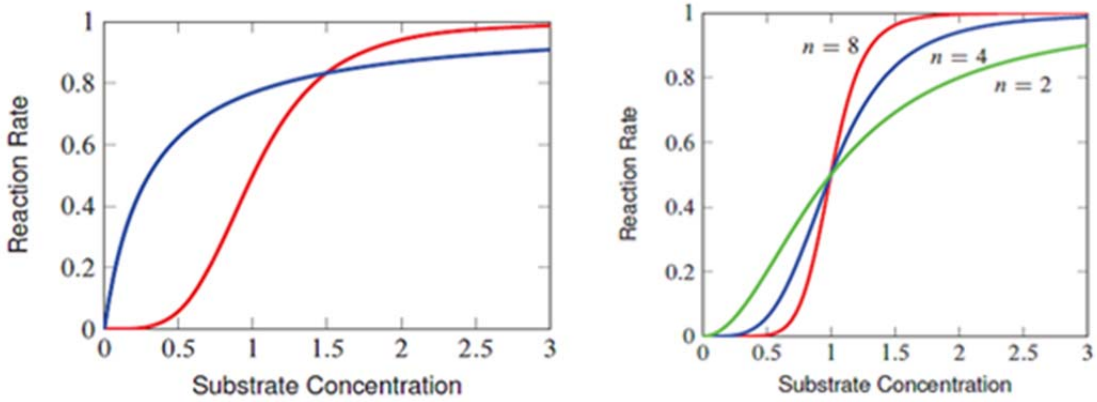

Figure 6: Left: Comparison between hyperbolic and sigmoidal dependence of reaction rate versus ligand concentration indicating lack of cooperativity (blue hyperbola line) and positive cooperativity (red sigmoid curve), respectively. Right: By varying the Hill parameter, sigmoid curves are able to describe a multitude of positive cooperative phenomena. Adapted from [55].

4.3. ENHANCED KINETIC MODEL FOR GRAPHITE OXIDATION

4.3.1 Site Cooperativity and Apparent Reaction Order

Fitting the LH model to experimental data on IG110 oxidation collected during 2015-2016 was more difficult than fitting the model to PCEA and NBG-17 data. It was shown in Fig. 1 that deviations from the LH model appear to be larger for graphite IG-110 than for the other grades. Deviations appear mostly at high temperatures. To understand the cause of temperature effects, we plotted in Figure 7 the apparent reaction order (*m*) calculated with Eq. (4) from the experimental data against the values predicted by the LH model with best fit parameters.

Figure 7 shows big differences between the trends predicted by the LH model and the experimentally observed variations of *m*. The LH model predicts a linear increase of the apparent reaction order with temperature. In contrast, the apparent reaction order obtained directly from experimental data (as the slope of ln(*Rate*) versus ln(P_{H2O}) plots) describes a sigmoid curve with values between 0 and 1. Interestingly, while IG-110 data spread over the full range of the sigmoid, NBG-17 data cover only the lower and middle ranges and PCEA data only the top range. In contrast, both variants of the LH predictions for graphite H-451 (based on digitized data from ref. [7]) show descending trends versus temperature; the values calculated directly from experimental observations are close to the predictions for the "low water" model at $P_{H2O} < 300$ Pa.

Other researchers observed that the apparent reaction order may vary during carbon oxidation. Querini and Fung [56] studied temperature-programmed oxidation (TPO) of highly coked catalysts and noted that coke reaction order can increase from near 0 to 1. Analyzing kinetics of charcoal and graphite oxidation at low O_2 partial pressure from TPO experiments, Li and Brown [57] used an exponential function to fit the observed variation of carbon reaction order on the fraction of unreacted carbon.

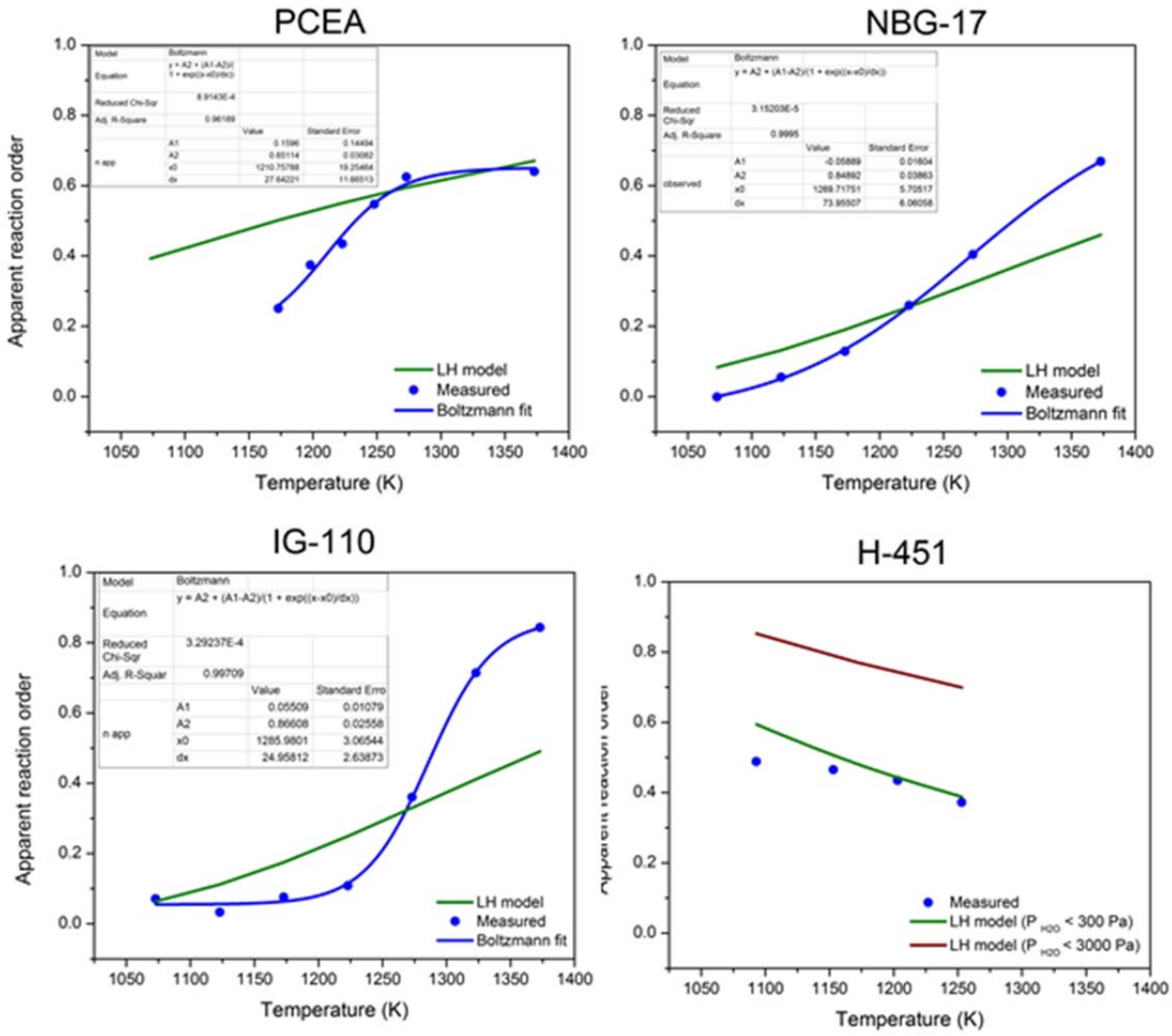

Figure 7: Temperature dependence of apparent reaction order calculated directly from experimental data compared with model predictions based on best fit LH parameters. Data for graphite grades PCEA, NBG-17 and IG-110 were obtained at ORNL and for graphite H-451 were derived by digitizing the plots from ref. [7]. Experimental data points were fitted with the Boltzmann cumulative distribution function.

We fitted the sigmoid temperature variations of apparent reaction order obtained from experiments (fig. 7) with the Boltzmann distribution function:

$$m(T) = m_{max} + \frac{m_{min} - m_{max}}{1 + exp\left(\frac{T - T_o}{\Delta T}\right)} \approx m_{max} \frac{exp\left(\frac{T - T_o}{\theta}\right)}{1 + exp\left(\frac{T - T_o}{\theta}\right)} \quad \text{(assume } m_{min} = 0\text{)} \qquad (9)$$

The cumulative Boltzmann distribution, Eq. (9), represents the probability distribution of apparent reaction order values (m) as a function of temperature. Here m_{max} and m_{min} are the upper and lower limits

of m (in the experimental range) and $0 \le m_{min} < m_{max}$; T_o is the temperature corresponding to the inflection point of the sigmoid curve and θ is the slope at T_o. Recall that the apparent reaction order is defined by the reaction stoichiometry. In the particular case of graphite gasification by moisture, the global equation can be written as:

$$C_f + m\ H_2O \rightarrow \ldots. \rightarrow x\ C_f + y\ CO + z\ H_2 \qquad \text{(VII)}$$

Because of formal similarity between schemes (VI) and (VII) we borrowed concepts from enzyme kinetics and applied them to graphite oxidation kinetics. The Hill coefficient, m, in Scheme (VI) is a variable stoichiometric coefficient in enzyme kinetics. In Scheme (VII) the stoichiometric coefficient m represents mechanistically the average number of H_2O molecules reacted per active carbon site. The global rate equation is proportional with P_{H2O} raised to the m-th power, as in Eq. (4) above, which is repeated here:

$$Rate\ (T) \cong k(P_{H2O})^m \cong A \exp\left(-\frac{E}{RT}\right)(P_{H2O})^{m(T)} \qquad (4')$$

In classical kinetics the temperature effect is expressed by the Arrhenius activation law: The rate constant k is the product of the frequency factor A and of the exponential function derived from the Boltzmann distribution of energy. Only those H_2O molecules impinging on the surface with energy higher than a threshold activation energy E will react.

The experimental data shown in Figure 7 demonstrate that the apparent reaction order m (or the stoichiometry of global oxidation reaction) also depends on temperature, and that dependence is described by a Boltzmann distribution. This empirical observation can be interpreted by observing that $1/m$ in Scheme (VII) is the average number of surface sites that participate in reaction with one H_2O molecule. This number is large at low temperatures (when m is small) and drops with the increase of temperature (m increases). This suggests that the cooperativity between surface sites able to participate in gasification by water is temperature-dependent, and follows the Boltzmann distribution function. In other words, increasing the temperature modifies the conditions at graphite surface and enhances the reactivity of surface sites: more and more sites that were stable at low temperatures become reactive at higher temperatures.

With this assumption the global rate equation should be written as

$$Rate\ (T) \cong k(T){P_{H2O}}^{m(T)} \cong A \exp\left(-\frac{E}{RT}\right){P_{H2O}}^{m(T)} \qquad (10)$$

where $m(T)$ is the Boltzmann distribution function and k is an oversimplified notation for the composed kinetic constants that support the LH model.

4.3.2 Enhanced LH Model with Boltzmann Activation of Surface Sites

Returning to the LH model for graphite gasification by water, we modified the classical LH equation, repeated below,

$$Rate(P_{H2O}, P_{H2}, T) = \frac{k_1 P_{H2O}}{1 + k_2 (P_{H2})^n + k_3 P_{H2O}} \qquad (1')$$

by replacing P_{H2O} at the numerator and denominator by ${P_{H2O}}^{m(T)}$. The new rate equation for the enhanced LH model that includes site cooperativity is then written as:

$$Rate(P_{H2O}, P_{H2}, T) = \frac{k_1 (P_{H2O})^{m(T)}}{1 + k_2 (P_{H2})^n + k_3 (P_{H2O})^{m(T)}} \quad (11)$$

where it is assumed that $n = 0.5$ (the exponent of P_{H2}) and the Arrhenius relationship holds for all three rate constants k_i. The *m(T)* exponent is modeled as the Boltzmann distribution function. The explicit form of Eq. (11) is as follows:

$$Rate(P_{H2O}, P_{H2}, T) = \frac{A_1 exp\left(-\frac{E_1}{RT}\right)(P_{H2O})^{\left[m_{max} + \frac{m_{min} - m_{max}}{1 + exp\left(\frac{T - T_O}{\theta}\right)}\right]}}{1 + A_2 exp\left(-\frac{E_2}{RT}\right)(P_{H2})^n + A_3 exp\left(-\frac{E_1}{RT}\right)(P_{H2O})^{\left[m_{max} + \frac{m_{min} - m_{max}}{1 + exp\left(\frac{T - T_O}{\theta}\right)}\right]}} \quad (12)$$

This 10-parameter equation of the LH model enhanced with the Boltzmann distribution function will be called Boltzmann-enhanced Langmuir-Hinshelwood (BLH) model. The new model was fitted to all experimental data points measured during 2015-2016 for graphite IG-110. The same model was then fit to data measured previously for graphite PCEA and NBG-17, and to data for graphite H-451 obtained by digitization of the plots in the 1978 GA report [7]. In general, the enhanced 10-parameters BLH model provides better fit than the 6-parameters classical LH variant.

4.3.3 Testing the Boltzmann-enhanced LH Model

Data analysis and statistical treatment was performed by Dr. Robert Mee at the University of Tennessee, Knoxville, TN. The estimation of parameters was done by the maximum likelihood estimation (MLE) method, which is a standard approach used in statistics. It is an indispensable modeling technique for non-linear modeling with non-normal data that offers sufficiency, consistency, efficiency, and parametrization invariance [58]. When applied to a set of data in combination with a parametrized model, MLE approach is able to simultaneously estimate the parameters that represent all data. The analysis returns parameters values, standard errors for estimates and correlations between estimates. This is essential for understanding the uncertainty in the parameters estimates.

In our analysis we found that not all experimental data were usable for parameters estimate. A preliminary validation step was performed after data collection was complete. Some data points were rejected because of experimental errors or unexpected events during experiments. All "negative oxidation rate" data (highlighted red in the Annex) were obviously wrong and were rejected. In general these were coming from measurements at low temperatures (mostly at 800 ^{o}C, a few at 850 ^{o}C) where oxidation rates are very slow and the relative error of weight loss measurements is higher. Some other data points were rejected because they were clearly in error with the rest of the data based on an empirical response surface model. Data rejected were coming from experiments perturbed by various reasons, either because of flow rate variations, gas composition instability, or other experimental errors. Valid observations retained for analysis were about 85 – 90 % of the bulk of total data collected for each graphite grade.

Analysis of valid data was performed by using the SAS Institute procedure MLMIXED for estimation of the 10 parameters of the enhanced LH model. The rate equation was rewritten in logarithmic form as follows:

$$\ln(Rate) = ln\left[\frac{(P_{H2O})^{\left[a_4+\frac{a_5-a_4}{1+exp\left(\frac{T-x_O}{dx}\right)}\right]}\times exp\left[a_1+\frac{b_1}{T}\right]}{1+\sqrt{P_{H2}}\times exp\left[a_2+\frac{b_2}{T}\right]+(P_{H2O})^{\left[a_4+\frac{a_5-a_4}{1+exp\left(\frac{T-x_O}{dx}\right)}\right]}\times exp\left[a_3+\frac{b_3}{T}\right]}\right] \quad (13)$$

The following notations link Eqs. (12) and (13):

$a_i = ln(A_i); i = 1,2,3$ so that $A_i = \exp(a_i)\,; i = 1,2,3$

$b_i = -\frac{E_i}{R}; i = 1,2,3; R = 8.314$ so that $E_i = -8.314 \times b_i$

and also $a_4 = m_{max}$; $a_5 = m_{min}$; $x_o = T_o$; $dx = \theta$. He variables are P_{H2O} (Pa), P_{H2} (Pa), and T (K). The units for A_i include pressure units (Pa) raised to a negative power equal to the appropriate value of the exponent defining the apparent kinetic order. In addition, the units of A_1 also include inverse time (s^{-1}). All E_i have the units of R, J/mol. The unit of *Rate* is s^{-1}. Rates are calculated as

$$Rate = (1/m_o) \times (\frac{\Delta m}{\Delta t}) \quad (14)$$

where Δm / Δt is the rate of weight loss (mg/s) at isothermal and constant gas composition conditions, and m_o (mg) is the apparent specimen weight at the beginning of isothermal constant conditions. The apparent specimen weight changes slightly when temperature, gas composition and flow rate change, but it is constant during isothermal and constant flow conditions. Corrections were made for every segment of constant conditions, starting from the known weight of the dry specimen at the beginning of the experiment.

5. RESULTS

5.1 GRAPHITE IG-110

As mentioned above, fitting the LH model to experimental data for graphite IG-110 was more difficult than LH fitting of PCEA and NBG-17 experimental data. Special attention was given to collecting data at low temperatures (800 and 850 °C) and low water vapor pressure (5 – 10 Pa) because these conditions are the closest to the normal operating conditions of HTGR (temperature range about 400 – 900 °C and P_{H2O} < 1 Pa) and practical for experiments. Because of the higher relative error of these measurements, the rate of rejections was higher for slow oxidation rates.

In typical runs the gas composition (P_{H2O} and P_{H2}) was kept constant and the temperature was raised in 50 °C increments (Method 1). In Figure 8 below, each Method 1 data point was collected on a different day, using a different graphite specimen. This day-to-day variation and differences between specimens as expected produces the scatter seen in these plots about the blue curves at low temperatures. In an effort to increase the precision of the pressure effect at low temperatures, Method 2 was attempted. In this procedure, each specimen was run at constant temperature, and only P_{H2O} was varied. As expected, this did reduce the scatter about the red curves, since measurements by Method 2 were taken using the same specimen on the same day. However, an unexpected result was observed. When we started at 800 °C with P_{H2O} = 200 Pa and repeatedly lowered the pressure at constant temperature to take additional measurements, the results showed an inexplicable increase in oxidation rate. A similar effect was observed when the Method 2 procedure was repeated at 850 °C (as shown in Figure 8) and 900 °C (not shown).

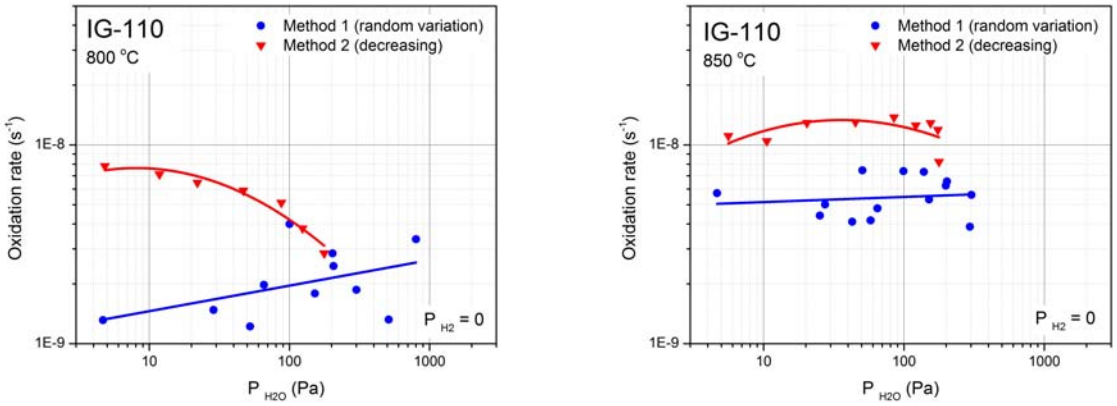

Figure 8: Experimental evidence of site cooperativity effects: Oxidation rates measured according to Method 1 (random P_{H2O} variation from multiple specimens) follow an increasing trend with $P_{H2O,}$ albeit scattered, while rates measured according to Method 2 (continuous P_{H2O} decrease on the same specimen) are higher and show a trend reversed to that expected.

This puzzling fact indicates that a certain "memory effect" was triggered on the graphite surface when the oxidation conditions changed from more aggressive at higher P_{H2O} to less aggressive at lower P_{H2O}. The surface reactivity of aggressively oxidized surfaces did not drop, as expected, when P_{H2O} was lowered at constant T. On the contrary, the rates increased. Figure 8 shows examples of this "memory effect". A similar observation was reported by Binford and Eyring [31] the reactivity of samples oxidized aggressively at high temperature continued even after lowering the graphite temperature by about 500 ^{o}C. This is experimental proof of the reality of cooperativity between active sites. Dynamic changes on the graphite surface are not necessarily reversible (in about 12 h timeframe). Our results confirm theoretical conclusions by Espinal et al. [52] that heavily oxidized surfaces can be more reactive than clean surfaces toward reactions with water. The explanation is that oxygenated species on graphite surface (from aggressive oxidation at higher P_{H2O}) act as centers for water clustering and migration in pores, and thus favors further chemisorption of water by lowering the barrier to H_2O dissociation. After we obtained evidence of the irreversibility of dynamic changes, all data collected in Method 2 were dropped from the MLE analysis.

All physical parameters of IG-110 specimens and their change after oxidation are listed in Annex 1. All oxidation rate values and their corresponding experimental conditions are reported in Annex 2. From a total of 308 data points, 29 observations were rejected because they were either affected by experimental errors, instrumental instability, or simply the oxidation rate values were zero or negative. Another lot of 70 data points were collected with Method 2 procedure and could not be used for model fitting. In the lot of valid observations, 103 data points measured in H_2O/He mixtures and 106 data points measured in (H_2O + H_2)/He mixtures were retained.

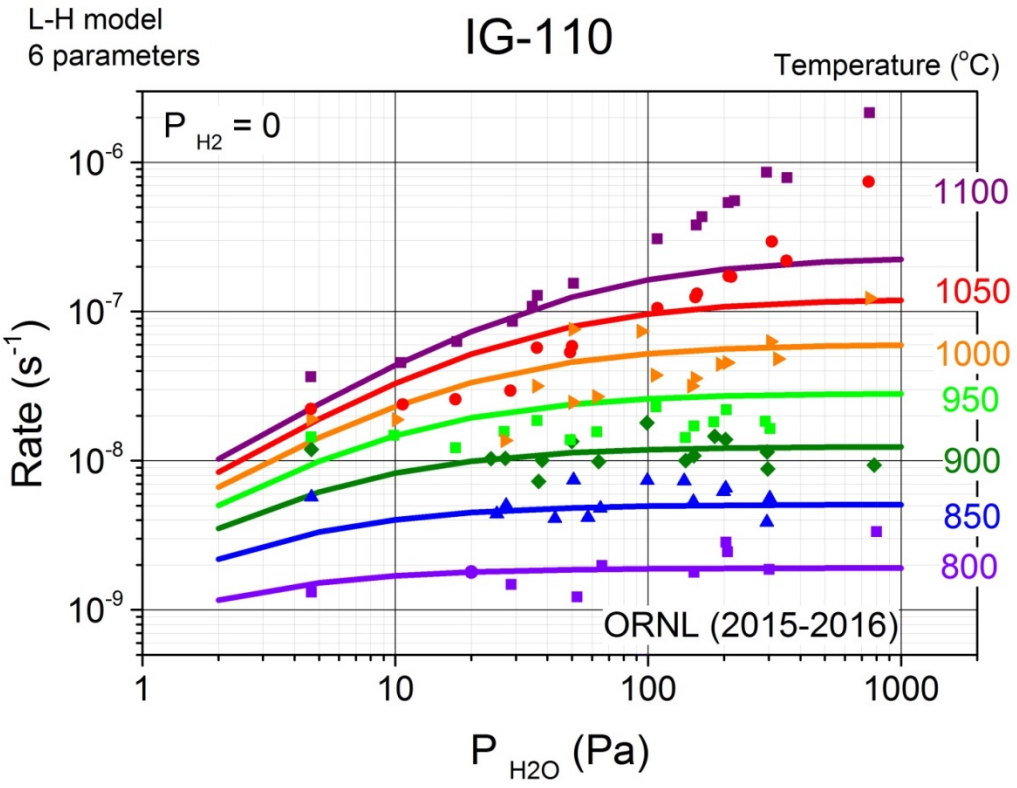

Figure 9: Oxidation rates measured for graphite IG-110 and the trends predicted by LH model with 6 parameters. Deviations are visible at high temperature and high water vapor pressure.

The best fit LH parameters for graphite IG-110 are shown in Table 1:

Table 1
Best fit LH parameters for graphite IG-110

$A_1 = 8.29 \times 10^{-6}$ Pa^{-1} s^{-1}	$E_1 =$ 85.75 kJ/mol	
$A_2 = 4.18 \times 10^{-8}$ Pa$^{-1/2}$	$E_2 =$ -193.23 kJ/mol	$n = 0.5$
$A_3 = 6.29 \times 10^{-11}$ Pa^{-1}	$E_3 =$ - 210.53 kJ/mol	

Figure 9 show shows that the trends calculated with the best fitted LH parameters do not reproduce faithfully the measured data. Large deviations are seen at high pressures and high temperatures, where predicted rates are lower than the observed rates. The LH model predicts that the apparent reaction order is larger at low P_{H2O} and smaller at high P_{H2O}. Accordingly, the LH trends in Fig. 9 (continuous lines) change the slope before P_{H2O} = 100 Pa, but the observed rates do not follow this trend. Figure 10 compares all measured rates versus the LH model prediction. The correlation is not as good as expected.

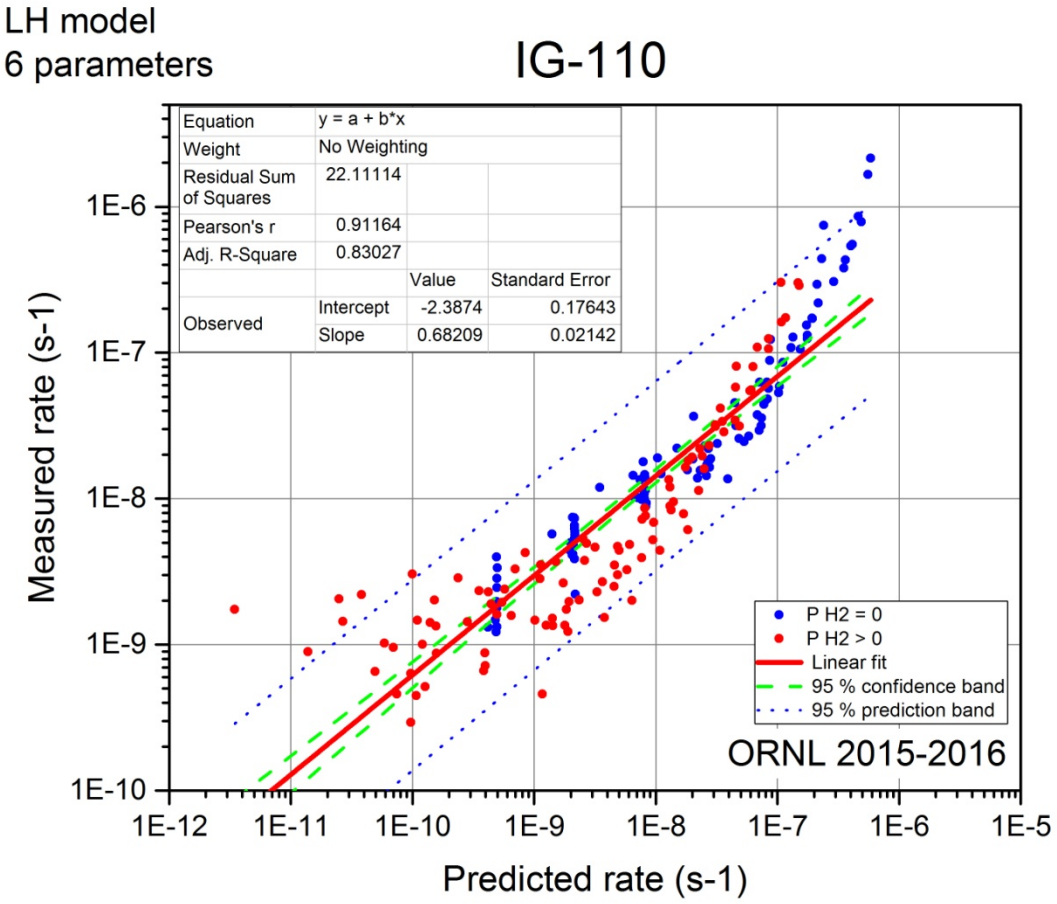

Figure 10: Comparison between rates measured for oxidation of IG-110 graphite and rates predicted by the LH model. Data shown include measurements in H_2O / He and (H_2O + H_2) / He mixtures.

The fact that fitting of 6-parameters LH model was not very successful for IG-110 is shown by the log-log plot of measured and predicted rates in Figure 10. Large deviations are seen for fast rates at H_2-free conditions and for slow rates in presence of H_2.

A much better agreement between experimental measurements and model predictions was obtained with the Boltzmann-enhanced LH model, introduced by Eqs. (12) and (13) above. Figure 11 compares the trends predicted at $P_{H2} = 0$ with the experimentally measured rates.

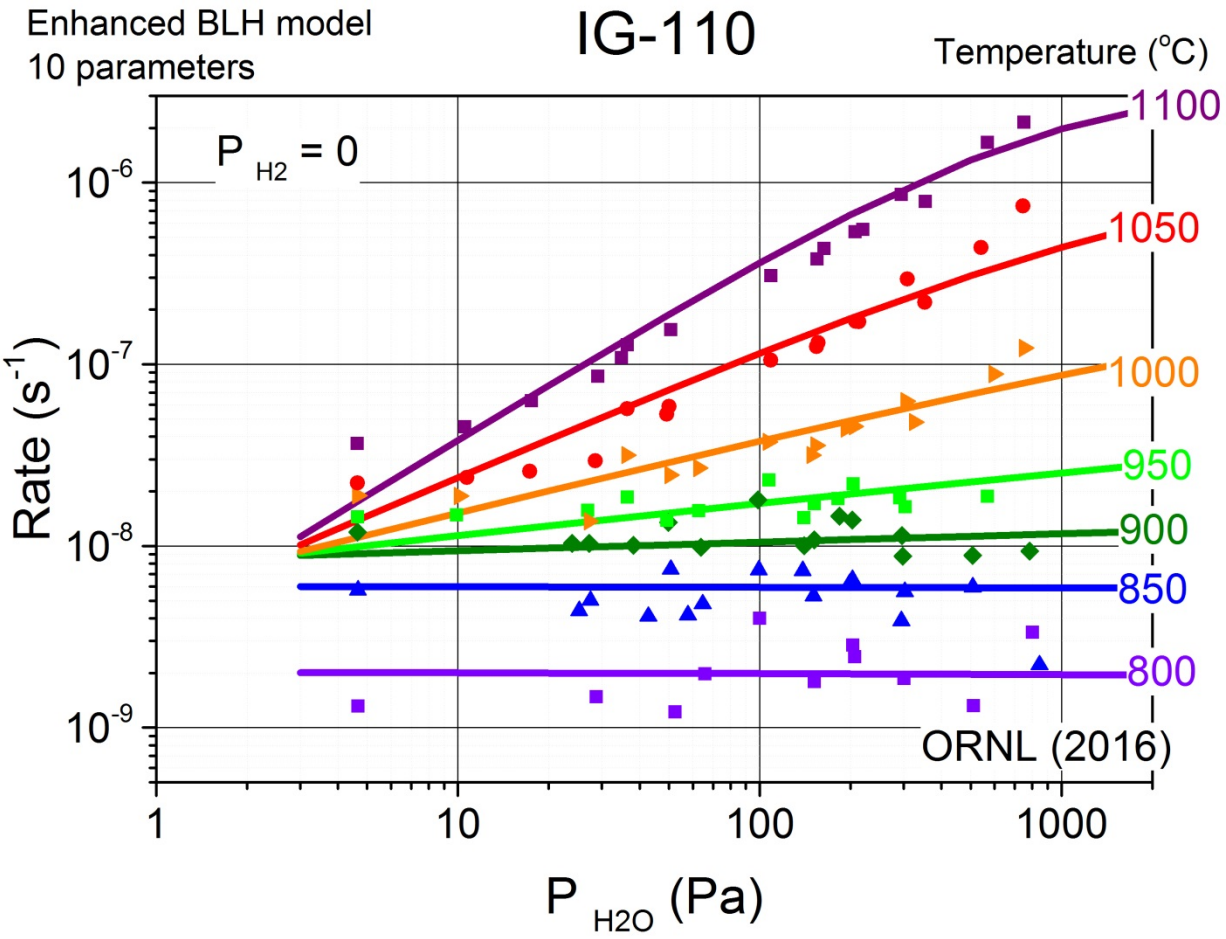

Figure 11: Oxidation rates measured for graphite IG-110 and the trends predicted by the Boltzmann-enhanced LH model (10 parameters). This model fits the data better, including observations at high temperature and high water pressure.

Table 2
Best fit parameters for graphite IG-110 using the Boltzmann-enhanced LH model

$A_1 = 7.64 \times 10^{-12}$ Pa^{-1} s^{-1}	$E_1 = -70.55$ kJ/mol	$m_{max} = 1.5$
$A_2 = 1.88 \times 10^{-2}$ Pa$^{-1/2}$	$E_2 = -39.61$ kJ/mol	$m_{min} = 0$
$A_3 = 6.07 \times 10^{-18}$ Pa^{-1}	$E_3 = -373.52$ kJ/mol	$T_o = 1327$ K
	$n = 0.5$	$\theta = 34.2$ K

Figure 12 compares rate measured versus rate predictions using the Boltzmann-enhanced LH model for this graphite. The linear fit in the log-log coordinates of Fig. 12 is of better quality than the corresponding fit shown in Fig. 10. This demonstrates that the enhanced model that includes site cooperativity and Boltzmann activation is able to more faithfully reproduce the experimental data over more than three ranges.

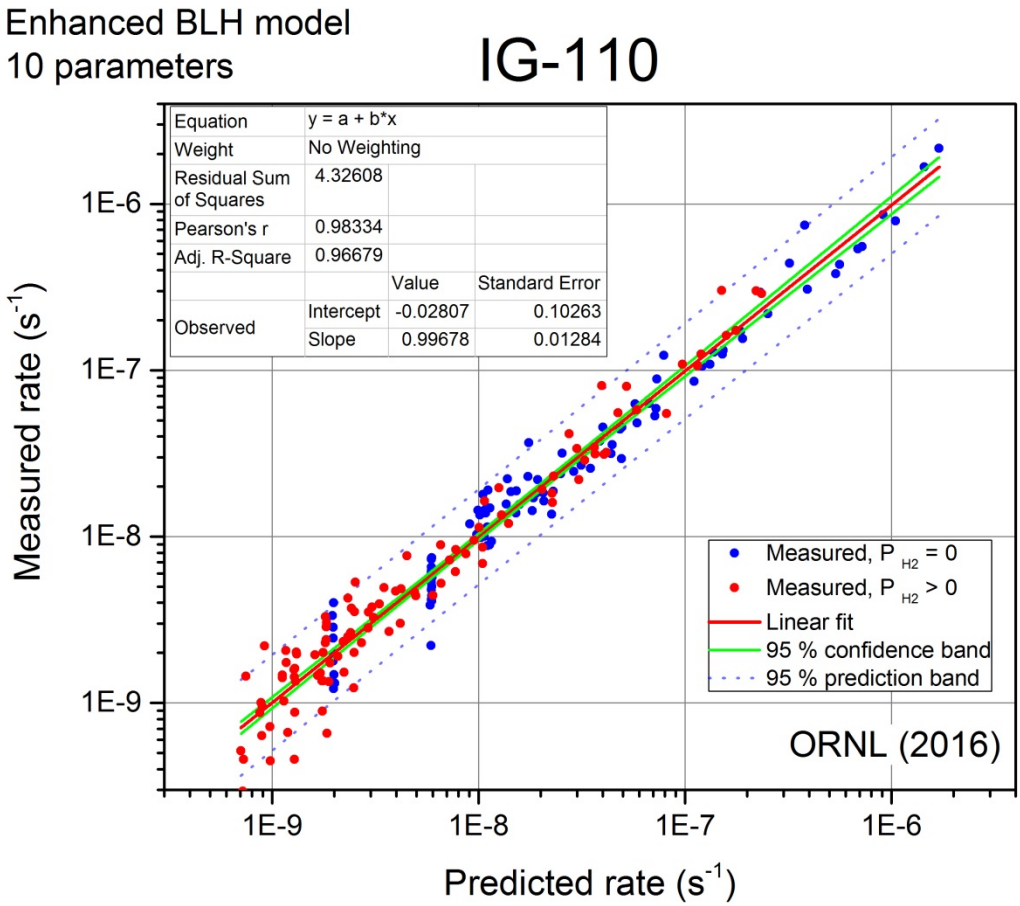

Figure 12: Comparison between rates measured for oxidation of IG-110 graphite and the rates predicted by the Boltzmann-enhanced LH model. Data shown include measurements in H_2O / He and (H_2O + H_2) / He mixtures.

5.2 GRAPHITE NBG-17

In the 2015 report on oxidation by moisture of graphite NBG-17 [13] we acknowledged that the LH model did not fit correctly all experimental data. The valid data lot consisted of 269 data points of which 195 were from measurements in moist He only and 74 were measurements in moist He with added

hydrogen. A number of 34 data points were invalidated because of the reasons explained above. Figure 13 shows the fit of LH model for data collected at $P_{H2} = 0$ and $P_{H2} = 26$ Pa. The same data were refitted using the augmented model with site cooperativity. The fit shown in Fig. 14 is a better model for experimental data.

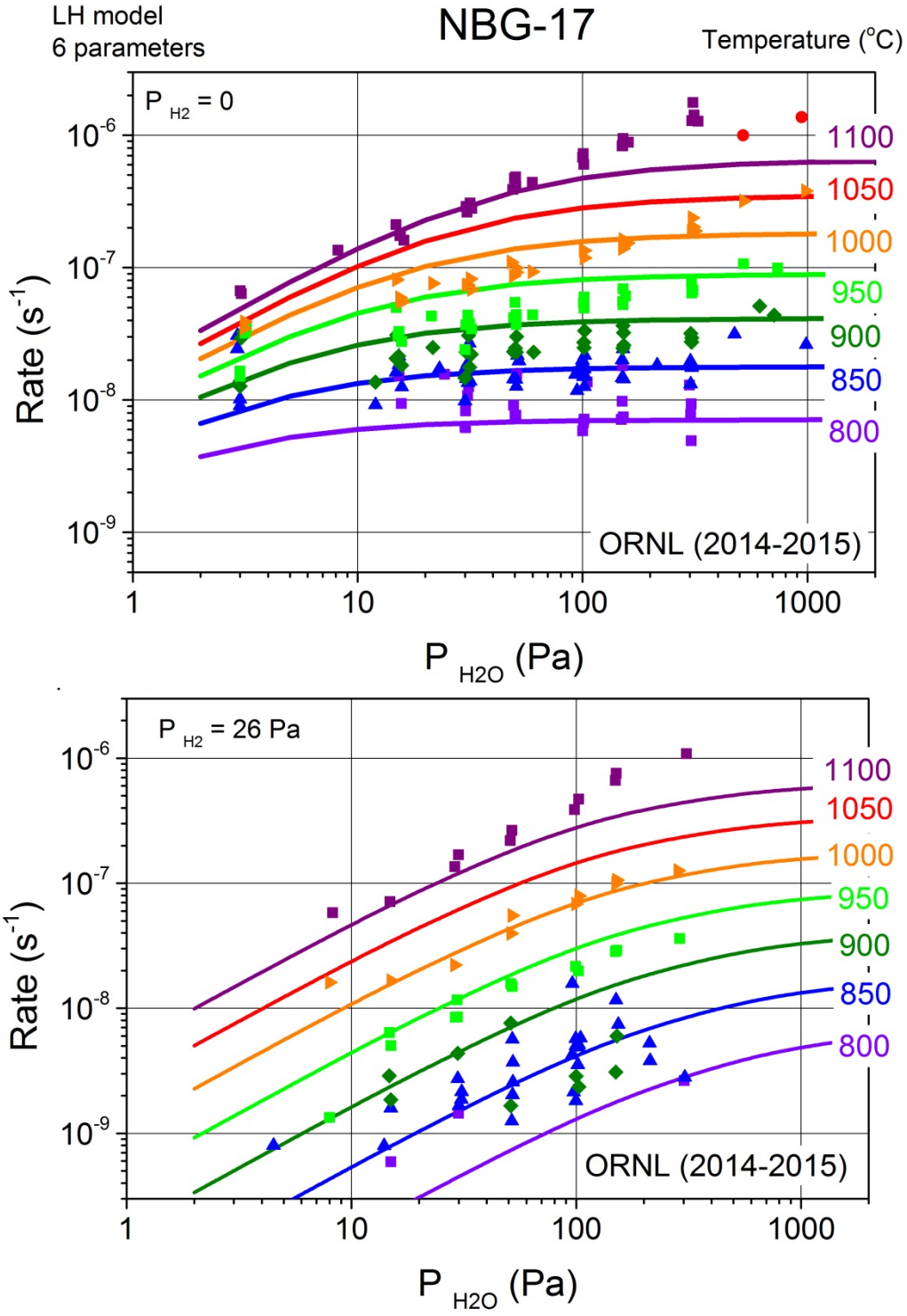

Figure 13: Fit of LH model to oxidation data for graphite NBG-17 at $P_{H2} = 0$ and $P_{H2} = 26$ Pa.

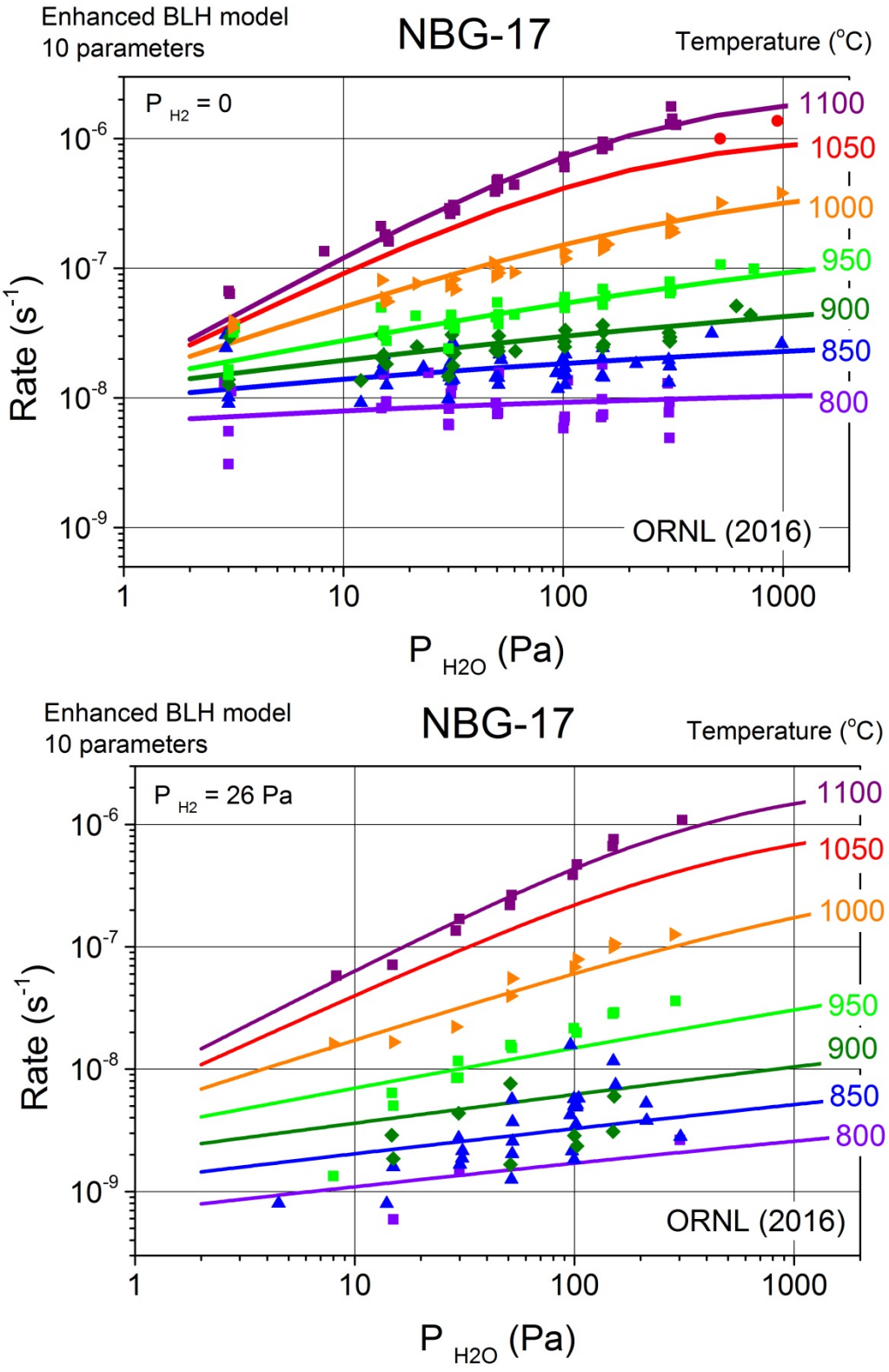

Figure 14: Fit of Boltzmann-enhanced LH model to oxidation data collected for graphite NBG-17 at $P_{H2} = 0$ and $P_{H2} = 26$ Pa.

Figure 15 compares the goodness of fit of the two models. The superiority of the Boltzmann-enhanced LH model is reflected in the lower scatter of the log-log comparison of measured versus predicted results, and the narrower prediction and confidence bands of the plots.

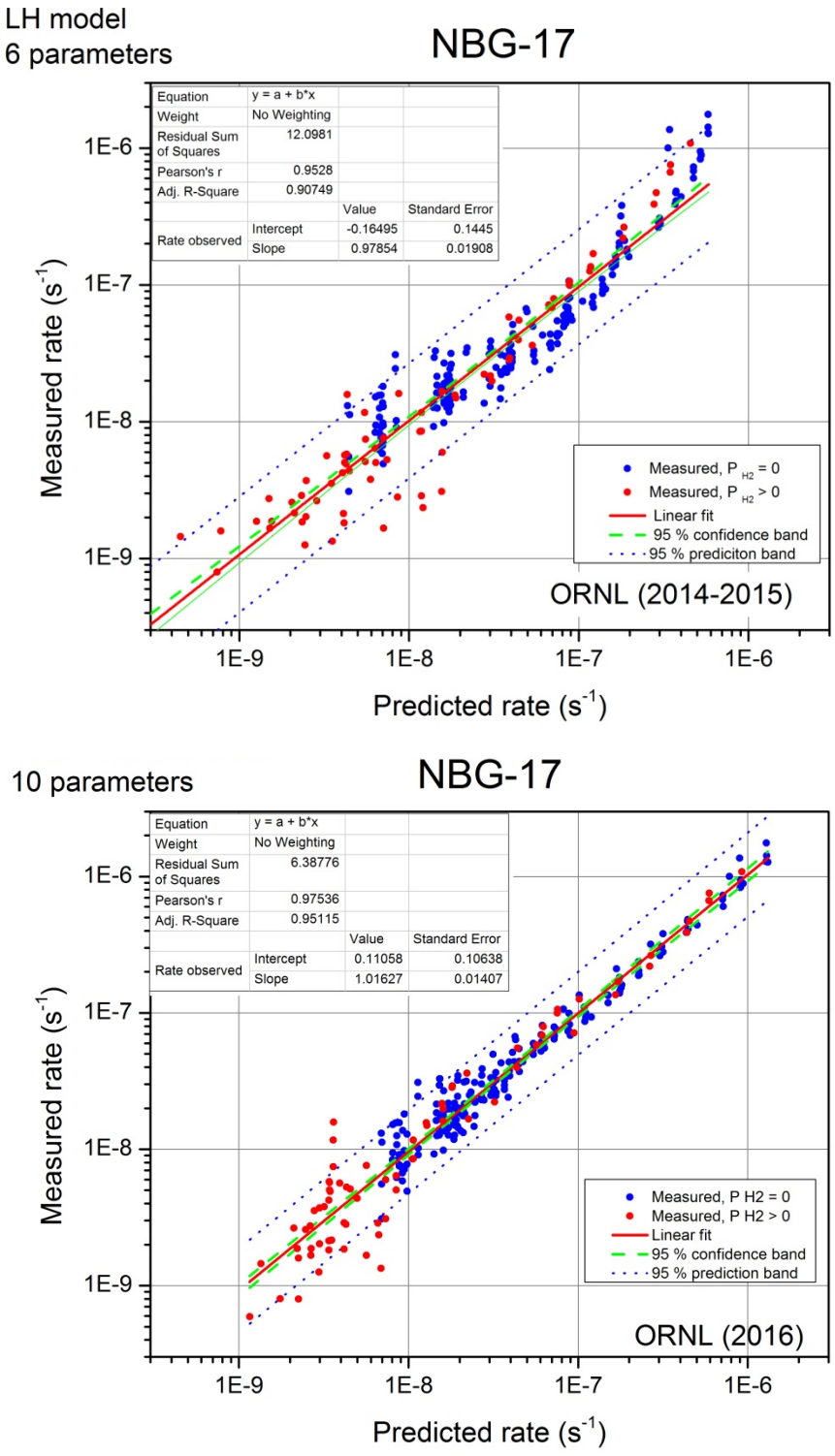

Figure 15: Goodness of fit comparison between the LH model and the Boltzmann-enhanced LH model applied to graphite NBG-17oxidation by moisture.

The parameters used for the LH fit (2014) and Boltzmann-enhanced LH fit (2016) of graphite NBG-17 oxidation data are listed below.

Table 3
Best fit LH parameters for graphite NBG-17 [13]

$A_1 = 3.85 \times 10^{-6}$ Pa^{-1} s^{-1}	$E_1 = 61.464$ kJ/mol	
$A_2 = 4.00 \times 10^{-8}$ Pa^{-1}	$E_2 = -186.561$ kJ/mol	$n = 0.5$
$A_3 = 5.79 \times 10^{-7}$ Pa^{-1}	$E_3 = -122.827$ kJ/mol	

Table 4
Best fit parameters for graphite IG-110 using the Boltzmann-enhanced LH model

$A_1 = 4.3 \times 10^{-8}$ Pa^{-1} s^{-1}	$E_1 = 11.37$ kJ/mol	$m_{max} = 0.93$
$A_2 = 3.9 \times 10^{-6}$ Pa$^{-1/2}$	$E_2 = -121.70$ kJ/mol	$m_{min} = 0.23$
$A_3 = 1.2 \times 10^{-10}$ Pa^{-1}	$E_3 = -203.18$ kJ/mol	$T_o = 1275$ K
	$n = 0.5$	$\theta = 32.5$ K

5.3 GRAPHITE PCEA

From a total to 355 data points, the lot of valid oxidation data for graphite PCEA [12] consisted of 144 data points measured at $P_{H2} = 0$ and 48 data points measured at 30 Pa < P_{H2} < 150 Pa. All physical measurements data and oxidation rate data measured for graphite PCEA are presented in Annex 5 and 6. The parameters used for the LH fit (2013) and Boltzmann-enhanced LH fit (2016) of graphite PCEA oxidation data are listed in Tables 5 and 6.

Table 5
Best fit LH parameters for graphite PCEA [12]

$A_1 = 5.9 \times 10^{-1}$ Pa^{-1} s^{-1}	$E_1 = 198.68$ kJ/mol	
$A_2 = 5.4 \times 10^{9}$ Pa$^{-1/2}$	$E_2 = 279.54$ kJ/mol	$n = 0.5$
$A_3 = 4.0 \times 10^{-4}$ Pa^{-1}	$E_3 = -38.98$ kJ/mol	

Table 6
Best fit parameters for graphite PCEA using the Boltzmann-enhanced LH model

$A_1 = 5.9 \times 10^{-2}$ Pa^{-1} s^{-1}	$E_1 = 161.71$ kJ/mol	$m_{max} = 0.64$
$A_2 = 2.1 \times 10^{5}$ Pa$^{-1/2}$	$E_2 = 166.79$ kJ/mol	$m_{min} = 0.44$
$A_3 = 1.4 \times 10^{-15}$ Pa^{-1}	$E_3 = -292.64$ kJ/mol	$T_o = 1283$ K
	n = 0.5	$\theta = 10.8$ K

Figure 16 shows the LH model fit and the enhanced model fit of oxidation data for graphite PCEA. The LH trend lines change slope as P_{H2O} increases, while the enhanced model predicts constant slope. Figure 17 compares the goodness of fit in LH and augmented model. For this graphite the augmented model did not improve substantially the agreement with the experimental data, but the shape of the fit is quite different.

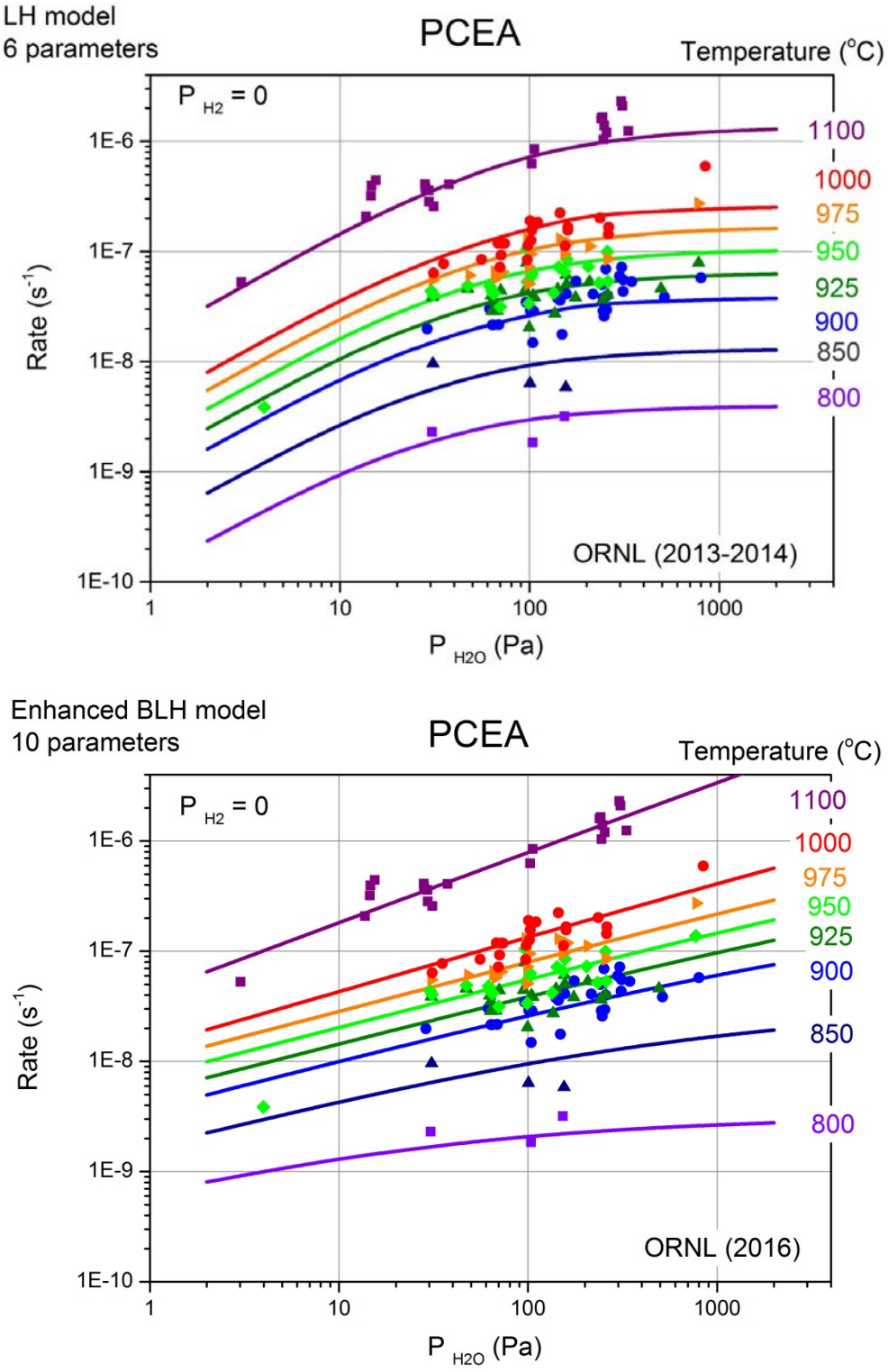

Figure 16: Fit of PCEA oxidation data using the LH model (top panel) and the Boltzmann-enhanced LH model (bottom panel)

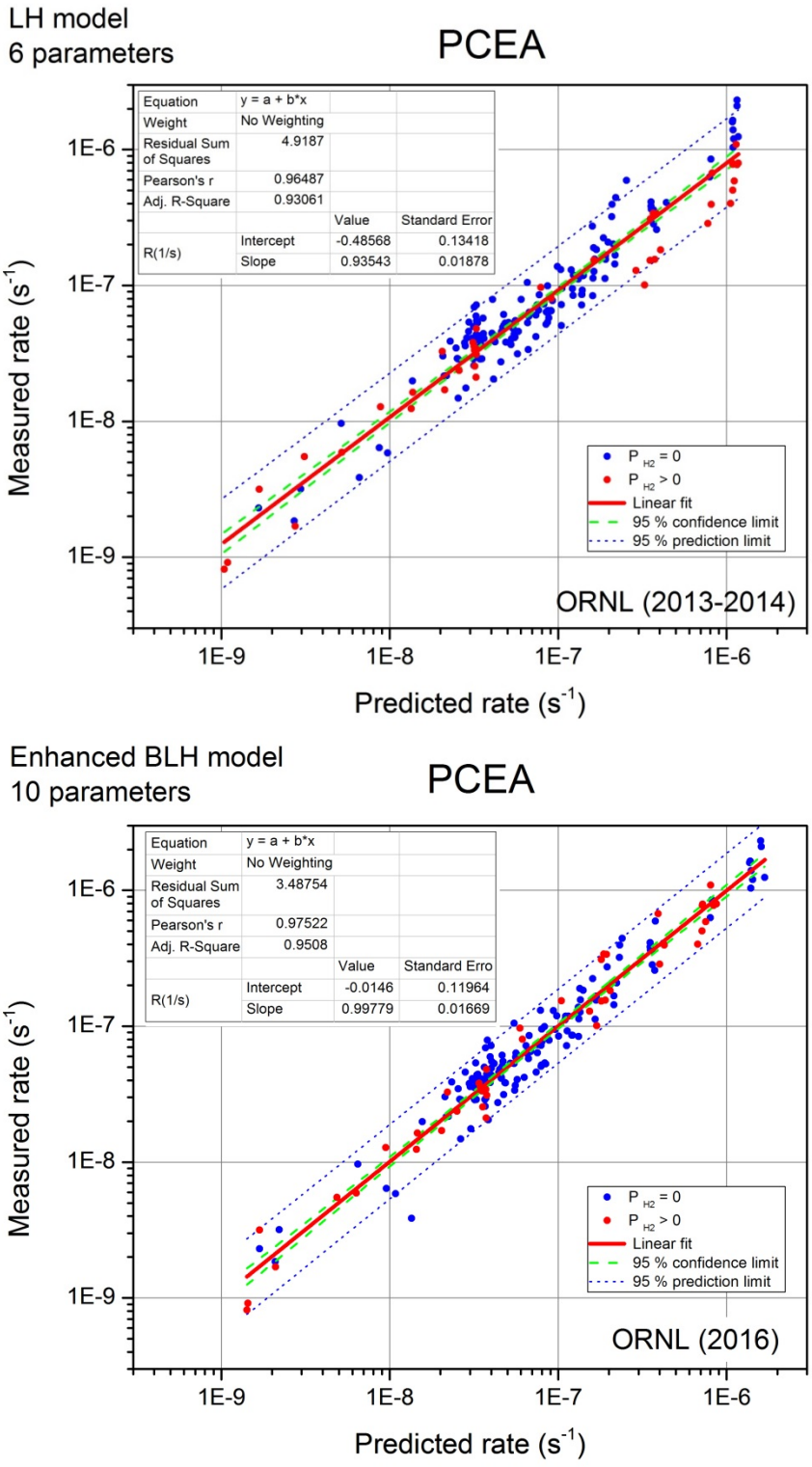

Figure 17: Goodness of fit comparison between LH model and Boltzmann-enhanced LH model applied to graphite PCEA oxidation by moisture

5.4 GRAPHITE H-451

The enhanced model was less successful in fitting the digitized data [7] available for graphite H-451. Figure 18 compares experimental and predicted data by the "low water" LH model and by the Boltzmann-enhanced LH model. The fitting parameters are comparable but the slope of the BLH model line is not close to 1, as it should be for good fitting.

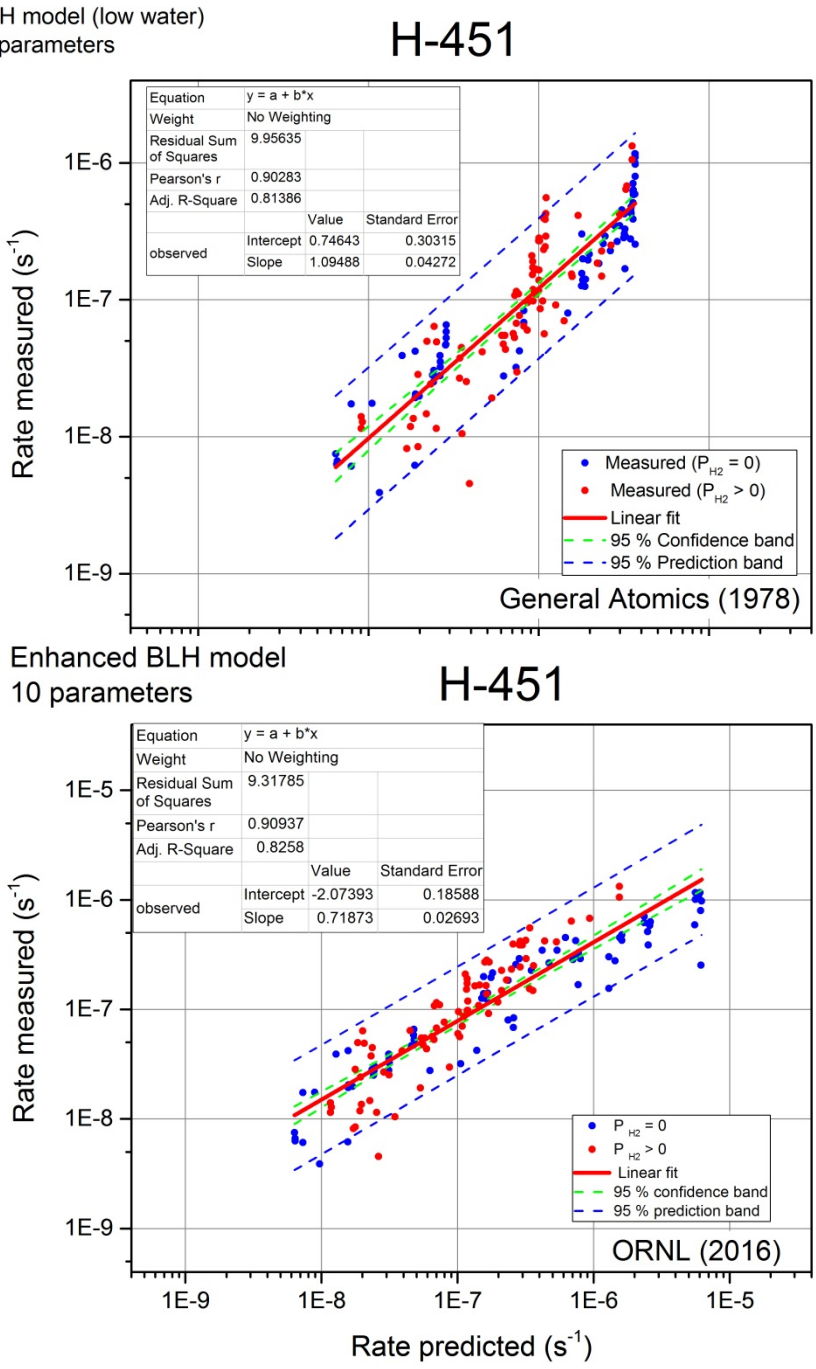

Figure 18: Goodness of fit comparison between LH and Boltzmann-enhanced LH applied to graphite H-451 oxidation by moisture [7]

The parameters used for fitting oxidation of H-451 graphite by the LH model ("low water" [7]) and the Boltzmann-enhanced LH model are shown in Tables 7 and 8.

Table 7

Best fit LH parameters for graphite H-451 ("low water" variant [7])

$A_1 = 2.0 \times 10^3$ Pa^{-1} s^{-1}	$E_1 =$ 274.00 kJ/mol	
$A_2 = 1.1 \times 10^2$ Pa$^{-1/2}$	$E_2 =$ 74.66 kJ/mol	$n = 0.75$
$A_3 = 2.0 \times 10^2$ Pa^{-1}	$E_3 =$ 95.85 kJ/mol	

Table 8

Best fit parameters for graphite H-451 using the Boltzmann-enhanced LH model

$A_1 = 6.6 \times 10^{-4}$ Pa^{-1} s^{-1}	$E_1 =$ 121.42 kJ/mol	$m_{max} = 1$
$A_2 = 9.2 \times 10^6$ Pa$^{-1/2}$	$E_2 =$ 180.359 kJ/mol	$m_{min} = 0.44$
$A_3 = 22.7$ Pa^{-1}	$E_3 =$ 84.38 kJ/mol	$T_o = 1194$ K
	$n = 0.5$	$\theta = 51.8$ K

5.5 COMPARISON OF THE TWO MODELS

Table 9 compares the residual sum of squares (RSS), Pearson's ρ parameter and the adjusted R-square parameter of observed and predicted rate plots, for each graphite grade and the two kinetic models available, the classical LH and the enhanced BLH model. All parameters are collected from the log-log plots shown in Figures 10 and 12 (for IG-110), 15 (for NBG-17), 17 (for PCEA) and 18 (for H-451).

Table 9

Comparison of scattered regression plots between observed and model-predicted rates

	IG-110		NBG-17		PCEA		H-451	
	LH	B LH	LH	B LH	LH	B LH	LH	B LH
Residual sum of squares	22.11	4.32	12.09	6.38	4.92	3.49	9.956	9.317
Pearson's ρ	0.911	0.983	0.953	0.975	0.965	0.975	0.903	0.909
Adjusted R-square	0.83	0.967	0.907	0.951	0.931	0.951	0.814	0.826

For each grade, the RSS corresponding to the BLH model is always smaller than that of the LH model. A small RSS indicates a tight fit of the model to the data. The Pearson's correlation parameter ρ and the adjusted R^2 correlation coefficient of linear regressions in the double logarithmic scale reflect a measure of correlation between observed and predicted oxidation rates. Most values are higher than 0.95 for the new graphite grades, showing good correlation (with the singular exception of LH model applied to graphite IG-110). Again, the BLH model shows systematically better correlations for each grade of graphite, although the improvement is not equal for all grades. The correlation is weaker, however, for graphite H-451 based on the digitized values from the 1978 report [7].

6. DISCUSSION

The results presented above indicate that the Boltzmann-enhanced LH model is able to better reproduce the experimental oxidation rates by moisture measured for several grades of nuclear graphite. Noticeably, the Boltzmann-enhanced LH model fits the deviations from the LH model, observed in general at high temperatures and high P_{H2O}, where measured rates are faster than what the classical LH model predicts.

The improvement is due to the recognition of the fact that active sites on graphite surface are not identical, not isolated, and their number is not constant. These principles are at the basis of classical Langmuir- and Langmuir – Hinshelwood models that have numerous applications in gas adsorption and heterogeneous catalysis. However, these models do not correctly represent the complex surface of graphite (or carbon) materials. The reactive surface sites on graphite are located mostly at the edge atoms of graphene sheets, or (in a lesser extent) at defects and dislocations on basal planes. The edge sites are not equivalent: zig-zag sites have high density of single electron states, and therefore high reactivity, while such states are absent in armchair sites. Figure 19 shows atomic resolution scanning tunneling microscopy (STM) images of nanoholes in graphene structures [59] and illustrate these differences. The brighter spots represent zig-zag sites with localized π state electrons that enhance tunneling in STM. The less luminous spots correspond to armchair sites, with no such states.

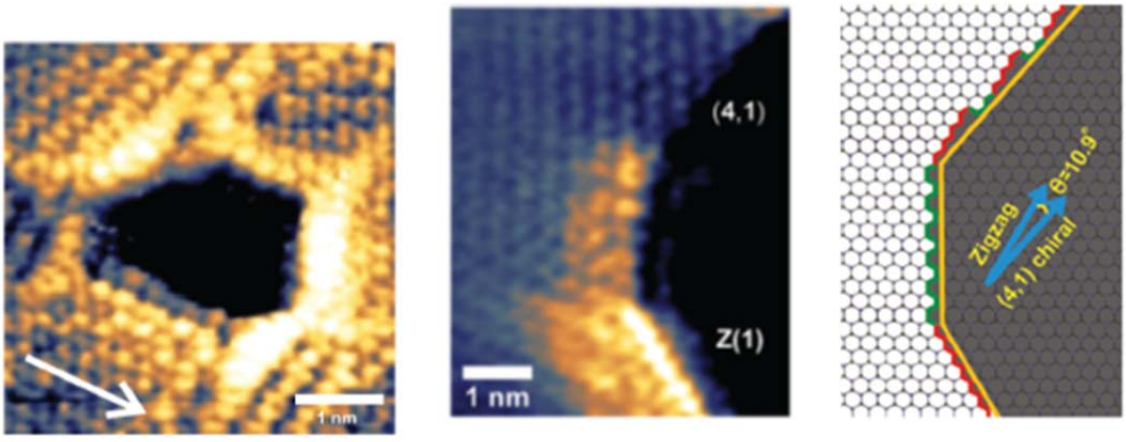

Figure 19: Visualization of electronic states localized at edge carbon atoms of graphene with different number of hydrogen atoms. Zig-zag atoms have local density of states if no H atoms are attached (left and center panel) or no localized states if H atoms are attached (center panel). Armchair atoms do not have local density of states (left panel) but partial bonding of H atoms enhances the local density of states at the boundary (center panel). The nanohole (left panel) has mostly zig-zag edges stabilized by spontaneous reconstruction [59].

Adding to the structural variety of atomic positions in graphene, and to defect creation and annihilation through physical actions (temperature, neutron irradiation), the delocalized π electrons link neighboring carbon atoms and mediate interactions between distant sites. Figure 19 shows very vividly how chemical changes occurring at some edge carbon sites propagate and modify the density of states of other, quite distant carbon sites. Bonding of H atoms on zig-zag edges extinguishes the localized states on that edge, while partial hydrogenation of armchair sites enhances the density of states. The inductive effect of functional groups in aromatic compounds, which is well known in organic chemistry, cannot be neglected in graphite chemistry.

Computational chemistry results cited above [52] support the proposal that water chemisorbs dissociatively on graphite edges, and chemisorbed states stabilize through rearrangement and migration of hydrogen atoms. The surface complexes formed by water chemisorption have a multitude of transformation routes, most of them being endothermic, which means they are favored by temperature. The multitude of surface complex transformations, beginning with water chemisorption and ending with elimination of H_2 and CO, and the fact that they do not occur in isolation, justifies the using of the cooperativity concept. It is known that temperature has an important role in reconstruction of carbon skeleton, even in the absence of chemical changes. When chemical changes are triggered by temperature (desorption of less stable surface complexes), temperature becomes an important factor that controls the number and reactivity of active surface sites, and therefore the global stoichiometry of gasification processes. The Boltzmann-enhanced LH model incorporates the effect of temperature through the variable stoichiometric coefficient *m(T)* which is modeled by a Gauss distribution function. In this way, the temperature control of graphite gasification rate occurs via two independent mechanisms: on one hand, water molecule impinging the surface must have energy above a certain threshold (the activation energy) in order to successfully initiate a chemical reaction. The higher the temperature, the more "activated" molecules will collide on the surface. On the other hand, the configuration of surface sites and their reactivity change with temperature. Desorption of stable complexes will leave vacant sites as the temperature increases. Higher density of vacant sites will cause faster turnover at constant pressure, and will also increase the electronic interactions between sites. This second mechanism of reactivity (and stoichiometry) controlled by temperature is introduced in the enhanced model by the Boltzmann distribution function. It shows the "activation" of surface sites on the increase of temperature. Formally, *m(T)* is also an apparent reaction order for the global oxidation reaction. The microstructure differences between graphite grades (and the associated diversity of local structures at the nanoscale) determine various shapes of the *m(T)* function, as shown by the slope variation of ln *(Rate)* versus ln (P_{H2O}) curves.

The Boltzmann-enhanced LH model proposed here offers a robust, comprehensive mathematical equation that fits kinetic data collected over large variations of experimental conditions (temperature, gas composition). The classic LH model may still fit data over narrower ranges of conditions. Moreover, the structural properties of each graphite grade determine that the Boltzmann-enhanced LH model is not equally successful for all grades. The IG-110 data could not be fitted without the enhanced model. This is a fine grade graphite (about 20-40 μm grain size) with a higher than average BET surface area and one single class of fine pores (about 0.01 μm diameter). The other two grades have larger grain sizes (0.8 mm), smaller BET surface areas and bimodal pore size distribution (larger pores of about 20 μm diameter and narrower pores of about 0.02 μm diameter) [60]. At this time we can only speculate that differences in oxidation kinetics by water reflect the degree of surface sites exposure in microstructure.

Being a better tool for modeling graphite oxidation kinetics, the Boltzmann-enhanced LH is in no way able to provide information on the mechanism of elementary steps. In fact, kinetics models are not regarded as sources of reaction mechanisms; on the contrary, they are rather used to validate mechanisms postulated independently, on different foundations. The parameters returned by fitting should not be compared using kinetic notions that are popular for reactions in gas phase. They are just fitting parameters and represent "apparent" (i.e. model-dependent) constants. For that reason, the occurrence of non-positive terms under the exponential sign is not paradoxical. As we have seen, even early applications of LH model for graphite oxidation by moisture contain examples of negative "activation energies". Moreover, reactions with negative activation energies are not impossible and do occur even though the elementary steps that compose the global process have non-negative activation energies [61].

7 . SUMMARY AND CONCLUSION

Graphite will undergo extremely slow, but continuous, oxidation by traces of moisture that will be present, albeit at very low levels, in the helium coolant of HTGR. This chronic oxidation may cause degradation of mechanical strength and thermal properties of graphite components, if a porous oxidation layer develops on the surface and then penetrates deeper in the bulk of graphite components during the lifetime of the reactor. The current research on graphite chronic oxidation is motivated by the acute need to understand the behavior of each graphite grade during prolonged exposure to high temperature chemical attack by moisture. The goal is to provide the elements needed to develop predictive models for long-time oxidation behavior of graphite components in the cooling helium of HTGR.

The tasks derived from this goal are structured on three directions:

(1) Oxidation rate measurements in conditions of kinetic control in order to determine and validate a comprehensive model suitable for prediction of intrinsic oxidation rates as a function of temperature and oxidant gas composition;
(2) Characterization of effective diffusivity of water vapor in the graphite pore system in order to account for the in-pore transport of moisture through the particular graphite microstructure;
(3) Development and validation of a predictive model for the penetration depth of the oxidized layer, in order to assess the risk of oxidation caused damage of particular graphite grades after prolonged exposure to the environment of helium coolant in HTGR.

The most important – and most time consuming – of these tasks is the measurement of oxidation rates in accelerated oxidation tests (but still under kinetic control) and the development of a reliable kinetic model. Because of that, this report is focused on the progress of kinetic measurements, validation of results, and improvement of the available models. Analysis of current and past results obtained with three grades of graphite showed that the classical Langmuir-Hinshelwood model cannot reproduce all data with a unique set of parameters. Starting from here, we propose a modification of the LH model that includes temperature activation of surface sites, modeled as a Boltzmann activation function. The enhanced Boltzmann-Langmuir-Hinshelwood model (BLH) was tested successfully on three grades of graphite. The model is a robust, comprehensive mathematical function that allows better fitting of experimental results collected over a wide range of temperature and partial pressures of water vapor and hydrogen. We found that the new model did improve the accuracy of data fitting for all three grades of graphite, although at different rates. The BLH model was essential for fitting oxidation of IG-110 graphite, but could not be used with the data for graphite H-451 extracted from the GA report [7].

Current activities still need to analyze the oxidized layer profile in graphite NBG-17, for which kinetic and water diffusivity results are now available. Combining kinetic and transport results will allow us to confirm (or not) the viability of the predictive model for the maximum penetration of the oxidation and its temperature dependence, which is an important goal of this research. At this time we have only checked the validity of the model and obtained confirmation only for PCEA graphite [18]. This task will be completed during FY 2016.

In the near future we plan to complete effective diffusivity measurements for graphite IG-110 and to prepare oxidized samples at 5-6 % weight loss for oxidized layer profile characterization. Combining kinetic results on IG-110 (now available) with effective diffusivity and oxidized layer profile will provide one more verification point of the predictive model.

We also plan to use the thermogravimetric equipment and the mass spectrometer available at ORNL for measurements of the desorption energy distribution function, $f(E_{des})$, of surface complexes formed by water on several grades of graphite (IG-110, NBG-17, PCEA). Then we will try to use this information in a variant of the stochastic oxidation model proposed by other researchers [43,44] for modeling of graphite gasification by air.

The long term plan is to extend these studies to graphite grades 2114 and 2160 produced by Mersen.

This page was intentionally left blank

REFERENCES

1. M P Kissane, A review of radionuclide behavior in the primary system of a very-high temperature reactor, *Nucl. Eng. Design,* **239** (2009) 3076−3091.
2. X Yu, S Yu, Analysis of fuel element matrix graphite corrosion in HTR-PM for normal operating conditions, *Nucl. Eng. Design,* **240** (2010) 738−743.
3. E R Corwin, Generation IV Reactors Integrated Materials Technology Program Plan: Focus on Very High Temperature Reactor Materials, ORNL/TM-2008/129 (2008).
4. M Fechter, Graphite Oxidation Modeling for a 250 MW Pebble Bed Reactor, ORNL presentation, July 2010.
5. B Castle, NGNP Reactor Coolant Chemistry Control Study, INL/EXT-10-10533.
6. R N Wright, Kinetics of Gas Reactions and Environmental Degradation in NGNP Helium, INL/EXT-06-11494.
7. C Velasquez, G Hightower, R Burnette, The Oxidation of H-451 Graphite by Steam. Part 1: Reaction Kinetics, General Atomic Company, GA-A14951 (1978).
8. M B Richards, Reaction of nuclear grade graphite with low concentrations of steam in the helium coolant of an MHTGR, *Energy* **15** (1990) 729-739
9. C. I. Contescu, T. Guldan, P. Wang, T. D. Burchell, The effect of microstructure on air oxidation resistance of nuclear graphite, *Carbon* **50** (2012) 3354-3366.
10. C I Contescu, Microstructure effect on air oxidation behavior of three nuclear grade materials: NBG-18, PCEA, and IG-110, ORNL/TM-2011/324 (2011)
11. C. I. Contescu, T. D. Burchell, R. W. Mee, Accelerated oxidation studies of PCEA nuclear graphite by low concentrations of water and hydrogen in helium, ORNL/TM-2013/524 (2013).
12. C.I. Contescu, R.W. Mee, P. Wang, A.V. Romanova, T.D. Burchell, oxidation of PCEA nuclear graphite by low water concentrations in helium, *J. Nucl. Mater*. **453** (2014) 225-232
13. C.I. Contescu, T.D. Burchell, R.W. Mee, Kinetics of chronic oxidation of NBG-17 nuclear graphite by water vapor, ORNL/TM-2015/142 (2015).
14. C.I. Contescu, T.D. Burchell, Water vapor transport in nuclear graphite, ORNL/TM-2015/88 (2015).
15. D Miller, I Lewis, M Santana, Isotropic graphite from needle coke, http://acs.omnibooksonline.com/data/papers/2004_K003.pdf (accessed January 5, 2015)
16. P Beghein, G Berlioux, B du Mesnildot, F Hiltmannm M Melin, NBG-17 – An improved graphite grade for HTRs and VHTRs, *Nucl. Eng. Des*. **251** (2012) 146-149
17. "Standard test method for water vapor diffusion resistance and air flow resistance of clothing materials using the dynamic moisture permeation cell", ASTM F2298-03 (reapproved 2009).
18. C. Contescu, J. Kane, R. Mee, A, Bontorno, N. Gallego, T. Burchell, W. Windes, Reactivity differences between graphite grades during long time exposure in the helium coolant, INGSM-16, International Nuclear Graphite Specialists Meeting, Nottingham, UK, September 13-17, 2015.
19. J Gadsby, C N Hinshelwood, K W Sykes, Kinetics of the reactions of steam-carbon system, *Proc Roy Soc (London) A* **187** (1946) 129-151.
20. R C Giberson, J P Walker, Reaction of nuclear graphite with water vapor. Part I: Effect of hydrogen and water vapor partial pressure, *Carbon* **3** (1966) 521-525
21. F J Long, K W Sykes, The mechanism of steam-carbon reaction, *Proc. Roy Soc. (London) A* **193** (1948) 377-399

22. J Gadsby, F J Long, P Sleightholmm K W Sykes, The mechanism of the carbon dioxide – carbon reaction, *Proc Roy Soc (London) A* **193** (1948) 357-376
23. Graphite Design Handbook, General Atomics Company, DOE-HTGR-88111/Rev 0 (September 1988)
24. H F Johnstone, C Y Chen, D S Scott, Kinetics of the steam-carbon reaction in porous graphite tubes, *Ind. Eng. Chem.* **44** (1952) 1564-
25. J D Blackwood, F McGrory, The carbon-steam reaction at high pressure, *Australian J Chem* **11** (1958) 16-33
26. J E Antill, K A Peakall, Attack of graphite by an oxidizing gas at low partial pressures and high temperatures, *J. Nucl Mater* **2** (1960) 31-38
27. K Huttinger, Mechanism of water vapor gasification at high hydrogen levels, *Carbon* **26** (1988) 79-87
28. R T Yang, K L Yang, Kinetics and mechanism of the carbon-steam reaction on the monolayer and multilayer edges of graphite, *Carbon* **23** (1985) 537-547
29. L G Overholser, J P Blakely, Oxidation of graphite by low concentration of water vapor and crabon dioxide in helium, *Carbon* **2** (1965) 385-394
30. J P Blakely, L GL Overholser, Oxidation of ATJ graphite by low concentrations of water vapor and carbon dioxide in helium, *Carbon* **3** (1965) 269-275
31. J S Binford, H Eyring, Kinetics of the steam-carbon reaction, *J Phys Chem* **60** (1956) 486-491
32. R F Strickland-Constable, The interaction of carbon filaments at high temperatures with nitrous oxide, carbon dioxide and water vapor, *Trans. Faraday Soc*. **43** (1947) 769-778
33. P Magne, RF Sauvageot, X Duval, Etude de la formation d'un complexe de surface graphie-eau relation avec la reaction d'oxydation, *Carbon* **11** (1973) 485-495
34. R F Strickland-Constable, Interaction of steam and charcoal at low pressures, *Proc. Roy Soc (London) A* **189** (1947) 1-10
35. G Blyholder, H Eyring, Kinetics of the steam-carbon reaction, *J Phys Chem* **63** (1959) 693-696
36. D R Olander, T R Acharaya, A Z Ullman, Reactions of modulated molecular beams with pyrolytic graphite. IV Water vapor, *J Chem Phys* **67** (1977) 3549-3562
37. K Miura, T Morimoto, Adsorption sites for water on graphite: 4. Chemisorption of water on graphite at room temperature, *Langmuir* **4** (1988) 1283-1288
38. M G Lussier, Z Zhang, D J Miller, Characterizing rate inhibition in steam/hydrogen gasification via analysis of adsorbed hydrogen, *Carbon* **36** (1998) 1361-1369
39. B S Haynes, A turnover model for carbon reactivity. I. Development, *Combust. Flame*, **126** (2001) 1421-1432
40. A E Lear, T C Brown, B S Haynes, Formation of metastable oxide complexes during the oxidation of carbons at low temperatures, 33rd Symposium (International) on Combustion. *The Combustion Institute* (1990) 1191-1197
41. A Sibbra, T G. Newbury, B S Haynes, The reactions of hydrogen and carbon monoxide with surface-bound oxides on carbon, *Combust. Flame* **120** (2000) 515-525
42. B S Haynes, T G Newbury, Oxyreactivity of carbon surface oxides, *Proc. Combust. Inst.* **28** (2000) 2197-2203
43. R H Hurt, J M Calo, Semi-global intrinsic kinetics for char combustion modeling, *Combust. Flame* **125** (2001) 1138-1149
44. R H Hurt, B S Haynes, On the origin of power-law kinetics in carbon oxidation, *Proc. Combust.*

Inst. **30** (2005) 2161-2168
45. M S El-Genk, J-M Tournier, Development and validation of a model for the chemical kinetics of graphite oxidation, *J. Nucl. Mat*. **411** (2011) 193-207
46. B Marchon, J Carrazza, H Heinemann, G A Somorjai, TPD and XPS studies of)$_2$, CO_2, and H_2O adsorption on clean polycrystalline graphite, *Carbon* **26** (1988) 507-514
47. V J Garcia, J M Briceno-Valero, L Martinez, Kinetic parameters from a single thermal desorption spectrum, *Surf Sci* **339** (1995) 189-193
48. M Battacharya, W G Devi, P S Mazumdar, Determination of kinetic parameters from temperature programmed desorption curves, *Appl Surf Sci* **218** (2003) 1-6
49. M C Ma, B S Haynes, Surface heterogeneity in the formation and decomposition of carbon surface oxides. *26th Symposium (International) on Combustion / The Combustion Institute* (1996) 3119-3125
50. A Allouche, Y Ferro, Dissociative adsorption of small molecules at vacancies on the graphite (0001) surface, *Carbon* **44** (2006) 3320-3327
51. P Cabrera-Sanfelix, G B Darling, Dissociative adsorption of water at vacancy defects in graphite, *J. Phys Chem C* **111** (2007) 18258-18263
52. J F Espinal, F Mondragon, T N Truong, Thermodynamic evaluation of steam gasification mechanisms of carbonaceous materials, *Carbon* **47** (2009) 3010-3018
53. E Agliari, A Barra, R Burioni, A Di Biasio, G. Uguzzoni, Collective behaviours: from biochemical kinetics to electronic circuits, *Sci. Rep*. **3** (2013) 3458; doi:10.1038/srep0.458
54. A Di Biasio, E Agliari, A Barra, R Burioni, Mean-field cooperativity in chemical kinetics, *Theor. Chem. Acc.* **131** (2012) 1104; doi: 10.1007/s00214-012-1104-3
55. http://sys-bio.org/wp-content/uploads/downloads/2012/03/CB_Chapter3.pdf (accessed April 26, 2016)
56. C A Querini, S C Fung, Coke characterization by temperature-programmed techniques, *Catal. Today* **37** (1997) 277-283
57. C Li, T C Brown, Carbon oxidation kinetics from evolved carbon oxide analysis during temperature-programmed oxidation, *Carbon* **39** (2001) 725-732
58. I J Myung, Tutorial on maximum likelihood estimation, *J. Math Psychology* **47** (2003) 90-100
59. M Ziatdinov, S Fuji, K Kusabe, M Kiguchi, T Mori, T Enoki, Visualization of electronic states on atomically smooth graphitic edhs with different types of hydrogen termination, *Phys Rev B* **87** (2013) 115427
60. T Burchell, S Nunn, J Strizak, M Williams, AGC-1 sister specimen testing data report, ORNL/TM-2009/025
61. L E Revell, B E Williamson, Why are some reactions slower at higher temperatures *?, J Chem Educ* **90** (2013) 1024-1027

ANNEXES

PHYSICAL MEASUREMENTS AND TEST CONDITIONS

ANNEX 1 PHYSICAL MEASUREMENTS ON GRAPHITE IG-110 SPECIMENS BEFORE AND AFTER TESTS

		Before test				Test Conditions		After test				
Test Date	Specimen ID	Weight mg	Average L mm	Average D mm	Density g/cm3	P H2O Pa	P H2 Pa	Weight mg	Average L mm	Average D mm	Density g/cm3	Method
3/2/2015	IG-1	464.71	20.02	4.00	1.849	100; 50	0	456.37	20.01	3.99	1.822	1
3/10/2015	IG-2	462.88	19.92	4.10	1.765	100; 51	0	459.61	19.90	4.08	1.769	1
3/11/2015	IG-3	452.82	20.09	4.03	1.772	100; 52	0	445.21	20.07	4.02	1.752	1
3/18/2015	IG-4	453.25	20.00	4.05	1.764	300, air	0	445.71	19.98	4.04	1.744	1
3/27/2015	IG-5	456.12	20.07	4.04	1.778	300 (bad)	0	448.59	20.06	4.02	1.762	1
3/31/2015	IG-6	461.91	20.05	4.06	1.783	300 (bad)	0	454.45	20.05	4.07	1.746	1
4/8/2015	IG-7	463.58	19.95	4.08	1.778	30	0	462.45	19.92	4.07	1.782	1
4/13/2015	IG-8	451.83	20.04	4.03	1.765	50	0	450.3	20.05	4.03	1.766	1
4/19/2015	IG-9	458.7	19.96	4.06	1.776	100	0	455.91	19.95	4.06	1.763	1
4/28/2015	IG-10	467.94	20.06	4.08	1.786	200	0	463.56	20.05	4.09	1.760	1
4/30/2015	IG-11	452.27	20.01	4.03	1.773	25	0	451.42	19.99	4.02	1.782	1
5/4/2015	IG-12	449.18	20.03	4.02	1.771	5	0	448.33	20.04	4.02	1.762	1
5/7/2015	IG-13	450.92	20.16	4.02	1.767	50; 30	0	449.32	20.17	4.01	1.764	1
5/13/2015	IG-14	458.71	20.12	4.05	1.770	300	0	452.97	20.12	4.04	1.760	1
5/27/2015	IG-15	453.86	20.18	4.02	1.776	50	0	452.53	20.17	4.02	1.767	1
5/29/2015	IG-16	458.61	19.98	4.06	1.771	150	0	455.53	19.98	4.07	1.758	1
6/2/2015	IG-17	454.02	20.25	4.02	1.766	200	0	449.82	20.26	4.02	1.755	1
6/8/2015	IG-18	453.84	20.09	4.02	1.782	200	20	451.47	20.09	4.02	1.773	1
6/10/2015	IG-19	457.44	20.16	4.03	1.779	100	20	456.37	20.16	4.03	1.777	1
6/12/2015	IG-20	447.79	20.09	4.02	1.756	50	20	447.1	20.08	4.02	1.758	1
6/13/2015	IG-21	459.88	20.12	4.06	1.770	25	20	459.38	20.12	4.05	1.771	1
6/15/2015	IG-22	462.15	20.08	4.07	1.774	100	50	461.55	20.07	4.07	1.771	1
6/19/2015	IG-23	452.72	20.14	4.03	1.764	50	50	452.2	20.16	4.03	1.762	1
6/30/2015	IG-24	461.93	19.93	4.09	1.763	150	50	460.7	19.92	4.09	1.764	1
7/2/2015	IG-25	450.75	20.09	4.02	1.771	200	50	449.55	20.09	4.01	1.772	1
7/8/2015	IG-26	452.81	20.14	4.02	1.776	300	50	450.79	20.14	4.02	1.768	1
7/27/2015	IG-27	451.25	20.11	4.02	1.769	300	100	450.06	20.11	4.03	1.758	1
8/13/2015	IG-28	449.77	20.07	4.00	1.781	100	100	449.21	20.08	4.02	1.767	1

		Before test				Test Conditions		After test				
Test Date	Specimen ID	Weight mg	Average L mm	Average D mm	Density g/cm3	P H2O Pa	P H2 Pa	Weight mg	Average L mm	Average D mm	Density g/cm3	Method
8/18/2015	IG-29	453.23	20.08	4.02	1.777	increasing	0	452.47	20.08	4.03	1.768	2
8/24/2015	IG-30	452.98	20.21	4.02	1.771	increasing	0	451.17	20.21	4.00	1.777	2
8/31/2015	IG-31	457.81	19.89	4.08	1.764	decreasing	0	455.85	19.89	4.07	1.764	2
9/4/2015	IG-32	452.47	20.21	4.01	1.777	increasing	0	450.03	20.21	4.00	1.770	2
9/28/2015	IG-33	455.39	20.14	4.02	1.782	decreasing	0	454.44	20.14	4.02	1.781	2
10/2/2015	IG-34	455.79	20.12	4.03	1.776	decreasing	0	452.97	20.11	4.02	1.773	2
10/8/2015	IG-35	455.15	20.16	4.03	1.775	random	0	450.46	20.15	4.02	1.764	2
11/2/2015	IG-36	450.82	20.06	4.03	1.765	random	0	443.82	20.06	4.01	1.752	2
11/6/2015	IG-37	448.76	20.22	3.99	1.774	random	0	447.2	20.22	3.99	1.769	2
11/18/2015	IG-38	466.41	20.07	4.07	1.784	random	0	464.34	20.08	4.08	1.773	2
3/7/2016	IG-39	450.09	20.04	4.03	1.766	200	100	448.74	20.03	4.03	1.762	1
3/9/2016	IG-40	452.74	20.02	4.04	1.769	150	100	451.9	20.01	4.03	1.769	1
3/12/2016	IG-41	452.09	20.04	4.03	1.772	50	100	451.75	20.04	4.03	1.765	1
3/13/2016	IG-42	456.13	19.93	4.06	1.769	0	20	455.89	19.94	4.06	1.772	1
3/16/2016	IG-43	450.29	20.06	4.03	1.759	150	20	448.04	20.08	4.02	1.760	1
3/17/2016	IG-44	462.12	20.08	4.07	1.768	500	0	449.98	20.06	4.06	1.735	1
3/19/2016	IG-45	455.29	20.08	4.03	1.781	300	0	447.55	20.07	4.02	1.761	1
3/24/2016	IG-46	455.33	20.21	4.01	1.784	1000	0	432.93	20.19	4.00	1.709	1

ANNEX 2 LOG OF EXPERIMENTAL RESULTS - GRAPHITE IG-110

Exp data number	Test Date	Specimen ID	H2O Pressure target	H2O Pressure actual [&]	H2 Pressure	Temperature	Weight before	Weight after	Time in the Test before	Time in the Test after	Rate	Weight loss % before	Weight loss % after	Sample preparaton duration	Sample preparaton temperature	Wt loss in outgassing	Notes
			Pa	Pa	Pa	°C	mg	mg	hr	hr	s^{-1}	%	%	h	°C	mg	
METHOD 1 (constant gas composition, incremental temepratures) 212 data																	
16	3/10/15	IG-2	150	139	0	850	461.94	461.90	8.71	11.42	7.32E-09	0.20	0.20	2	1200	0.028	
17	3/10/15	IG-2	150	141	0	900	461.84	461.80	11.94	14.46	1.00E-08	0.22	0.23	2	1200	0.028	
18	3/10/15	IG-2	150	140	0	950	461.72	461.66	15.11	17.59	1.43E-08	0.25	0.26	2	1200	0.028	
19	3/10/15	IG-2	150	149	0	1000	461.58	461.45	17.99	20.56	3.16E-08	0.27	0.30	2	1200	0.028	
20	3/10/15	IG-2	150	156	0	1050	461.33	460.76	21.09	23.70	1.31E-07	0.33	0.45	2	1200	0.028	
21	3/10/15	IG-2	150	163	1	1100	460.51	458.59	24.13	26.80	4.33E-07	0.51	0.92	2	1200	0.028	
23	3/12/15	IG-3	30	43	0	850	451.29	451.27	8.69	11.54	4.10E-09	0.17	0.18	2	1200	0.013	
27	3/12/15	IG-3	30	17	0	1050	450.85	450.74	21.04	23.84	2.57E-08	0.27	0.29	2	1200	0.013	
28	3/12/15	IG-3	30	18	0	1100	450.65	450.35	24.07	26.95	6.29E-08	0.31	0.38	2	1200	0.013	
30	4/8/15	IG-7	30	27	0	850	463.14	463.11	8.71	11.46	5.02E-09	0.01	0.02	2	1200	0.376	
31	4/8/15	IG-7	30	27	0	900	463.11	463.06	11.75	14.59	1.03E-08	0.02	0.03	2	1200	0.376	
32	4/8/15	IG-7	30	27	0	950	463.06	462.99	14.82	17.69	1.57E-08	0.03	0.04	2	1200	0.376	
33	4/8/15	IG-7	30	27	0	1000	462.99	462.93	17.95	20.76	1.37E-08	0.04	0.06	2	1200	0.376	
34	4/8/15	IG-7	30	29	0	1050	462.93	462.79	21.09	23.76	2.94E-08	0.06	0.09	2	1200	0.376	
35	4/8/15	IG-7	30	29	1	1100	462.79	462.37	24.02	26.96	8.57E-08	0.09	0.18	2	1200	0.376	
36	4/13/15	IG-8	50	52	0	800	451.33	451.33	5.87	8.39	1.22E-09	-0.11	-0.11	2	1200	0.497	
37	4/13/15	IG-8	50	51	0	850	451.33	451.29	8.71	11.52	7.45E-09	-0.11	-0.10	2	1200	0.497	
38	4/13/15	IG-8	50	50	0	900	451.29	451.23	11.78	14.66	1.35E-08	-0.10	-0.09	2	1200	0.497	
39	4/13/15	IG-8	50	49	0	950	451.23	451.16	14.82	17.89	1.38E-08	-0.09	-0.07	2	1200	0.497	
40	4/13/15	IG-8	50	50	0	1000	451.16	451.06	18.21	20.79	2.46E-08	-0.07	-0.05	2	1200	0.497	
41	4/13/15	IG-8	50	50	0	1050	451.06	450.80	21.06	23.83	5.87E-08	-0.05	0.01	2	1200	0.497	
42	4/13/15	IG-8	50	51	1	1100	450.80	450.09	24.13	26.93	1.55E-07	0.01	0.17	2	1200	0.497	
43	4/19/15	IG-9	100	100	0	800	458.15	458.14	5.67	8.25	3.99E-09	-0.11	-0.11	2	1200	0.526	
44	4/19/15	IG-9	100	99	0	850	458.14	458.10	8.71	11.42	7.38E-09	-0.11	-0.10	2	1200	0.526	
45	4/19/15	IG-9	100	99	0	900	458.10	458.02	11.78	14.59	1.79E-08	-0.10	-0.09	2	1200	0.526	
46	4/19/15	IG-9	100	107	0	950	458.02	457.97	14.82	16.19	2.30E-08	-0.09	-0.07	2	1200	0.526	
47	4/19/15	IG-9	100	107	0	1000	457.97	457.81	18.05	20.56	3.75E-08	-0.07	-0.04	2	1200	0.526	
48	4/19/15	IG-9	100	109	0	1050	457.81	457.32	20.96	23.83	1.05E-07	-0.04	0.07	2	1200	0.526	
49	4/19/15	IG-9	100	109	0	1100	457.32	455.88	24.06	26.90	3.07E-07	0.07	0.38	2	1200	0.526	
50	4/28/15	IG-10	200	206	0	800	467.47	467.46	5.90	8.32	2.46E-09	-0.10	-0.10	2	1200	0.010	
51	4/28/15	IG-10	200	199	0	850	467.46	467.43	8.74	11.22	6.23E-09	-0.10	-0.09	2	1200	0.010	
52	4/28/15	IG-10	200	184	0	900	467.43	467.37	11.85	14.46	1.46E-08	-0.09	-0.08	2	1200	0.010	
53	4/28/15	IG-10	200	182	0	950	467.37	467.28	14.82	17.53	1.82E-08	-0.08	-0.06	2	1200	0.010	
54	4/28/15	IG-10	200	193	0	1000	467.28	467.08	17.95	20.69	4.43E-08	-0.06	-0.02	2	1200	0.010	
55	4/28/15	IG-10	200	213	0	1050	467.08	466.29	21.02	23.76	1.71E-07	-0.02	0.15	2	1200	0.010	
56	4/28/15	IG-10	200	220	0	1100	466.29	463.62	24.09	26.96	5.54E-07	0.15	0.72	2	1200	0.010	
57	4/30/15	IG-11	25	29	0	800	451.77	451.77	5.48	8.39	1.48E-09	-0.11	-0.11	2	1200	0.025	
58	4/30/15	IG-11	25	25	0	850	451.77	451.75	8.71	11.36	4.41E-09	-0.11	-0.10	2	1200	0.025	
59	4/30/15	IG-11	25	24	0	900	451.75	451.70	11.78	14.58	1.03E-08	-0.10	-0.09	2	1200	0.025	
60	4/30/15	IG-11	25	10	0	950	451.70	451.64	15.14	17.63	1.48E-08	-0.09	-0.08	2	1200	0.025	
61	4/30/15	IG-11	25	10	0	1000	451.64	451.56	17.95	20.73	1.88E-08	-0.08	-0.06	2	1200	0.025	
62	4/30/15	IG-11	25	11	0	1050	451.56	451.45	21.02	23.76	2.38E-08	-0.06	-0.04	2	1200	0.025	
63	4/30/15	IG-11	25	11	0	1100	451.45	451.25	24.13	26.83	4.54E-08	-0.04	0.01	2	1200	0.025	
64	5/4/15	IG-12	3	5	0	800	448.64	448.63	5.40	8.23	1.31E-09	-0.12	-0.12	2	1200	0.036	
65	5/4/15	IG-12	3	5	0	850	448.63	448.61	8.76	11.36	5.72E-09	-0.12	-0.11	2	1200	0.036	
66	5/4/15	IG-12	3	5	0	900	448.61	448.56	11.77	14.52	1.19E-08	-0.11	-0.10	2	1200	0.036	
67	5/4/15	IG-12	3	5	0	950	448.56	448.49	14.89	17.51	1.44E-08	-0.10	-0.09	2	1200	0.036	
68	5/4/15	IG-12	3	5	0	1000	448.49	448.41	17.93	20.80	1.90E-08	-0.09	-0.07	2	1200	0.036	
69	5/4/15	IG-12	3	5	0	1050	448.41	448.31	21.01	23.80	2.22E-08	-0.07	-0.05	2	1200	0.036	
70	5/4/15	IG-12	3	5	0	1100	448.31	448.15	24.17	26.83	3.66E-08	-0.05	-0.01	2	1200	0.036	

Exp data number	Test Date	Specimen ID	H2O Pressure target	H2O Pressure actual [&]	H2 Pressure	Temperature	Weight before	Weight after	Time in the Test before	Time in the Test after	Rate	Weight loss % before	Weight loss % after	Sample preparaton duration	Sample preparaton temperature	Wt loss in outgassing	Notes
			Pa	Pa	Pa	°C	mg	mg	hr	hr	s^{-1}	%	%	h	°C	mg	
71	5/8/15	IG-13	50	95	0	800	450.90	450.89	5.71	8.39	4.60E-10	-0.01	-0.01	2	1200	0.024	
72	5/8/15	IG-13	50	58	0	850	450.89	450.88	8.76	11.42	4.17E-09	-0.01	0.00	2	1200	0.024	
73	5/8/15	IG-13	50	38	0	900	450.88	450.83	11.75	14.56	1.01E-08	0.00	0.01	2	1200	0.024	
74	5/8/15	IG-13	50	36	0	950	450.83	450.75	14.85	17.63	1.86E-08	0.01	0.03	2	1200	0.024	
75	5/8/15	IG-13	50	36	0	1000	450.75	450.60	17.89	20.79	3.17E-08	0.03	0.06	2	1200	0.024	
76	5/8/15	IG-13	50	36	0	1050	450.60	450.34	21.02	23.83	5.70E-08	0.06	0.12	2	1200	0.024	
77	5/8/15	IG-13	50	36	1	1100	450.34	449.74	24.02	26.90	1.28E-07	0.12	0.25	2	1200	0.024	
79	5/13/15	IG-14	300	303	0	850	458.18	458.15	8.71	11.52	5.61E-09	-0.12	-0.11	2	1200	0.037	
80	5/13/15	IG-14	300	296	0	900	458.15	458.10	11.78	14.59	1.14E-08	-0.11	-0.10	2	1200	0.037	
81	5/13/15	IG-14	300	291	0	950	458.10	458.01	14.85	17.69	1.84E-08	-0.10	-0.08	2	1200	0.037	
82	5/13/15	IG-14	300	326	0	1000	458.01	457.79	17.92	20.73	4.81E-08	-0.08	-0.04	2	1200	0.037	
83	5/13/15	IG-14	300	352	0	1050	457.79	456.77	20.93	23.76	2.19E-07	-0.04	0.19	2	1200	0.037	
84	5/13/15	IG-14	300	354	0	1100	456.77	453.05	24.06	26.93	7.88E-07	0.19	1.00	2	1200	0.037	
85	5/27/15	IG-15	50	66	0	800	453.27	453.26	5.84	8.32	1.98E-09	-0.13	-0.13	2	1200	0.034	
86	5/27/15	IG-15	50	65	0	850	453.26	453.24	8.78	11.46	4.80E-09	-0.13	-0.12	2	1200	0.034	
87	5/27/15	IG-15	50	64	0	900	453.24	453.20	11.88	14.49	9.86E-09	-0.12	-0.11	2	1200	0.034	
88	5/27/15	IG-15	50	63	0	950	453.20	453.13	14.92	17.59	1.56E-08	-0.11	-0.10	2	1200	0.034	
89	5/27/15	IG-15	50	63	0	1000	453.13	453.01	18.02	20.69	2.69E-08	-0.10	-0.07	2	1200	0.034	
90	5/27/15	IG-15	50	49	0	1050	453.01	452.77	21.02	23.83	5.32E-08	-0.07	-0.02	2	1200	0.034	
91	5/27/15	IG-15	50	35	0	1100	452.77	452.27	24.09	26.90	1.09E-07	-0.02	0.09	2	1200	0.034	
92	5/29/15	IG-16	150	152	0	800	458.07	458.06	5.61	8.32	1.79E-09	-0.12	-0.12	2	1200	0.031	
93	5/29/15	IG-16	150	151	0	850	451.24	451.24	8.78	11.52	5.31E-09	-0.12	-0.11	2	1200	0.031	
94	5/29/15	IG-16	150	152	0	900	451.24	451.23	11.81	14.56	1.08E-08	-0.11	-0.10	2	1200	0.031	
95	5/29/15	IG-16	150	152	0	950	451.23	451.22	14.85	17.66	1.71E-08	-0.10	-0.08	2	1200	0.031	
96	5/29/15	IG-16	150	153	0	1000	451.22	451.19	17.89	20.66	3.57E-08	-0.08	-0.05	2	1200	0.031	
97	5/29/15	IG-16	150	154	0	1050	451.19	451.05	21.02	23.76	1.25E-07	-0.05	0.08	2	1200	0.031	
98	5/29/15	IG-16	150	155	0	1100	451.05	450.26	24.02	26.83	3.81E-07	0.08	0.46	2	1200	0.031	
99	6/2/15	IG-17	200	203	0	800	453.49	453.48	5.22	8.45	2.84E-09	-0.12	-0.11	2	1200	0.526	
100	6/2/15	IG-17	200	203	0	850	453.48	453.45	8.71	11.42	6.55E-09	-0.11	-0.11	2	1200	0.526	
101	6/2/15	IG-17	200	203	0	900	453.45	453.39	11.75	14.62	1.39E-08	-0.11	-0.09	2	1200	0.526	
102	6/2/15	IG-17	200	204	0	950	453.39	453.28	14.82	17.66	2.20E-08	-0.09	-0.07	2	1200	0.526	
103	6/2/15	IG-17	200	205	0	1000	453.28	453.07	17.92	20.76	4.55E-08	-0.07	-0.02	2	1200	0.526	
104	6/2/15	IG-17	200	208	0	1050	453.07	452.30	20.99	23.73	1.73E-07	-0.02	0.15	2	1200	0.526	
105	6/2/15	IG-17	200	207	0	1100	452.30	449.79	24.06	26.93	5.37E-07	0.15	0.70	2	1200	0.526	
107	6/8/15	IG-18	20	204	17	850	453.83	453.81	8.68	11.46	3.30E-09	-0.02	-0.01	2	1200	0.063	
108	6/8/15	IG-18	20	203	17	900	453.81	453.79	11.75	14.62	5.33E-09	-0.01	-0.01	2	1200	0.063	
109	6/8/15	IG-18	20	203	17	950	453.79	453.75	14.75	17.63	7.65E-09	-0.01	0.00	2	1200	0.063	
110	6/8/15	IG-18	20	203	17	1000	453.75	453.66	17.95	20.79	1.96E-08	0.00	0.02	2	1200	0.063	
111	6/8/15	IG-18	20	204	17	1050	453.66	453.29	20.96	23.83	8.00E-08	0.02	0.10	2	1200	0.063	
112	6/8/15	IG-18	20	202	17	1100	453.29	451.91	24.16	26.96	3.00E-07	0.10	0.40	2	1200	0.063	
113	6/10/15	IG-19	100	113	17	800	457.41	457.41	6.07	7.31	1.47E-09	-0.01	-0.01	2	1200	0.028	
114	6/10/15	IG-19	100	104	17	850	457.41	457.40	8.78	11.42	2.30E-09	-0.01	0.00	2	1200	0.028	
115	6/10/15	IG-19	100	104	17	900	457.40	457.38	11.78	14.56	3.71E-09	0.00	0.00	2	1200	0.028	
116	6/10/15	IG-19	100	103	17	950	457.38	457.36	14.92	17.63	4.71E-09	0.00	0.01	2	1200	0.028	
117	6/10/15	IG-19	100	103	17	1000	457.36	457.32	17.95	20.69	9.53E-09	0.01	0.01	2	1200	0.028	
118	6/10/15	IG-19	100	103	17	1050	457.32	457.19	20.96	23.73	2.87E-08	0.01	0.04	2	1200	0.028	
119	6/10/15	IG-19	100	103	17	1100	457.19	456.69	24.02	26.87	1.06E-07	0.04	0.15	2	1200	0.028	
120	6/12/15	IG-20	20	53	17	800	447.75	447.74	6.00	8.42	1.03E-09	-0.01	-0.01	2	1200	0.038	
121	6/12/15	IG-20	20	53	17	850	447.74	447.73	8.68	11.49	2.87E-09	-0.01	-0.01	2	1200	0.038	
122	6/12/15	IG-20	20	52	17	900	447.73	447.71	11.68	14.59	4.26E-09	-0.01	0.00	2	1200	0.038	
123	6/12/15	IG-20	20	52	17	950	447.71	447.69	14.82	17.59	4.93E-09	0.00	0.00	2	1200	0.038	
124	6/12/15	IG-20	20	53	17	1000	447.69	447.65	17.92	20.76	7.21E-09	0.00	0.01	2	1200	0.038	
125	6/12/15	IG-20	20	52	17	1050	447.65	447.56	20.93	23.86	1.93E-08	0.01	0.03	2	1200	0.038	

Exp data number	Test Date	Specimen ID	H2O Pressure target	H2O Pressure actual [&]	H2 Pressure	Temperature	Weight before	Weight after	Time in the Test before	Time in the Test after	Rate	Weight loss % before	Weight loss % after	Sample preparaton duration	Sample preparaton temperature	Wt loss in outgassing	Notes
			Pa	Pa	Pa	°C	mg	mg	hr	hr	s^{-1}	%	%	h	°C	mg	
126	6/12/15	IG-20	20	52	17	1100	447.56	447.30	23.99	26.83	5.79E-08	0.03	0.09	2	1200	0.038	
127	6/14/15	IG-21	20	21	17	800	459.53	459.52	5.81	8.45	2.06E-09	-0.08	-0.08	2	1200	0.035	
128	6/14/15	IG-21	20	21	17	850	459.52	459.50	8.68	11.46	3.04E-09	-0.08	-0.07	2	1200	0.035	
129	6/14/15	IG-21	20	21	17	900	459.50	459.49	11.75	14.59	2.34E-09	-0.07	-0.07	2	1200	0.035	
130	6/14/15	IG-21	20	21	17	950	459.49	459.48	14.85	17.63	2.83E-09	-0.07	-0.07	2	1200	0.035	
131	6/14/15	IG-21	20	20	17	1000	459.48	459.46	17.92	20.79	4.63E-09	-0.07	-0.06	2	1200	0.035	
132	6/14/15	IG-21	20	20	17	1050	459.46	459.42	20.96	23.83	8.64E-09	-0.06	-0.05	2	1200	0.035	
133	6/14/15	IG-21	20	20	17	1100	459.42	459.33	24.02	26.90	1.83E-08	-0.05	-0.03	2	1200	0.035	
134	6/15/15	IG-22	100	103	44	800	462.12	462.12	5.25	8.39	9.57E-10	-0.01	0.00	2	1200	0.028	
135	6/15/15	IG-22	100	103	44	850	462.12	462.11	8.58	11.52	1.43E-09	0.00	0.00	2	1200	0.028	
136	6/15/15	IG-22	100	103	44	900	462.11	462.10	11.75	14.62	1.47E-09	0.00	0.00	2	1200	0.028	
137	6/15/15	IG-22	100	104	44	950	462.10	462.09	14.82	17.69	2.30E-09	0.00	0.00	2	1200	0.028	
138	6/15/15	IG-22	100	103	44	1000	462.09	462.07	17.92	20.79	5.24E-09	0.00	0.01	2	1200	0.028	
139	6/15/15	IG-22	100	104	44	1050	462.07	461.99	20.96	23.89	1.60E-08	0.01	0.02	2	1200	0.028	
140	6/15/15	IG-22	100	104	44	1100	461.99	461.73	24.06	26.93	5.49E-08	0.02	0.08	2	1200	0.028	
141	6/19/15	IG-23	50	52	42	800	452.69	452.68	5.61	8.39	2.21E-09	-0.01	-0.01	2	1200	0.035	
142	6/19/15	IG-23	50	51	42	850	452.68	452.67	8.78	11.52	2.02E-09	-0.01	0.00	2	1200	0.035	
143	6/19/15	IG-23	50	51	42	900	452.67	452.66	11.75	14.59	1.94E-09	0.00	0.00	2	1200	0.035	
144	6/19/15	IG-23	50	51	42	950	452.66	452.65	14.88	17.66	2.65E-09	0.00	0.00	2	1200	0.035	
145	6/19/15	IG-23	50	51	42	1000	452.65	452.63	17.95	20.73	4.41E-09	0.00	0.01	2	1200	0.035	
146	6/19/15	IG-23	50	51	42	1050	452.63	452.57	20.96	23.83	1.20E-08	0.01	0.02	2	1200	0.035	
147	6/19/15	IG-23	50	51	42	1100	452.57	452.43	24.09	26.90	3.12E-08	0.02	0.05	2	1200	0.035	
148	6/30/15	IG-24	150	152	43	800	461.92	461.91	6.46	8.35	6.36E-10	0.00	0.00	2	1200	0.034	
149	6/30/15	IG-24	150	150	43	850	461.91	461.91	8.68	11.42	8.78E-10	0.00	0.00	2	1200	0.034	
150	6/30/15	IG-24	150	151	43	900	461.91	461.90	11.75	14.53	1.51E-09	0.00	0.00	2	1200	0.034	
151	6/30/15	IG-24	150	150	43	950	461.90	461.89	14.85	17.59	3.51E-09	0.00	0.00	2	1200	0.034	
152	6/30/15	IG-24	150	151	43	1000	461.89	461.85	17.89	20.69	8.38E-09	0.00	0.01	2	1200	0.034	
153	6/30/15	IG-24	150	151	43	1050	461.85	461.69	20.96	23.83	3.37E-08	0.01	0.05	2	1200	0.034	
154	6/30/15	IG-24	150	151	43	1100	461.69	461.13	24.13	26.83	1.25E-07	0.05	0.17	2	1200	0.034	
155	7/2/15	IG-25	200	202	43	800	450.74	450.73	6.00	8.45	1.01E-09	0.00	0.00	2	1200	0.028	
156	7/2/15	IG-25	200	202	43	850	450.73	450.73	8.74	11.42	1.61E-09	0.00	0.00	2	1200	0.028	
157	7/2/15	IG-25	200	200	43	900	450.73	450.72	11.81	14.53	1.36E-09	0.00	0.00	2	1200	0.028	
158	7/2/15	IG-25	200	201	43	950	450.72	450.70	14.82	17.66	3.26E-09	0.00	0.00	2	1200	0.028	
159	7/2/15	IG-25	200	200	43	1000	450.70	450.67	17.99	20.73	7.87E-09	0.00	0.01	2	1200	0.028	
160	7/2/15	IG-25	200	200	43	1050	450.67	450.51	20.99	23.80	3.44E-08	0.01	0.05	2	1200	0.028	
161	7/2/15	IG-25	200	202	43	1100	450.51	449.78	24.13	26.90	1.62E-07	0.05	0.21	2	1200	0.028	
162	7/8/15	IG-26	300	293	44	800	452.79	452.79	5.58	8.39	8.73E-10	0.00	0.00	2	1200	0.035	
163	7/8/15	IG-26	300	292	44	850	452.79	452.78	8.71	11.42	1.58E-09	0.00	0.00	2	1200	0.035	
164	7/8/15	IG-26	300	291	44	900	452.78	452.77	11.82	14.56	2.02E-09	0.00	0.00	2	1200	0.035	
165	7/8/15	IG-26	300	289	44	950	452.77	452.75	14.82	17.63	3.93E-09	0.00	0.00	2	1200	0.035	
166	7/8/15	IG-26	300	291	44	1000	452.75	452.70	17.92	20.73	1.14E-08	0.00	0.02	2	1200	0.035	
167	7/8/15	IG-26	300	295	44	1050	452.70	452.45	21.02	23.83	5.55E-08	0.02	0.07	2	1200	0.035	
168	7/8/15	IG-26	300	305	44	1100	452.45	451.09	24.09	26.98	2.89E-07	0.07	0.37	2	1200	0.035	
169	7/27/15	IG-27	300	307	87	800	451.24	451.24	6.00	8.39	5.15E-10	0.00	0.00	2	1200	0.033	
171	7/27/15	IG-27	300	317	87	900	451.24	451.23	11.72	14.53	1.97E-09	0.00	0.00	2	1200	0.033	
172	7/27/15	IG-27	300	320	87	950	451.23	451.22	14.92	17.68	2.01E-09	0.00	0.00	2	1200	0.033	
173	7/27/15	IG-27	300	313	87	1000	451.22	451.19	17.92	20.73	6.13E-09	0.00	0.01	2	1200	0.033	
174	7/27/15	IG-27	300	309	87	1050	451.19	451.05	20.93	23.73	3.14E-08	0.01	0.04	2	1200	0.033	
175	7/27/15	IG-27	300	301	87	1100	451.05	450.26	24.09	26.87	1.73E-07	0.04	0.21	2	1200	0.033	
178	8/13/15	IG-28	100	101	86	900	449.74	449.74	11.75	14.56	2.20E-10	-0.01	-0.01	2	1200	0.029	
179	8/13/15	IG-28	100	77	86	950	449.74	449.73	14.82	17.66	1.74E-09	-0.01	-0.01	2	1200	0.029	
180	8/13/15	IG-28	100	69	86	1000	449.73	449.72	17.89	20.76	3.01E-09	-0.01	0.00	2	1200	0.029	
181	8/13/15	IG-28	100	69	86	1050	449.72	449.65	20.99	23.83	1.35E-08	0.00	0.01	2	1200	0.029	

Exp data number	Test Date	Specimen ID	H2O Pressure target	H2O Pressure actual [&]	H2 Pressure	Temperature	Weight before	Weight after	Time in the Test before	Time in the Test after	Rate	Weight loss % before	Weight loss % after	Sample preparaton duration	Sample preparaton temperature	Wt loss in outgassing	Notes
			Pa	Pa	Pa	°C	mg	mg	hr	hr	s^{-1}	%	%	h	°C	mg	
182	8/13/15	IG-28	100	70	86	1100	449.65	449.50	24.02	26.93	3.21E-08	0.01	0.05	2	1200	0.029	
254	3/7/16	IG 39	200	213	85	800	449.44	449.44	6.29	8.39	2.94E-10	-0.15	-0.14	2	1200	0.023	
255	3/7/16	IG 39	200	214	85	850	449.44	449.44	8.81	11.39	7.19E-10	-0.14	-0.14	2	1200	0.023	
256	3/7/16	IG 39	200	213	85	900	449.44	449.43	11.81	14.56	1.35E-09	-0.14	-0.14	2	1200	0.023	
257	3/7/16	IG 39	200	209	85	950	449.43	449.42	14.88	17.59	2.51E-09	-0.14	-0.14	2	1200	0.023	
258	3/7/16	IG 39	200	205	85	1000	449.42	449.38	17.95	20.73	8.89E-09	-0.14	-0.13	2	1200	0.023	
259	3/7/16	IG 39	200	200	85	1050	449.38	449.19	21.02	23.80	4.16E-08	-0.13	-0.09	2	1200	0.023	
260	3/7/16	IG 39	200	201	85	1100	449.19	443.99	24.09	26.90	1.14E-06	-0.09	1.07	2	1200	0.023	
261	3/9/16	IG-40	150	155	85	800	452.21	452.21	7.05	8.39	4.58E-10	-0.12	-0.12	2	1200	0.023	
262	3/9/16	IG-40	150	161	85	850	452.21	452.21	8.71	11.42	0.00E+00	-0.12	-0.12	2	1200	0.023	
263	3/9/16	IG-40	150	168	85	900	452.21	452.21	11.85	14.53	4.58E-10	-0.12	-0.12	2	1200	0.023	
264	3/9/16	IG-40	150	168	85	950	452.21	452.20	14.85	17.66	1.53E-09	-0.12	-0.12	2	1200	0.023	
265	3/9/16	IG-40	150	165	85	1000	452.20	452.18	17.92	20.69	4.44E-09	-0.12	-0.11	2	1200	0.023	
266	3/9/16	IG-40	150	157	85	1050	452.18	452.07	20.99	23.83	2.31E-08	-0.11	-0.09	2	1200	0.023	
267	3/9/16	IG-40	150	162	85	1100	452.07	451.57	24.09	26.93	1.09E-07	-0.09	0.02	2	1200	0.023	
268	3/12/16	IG-41	50	51	86	800	452.09	452.09	6.75	8.45	1.45E-09	0.00	0.00	2	1200	0.027	
269	3/12/16	IG-41	50	50	86	850	452.09	452.09	8.68	11.42	4.48E-10	0.00	0.00	2	1200	0.027	
270	3/12/16	IG-41	50	50	85	900	452.09	452.08	11.81	14.59	6.63E-10	0.00	0.00	2	1200	0.027	
271	3/12/16	IG-41	50	51	85	950	452.08	452.08	14.82	17.53	1.36E-09	0.00	0.00	2	1200	0.027	
272	3/12/16	IG-41	50	51	85	1000	452.08	452.06	17.95	20.69	2.69E-09	0.00	0.01	2	1200	0.027	
273	3/12/16	IG-41	50	51	85	1050	452.06	452.03	21.12	23.80	6.88E-09	0.01	0.01	2	1200	0.027	
274	3/12/16	IG-41	50	51	85	1100	452.03	451.94	24.16	26.87	2.20E-08	0.01	0.03	2	1200	0.027	
275	3/13/2016	IG-42	0	3	20	800	455.54	455.53	5.63	8.42	1.75E-09	-0.130	-0.128	2	1200	0.03	
276	3/13/2016	IG-42	0	3	20	850	455.53	455.53	8.76	11.49	8.93E-10	-0.128	-0.127	2	1200	0.03	
277	3/13/2016	IG-42	0	3	20	900	455.53	455.52	11.76	14.55	6.56E-10	-0.127	-0.127	2	1200	0.03	
278	3/13/2016	IG-42	0	3	20	950	455.52	455.52	14.86	17.59	1.34E-09	-0.127	-0.126	2	1200	0.03	
279	3/13/2016	IG-42	0	3	20	1000	455.52	455.51	17.89	20.77	1.91E-09	-0.126	-0.124	2	1200	0.03	
280	3/13/2016	IG-42	0	3	20	1050	455.51	455.49	21.05	23.81	3.54E-09	-0.124	-0.120	2	1200	0.03	
281	3/13/2016	IG-42	0	3	20	1100	455.49	455.48	24.11	25.89	3.77E-09	-0.120	-0.118	2	1200	0.03	
282	3/16/16	IG-43	150	153	17	800	449.69	449.69	6.23	8.39	1.42E-09	-0.13	-0.13	2	1200	0.020	
283	3/16/16	IG-43	150	152	17	850	449.69	449.68	9.01	11.36	2.39E-09	-0.13	-0.13	2	1200	0.020	
284	3/16/16	IG-43	150	135	17	900	449.68	449.67	11.88	14.46	1.23E-09	-0.13	-0.13	2	1200	0.020	
285	3/16/16	IG-43	150	135	17	950	449.67	449.65	15.08	17.63	4.84E-09	-0.13	-0.12	2	1200	0.020	
286	3/16/16	IG-43	150	134	17	1000	449.65	449.58	18.02	20.66	1.64E-08	-0.12	-0.11	2	1200	0.020	
287	3/16/16	IG-43	150	134	17	1050	449.58	449.24	20.98	23.60	8.09E-08	-0.11	-0.03	2	1200	0.020	
288	3/16/16	IG-43	150	134	17	1100	449.24	447.95	24.22	26.87	3.02E-07	-0.03	0.26	2	1200	0.020	
289	3/17/16	IG-44	500	511	0	800	461.67	461.67	5.51	8.24	1.32E-09	-0.10	-0.10	2	1200	0.022	
290	3/17/16	IG-44	500	508	0	850	461.67	461.64	8.70	11.33	5.95E-09	-0.10	-0.09	2	1200	0.022	
291	3/17/16	IG-44	500	507	0	900	461.64	461.60	11.92	14.49	8.90E-09	-0.09	-0.08	2	1200	0.022	
292	3/17/16	IG-44	500	569	0	950	461.60	461.52	14.91	17.48	1.87E-08	-0.08	-0.06	2	1200	0.022	
293	3/17/16	IG-44	500	598	0	1000	461.52	461.16	18.19	20.67	8.83E-08	-0.06	0.01	2	1200	0.022	
294	3/17/16	IG-44	500	542	0	1050	461.16	459.74	21.09	23.04	4.39E-07	0.01	0.32	2	1200	0.022	
295	3/17/16	IG-44	500	568	0	1100	459.74	454.61	24.27	26.13	1.67E-06	0.32	1.44	2	1200	0.022	
296	3/19/16	IG-45	300	301	0	800	454.73	454.72	5.55	7.84	1.87E-09	-0.12	-0.12	2	1200	0.018	
297	3/19/16	IG-45	300	295	0	850	454.72	454.70	8.84	11.36	3.88E-09	-0.12	-0.12	2	1200	0.018	
298	3/19/16	IG-45	300	298	0	900	454.70	454.67	12.16	14.45	8.80E-09	-0.12	-0.11	2	1200	0.018	
299	3/19/16	IG-45	300	303	0	950	454.67	454.60	14.97	17.58	1.64E-08	-0.11	-0.10	2	1200	0.018	
300	3/19/16	IG-45	300	305	0	1000	454.60	454.34	18.09	20.61	6.28E-08	-0.10	-0.04	2	1200	0.018	
301	3/19/16	IG-45	300	308	0	1050	454.34	453.15	21.19	23.67	2.94E-07	-0.04	0.22	2	1200	0.018	
302	3/19/16	IG-45	300	295	0	1100	453.15	450.35	24.09	26.09	8.58E-07	0.22	0.84	2	1200	0.018	
303	3/24/16	IG-46	1000	801	0	800	455.36	455.34	5.51	8.24	3.35E-09	0.01	0.01	2	1200	0.028	
304	3/24/16	IG-46	1000	846	0	850	455.34	455.34	9.91	10.46	2.22E-09	0.01	0.01	2	1200	0.028	
305	3/24/16	IG-46	1000	785	0	900	455.34	455.30	11.98	14.46	9.35E-09	0.01	0.02	2	1200	0.028	

Exp data number	Test Date	Specimen ID	H2O Pressure target	H2O Pressure actual [&]	H2 Pressure	Temperature	Weight before	Weight after	Time in the Test before	Time in the Test after	Rate	Weight loss % before	Weight loss % after	Sample preparaton duration	Sample preparaton temperature	Wt loss in outgassing	Notes
			Pa	Pa	Pa	°C	mg	mg	hr	hr	s^{-1}	%	%	h	°C	mg	
307	3/24/16	IG-46	1000	753	0	1000	455.30	454.86	18.16	20.37	1.23E-07	0.02	0.12	2	1200	0.028	
308	3/24/16	IG-46	1000	746	0	1050	454.86	452.48	21.74	23.69	7.43E-07	0.12	0.64	2	1200	0.028	
309	3/24/16	IG-46	1000	751	0	1100	452.48	450.52	24.14	24.70	2.15E-06	0.64	1.07	2	1200	0.028	
							METHOD 2 (variable gas composition at constant temperature) 70 data										
183	8/18/15	IG-29	variable	4	0	800	453.20	453.16	7.18	21.30	2.00E-09	-0.01	0.00	2	1200	0.031	increasing
184	8/18/15	IG-29	variable	11	0	800	453.16	453.09	22.39	34.20	3.32E-09	0.00	0.02	2	1200	0.031	increasing
185	8/18/15	IG-29	variable	22	0	800	453.09	453.01	35.56	46.69	4.30E-09	0.02	0.04	2	1200	0.031	increasing
186	8/18/15	IG-29	variable	47	0	800	453.01	452.94	47.91	58.09	4.64E-09	0.04	0.05	2	1200	0.031	increasing
187	8/18/15	IG-29	variable	86	0	800	452.94	452.84	59.31	71.12	5.19E-09	0.05	0.07	2	1200	0.031	increasing
188	8/18/15	IG-29	variable	122	0	800	452.84	452.76	73.43	82.53	5.53E-09	0.07	0.09	2	1200	0.031	increasing
189	8/18/15	IG-29	variable	176	0	800	452.76	452.70	83.89	89.91	5.71E-09	0.09	0.10	2	1200	0.031	increasing
190	8/24/15	IG-30	variable	4	0	850	452.66	452.60	5.72	11.21	6.26E-09	-0.07	-0.06	2	1200	0.026	decreasing
191	8/24/15	IG-30	variable	11	0	850	452.60	452.40	11.77	22.28	1.16E-08	-0.06	-0.01	2	1200	0.026	decreasing
192	8/24/15	IG-30	variable	21	0	850	452.40	452.19	23.29	32.35	1.42E-08	-0.01	0.03	2	1200	0.026	decreasing
193	8/24/15	IG-30	variable	45	0	850	452.19	451.90	34.22	46.27	1.48E-08	0.03	0.10	2	1200	0.026	decreasing
194	8/24/15	IG-30	variable	86	0	850	451.90	451.65	47.59	57.81	1.49E-08	0.10	0.15	2	1200	0.026	decreasing
195	8/24/15	IG-30	variable	121	0	850	451.65	451.44	59.24	70.15	1.23E-08	0.15	0.20	2	1200	0.026	decreasing
197	8/24/15	IG-30	variable	174	0	850	451.44	451.20	70.68	82.66	1.21E-08	0.20	0.25	2	1200	0.026	decreasing
198	8/31/15	IG-31	variable	178	0	850	457.82	457.72	6.38	13.47	8.22E-09	0.00	0.02	2	1200	0.035	decreasing
199	8/31/15	IG-31	variable	175	0	850	457.72	457.55	13.47	22.18	1.19E-08	0.02	0.06	2	1200	0.035	decreasing
200	8/31/15	IG-31	variable	155	0	850	457.55	457.38	23.19	31.3	1.29E-08	0.06	0.10	2	1200	0.035	decreasing
201	8/31/15	IG-31	variable	121	0	850	457.38	457.28	31.3	35.95	1.25E-08	0.10	0.12	2	1200	0.035	decreasing
202	8/31/15	IG-31	variable	85	0	850	457.28	457.04	36.49	47.08	1.38E-08	0.12	0.17	2	1200	0.035	decreasing
203	8/31/15	IG-31	variable	45	0	850	457.04	456.78	48.01	60.33	1.30E-08	0.17	0.23	2	1200	0.035	decreasing
204	8/31/15	IG-31	variable	20	0	850	456.78	456.61	61.48	69.67	1.29E-08	0.23	0.27	2	1200	0.035	decreasing
205	8/31/15	IG-31	variable	11	0	850	456.61	456.40	72.33	84.61	1.05E-08	0.27	0.31	2	1200	0.035	decreasing
206	8/31/15	IG-31	variable	6	0	850	456.40	456.24	85.79	94.34	1.11E-08	0.31	0.35	2	1200	0.035	decreasing
207	9/4/15	IG-32	variable	5	0	900	452.42	452.33	6.16	11.03	1.21E-08	-0.01	0.01	2	1200	0.039	increasing
208	9/4/15	IG-32	variable	13	0	900	452.33	452.07	11.73	23.90	1.30E-08	0.01	0.07	2	1200	0.039	increasing
209	9/4/15	IG-32	variable	23	0	900	452.07	451.80	24.82	36.93	1.38E-08	0.07	0.13	2	1200	0.039	increasing
210	9/4/15	IG-32	variable	48	0	900	451.80	451.58	39.06	47.79	1.54E-08	0.13	0.18	2	1200	0.039	increasing
211	9/4/15	IG-32	variable	90	0	900	451.58	451.26	48.82	59.98	1.76E-08	0.18	0.25	2	1200	0.039	increasing
212	9/4/15	IG-32	variable	126	0	900	451.26	450.94	61.14	71.56	1.87E-08	0.25	0.32	2	1200	0.039	increasing
213	9/4/15	IG-32	variable	180	0	900	450.94	450.60	72.71	82.90	2.04E-08	0.32	0.39	2	1200	0.039	increasing
214	9/4/15	IG-32	variable	206	0	900	450.60	450.43	83.94	86.72	2.11E-08	0.39	0.43	2	1200	0.039	increasing
215	9/28/2015	IG-33	variable	177	0	800	455.35	455.30	7.08	19.7	2.85E-09	-0.008	0.005	2	1200	0.039	decreasing
216	9/28/2015	IG-33	variable	124	0	800	455.30	455.23	20.53	30.96	3.80E-09	0.005	0.019	2	1200	0.039	decreasing
217	9/28/2015	IG-33	variable	87	0	800	455.23	455.14	31.68	42.53	5.12E-09	0.019	0.039	2	1200	0.039	decreasing
218	9/28/2015	IG-33	variable	47	0	800	455.14	455.02	43.27	55.18	5.89E-09	0.039	0.065	2	1200	0.039	decreasing
219	9/28/2015	IG-33	variable	22	0	800	455.02	454.91	56.07	66.57	6.45E-09	0.065	0.089	2	1200	0.039	decreasing
220	9/28/2015	IG-33	variable	12	0	800	454.91	454.78	68.17	79.74	7.12E-09	0.089	0.119	2	1200	0.039	decreasing
221	9/28/2015	IG-33	variable	5	0	800	454.78	454.67	80.87	89.22	7.83E-09	0.119	0.142	2	1200	0.039	decreasing
222	10/2/15	IG-34	variable	159	0	900	455.76	455.64	6.47	11.48	1.46E-08	-0.01	0.02	2	1200	0.028	decreasing
223	10/2/15	IG-34	variable	109	0	900	455.64	455.33	12.27	23.53	1.69E-08	0.02	0.09	2	1200	0.028	decreasing
224	10/2/15	IG-34	variable	82	0	900	455.33	454.98	24.16	36.20	1.80E-08	0.09	0.17	2	1200	0.028	decreasing
225	10/2/15	IG-34	variable	46	0	900	454.98	454.67	36.91	47.00	1.88E-08	0.17	0.24	2	1200	0.028	decreasing
226	10/2/15	IG-34	variable	22	0	900	454.67	454.37	49.03	58.66	1.86E-08	0.24	0.30	2	1200	0.028	decreasing
227	10/2/15	IG-34	variable	12	0	900	454.37	454.18	59.59	66.07	1.79E-08	0.30	0.34	2	1200	0.028	decreasing
228	10/8/15	IG-35	variable	5	0	950	455.11	454.98	5.46	10.87	1.46E-08	-0.01	0.02	2	1200	0.040	random
229	10/8/15	IG-35	variable	13	0	950	454.98	454.64	11.43	21.69	2.04E-08	0.02	0.10	2	1200	0.040	random
230	10/8/15	IG-35	variable	23	0	950	454.64	454.17	23.80	34.33	2.73E-08	0.10	0.20	2	1200	0.040	random
231	10/8/15	IG-35	variable	47	0	950	454.17	453.53	35.02	47.58	3.14E-08	0.20	0.34	2	1200	0.040	random

Exp data number	Test Date	Specimen ID	H2O Pressure target	H2O Pressure actual [&]	H2 Pressure	Temperature	Weight before	Weight after	Time in the Test before	Time in the Test after	Rate	Weight loss % before	Weight loss % after	Sample preparaton duration	Sample preparaton temperature	Wt loss in outgassing	Notes
			Pa	Pa	Pa	°C	mg	mg	hr	hr	s^{-1}	%	%	h	°C	mg	
232	10/8/15	IG-35	variable	87	0	950	453.53	452.96	48.44	58.19	3.52E-08	0.34	0.46	2	1200	0.040	random
233	10/8/15	IG-35	variable	123	0	950	452.96	452.22	59.40	70.26	4.20E-08	0.46	0.63	2	1200	0.040	random
234	10/8/15	IG-35	variable	175	0	950	452.22	451.28	70.92	81.81	5.30E-08	0.63	0.83	2	1200	0.040	random
235	10/8/15	IG-35	variable	5	0	950	451.28	451.06	83.02	88.93	2.31E-08	0.83	0.88	2	1200	0.040	random
236	11/2/15	IG-36	variable	4	0	1000	450.76	450.62	6.19	10.24	2.01E-08	-0.01	0.01	2	1200	0.066	random
237	11/2/15	IG-36	variable	12	0	1000	450.62	450.18	11.41	21.89	2.61E-08	0.01	0.11	2	1200	0.066	random
238	11/2/15	IG-36	variable	22	0	1000	450.18	449.63	23.13	32.91	3.50E-08	0.11	0.24	2	1200	0.066	random
239	11/2/15	IG-36	variable	46	0	1000	449.63	448.73	34.93	45.18	5.39E-08	0.24	0.43	2	1200	0.066	random
240	11/2/15	IG-36	variable	35	0	1000	448.73	448.03	46.41	51.69	8.18E-08	0.43	0.59	2	1200	0.066	random
241	11/2/15	IG-36	variable	119	0	1000	448.03	447.12	52.82	58.20	1.05E-07	0.59	0.79	2	1200	0.066	random
242	11/2/15	IG-36	variable	12	0	1000	447.12	446.44	59.01	69.23	4.11E-08	0.79	0.94	2	1200	0.066	random
243	11/2/15	IG-36	variable	46	0	1000	446.44	445.31	70.20	79.47	7.64E-08	0.94	1.19	2	1200	0.066	random
244	11/2/15	IG-36	variable	4	0	1000	445.31	444.89	80.28	88.84	3.06E-08	1.19	1.29	2	1200	0.066	random
245	11/6/15	IG-37	variable	168	0	850	447.97	447.89	6.08	11.17	9.98E-09	-0.01	0.01	2	1200	0.037	random
246	11/6/15	IG-37	variable	4	0	850	447.89	447.61	11.75	25.28	1.29E-08	0.01	0.07	2	1200	0.037	random
247	11/18/15	IG-38	variable	3	0	900	466.43	466.19	5.74	19.34	1.05E-08	0.00	0.06	2	1200	0.031	random
248	11/18/15	IG-38	variable	44	0	900	466.19	465.97	20.32	31.22	1.16E-08	0.06	0.10	2	1200	0.031	random
249	11/18/15	IG-38	variable	10	0	900	465.97	465.80	32.43	42.21	1.08E-08	0.10	0.14	2	1200	0.031	random
250	11/18/15	IG-38	variable	19	0	900	465.80	465.57	45.51	55.57	1.32E-08	0.14	0.19	2	1200	0.031	random
251	11/18/15	IG-38	variable	117	0	900	465.57	465.34	57.23	67.51	1.36E-08	0.19	0.24	2	1200	0.031	random
252	11/18/15	IG-38	variable	83	0	900	465.34	465.06	68.91	80.37	1.45E-08	0.24	0.30	2	1200	0.031	random
253	11/18/15	IG-38	variable	167	0	900	465.06	464.87	81.39	88.90	1.53E-08	0.30	0.34	2	1200	0.031	random
								26 DATA REJECTED									
1	3/3/15	IG-1	100	95	0	800	464.54	464.52	7.01	8.42	1.23E-08	-0.06	-0.05	1	1200	0.264	Unstable
2	3/3/15	IG-1	100	93	0	850	464.45	464.41	8.78	11.39	9.17E-09	-0.05	-0.04	1	1200	0.264	Unstable
3	3/3/15	IG-1	100	94	0	900	464.34	464.28	11.85	14.43	1.32E-08	-0.04	-0.03	1	1200	0.264	Unstable
4	3/3/15	IG-1	100	94	0	950	464.20	464.05	14.88	17.59	3.33E-08	-0.03	0.00	1	1200	0.264	Unstable
5	3/3/15	IG-1	100	94	0	1000	463.95	463.62	17.95	20.60	7.39E-08	0.00	0.07	1	1200	0.264	Unstable
6	3/3/15	IG-1	100	97	0	1050	463.44	462.63	21.09	23.60	1.95E-07	0.07	0.25	1	1200	0.264	Unstable
7	3/3/15	IG-1	100	98	0	1100	462.28	460.07	24.16	26.87	4.89E-07	0.25	0.73	1	1200	0.264	Unstable
8	3/4/15	IG-1(2)	50	52	0	800	461.56	461.55	7.54	8.35	8.92E-09	-0.07	-0.07	1	1200	n/a	Unstable
9	3/4/15	IG-1(2)	50	49	0	850	461.48	461.44	8.71	11.42	9.33E-09	-0.05	-0.04	1	1200	n/a	Unstable
10	3/4/15	IG-1(2)	50	49	0	900	461.37	461.30	11.75	14.49	1.41E-08	-0.03	-0.01	1	1200	n/a	Unstable
11	3/4/15	IG-1(2)	50	51	0	950	461.24	461.12	14.85	17.63	2.69E-08	0.00	0.03	1	1200	n/a	Unstable
12	3/4/15	IG-1(2)	50	50	0	1000	461.00	460.67	17.99	20.63	7.60E-08	0.05	0.13	1	1200	n/a	Unstable
13	3/4/15	IG-1(2)	50	50	0	1050	460.54	459.75	20.99	23.80	1.68E-07	0.15	0.32	1	1200	n/a	Unstable
14	3/4/15	IG-1(2)	50	48	0	1100	459.49	457.90	24.22	26.90	3.60E-07	0.38	0.73	1	1200	n/a	Unstable
15	3/10/15	IG-2	150	138	0	800	462.12	462.00	5.02	8.32	2.30E-08	0.16	0.18	2	1200	0.028	Unstable
22	3/12/15	IG-3	30	35	0	800	451.43	451.35	5.04	8.44	1.43E-08	0.14	0.16	2	1200	0.013	Unstable
24	3/12/15	IG-3	30	37	0	900	451.21	451.17	11.70	14.58	7.27E-09	0.19	0.20	2	1200	0.013	Unstable
25	3/12/15	IG-3	30	17	0	950	451.10	451.04	14.85	17.68	1.22E-08	0.21	0.23	2	1200	0.013	Unstable
26	3/12/15	IG-3	30	17	0	1000	450.97	450.92	17.93	20.81	9.62E-09	0.24	0.25	2	1200	0.013	Unstable
29	4/8/15	IG-7	30	29	0	800	463.20	463.14	5.31	8.39	1.32E-08	0.00	0.01	2	1200	0.376	Unstable
78	5/13/15	IG-14	300	318	0	800	458.17	458.18	6.42	8.39	-2.15E-09	-0.12	-0.12	2	1200	0.037	Negative rate
106	6/8/15	IG-18	20	190	15	800	453.84	453.83	6.23	8.42	3.91E-09	-0.02	-0.02	2	1200	0.063	Unstable
170	7/27/15	IG-27	300	310	87	850	451.24	451.24	8.78	11.42	0.00E+00	0.00	0.00	2	1200	0.033	Zero rate
176	8/13/15	IG-28	100	110	86	800	449.74	449.74	6.20	8.45	0.00E+00	-0.01	-0.01	2	1200	0.029	Negative rate
177	8/13/15	IG-28	100	103	86	850	449.74	449.74	8.68	11.52	-2.17E-10	-0.01	-0.01	2	1200	0.029	Negative rate
306	3/24/16	IG-46	1000	unstable	0	950	455.30	455.30	0.00	0.00	#DIV/0!	0.02	0.02	2	1200	0.028	Unstable

ANNEX 3 PHYSICAL MEASUREMENTS ON GRAPHITE NBG-17 SPECIMENS BEFORE AND AFTER TESTS

		Before test				Test Conditions		After test				
Test Date	Specimen ID	Weight mg	Average L mm	Average D mm	Density g/cm3	P H2O Pa	P H2 Pa	Weight mg	Average L mm	Average D mm	Density g/cm3	Notes
11/25/2013	WG1-1	466.32	20.01	3.98	1.870	3	0	462.60	20.01	3.98	1.856	
11/26/2013	WG1-2	464.58	20.05	3.97	1.871	3	0	463.60	20.23	3.97	1.849	
12/3/2013	WG1-3	465.13	20.03	3.98	1.867	3	0	449.25	20.03	3.97	1.809	exp. error
12/5/2013	WG1-4	465.63	20.04	3.98	1.870	100	0	460.99	20.03	3.97	1.858	waiting in furnace
12/16/2013	WG1-5	464.92	20.00	3.99	1.859	100	0	459.77	20.00	3.99	1.840	
12/17/2013	WG1-6	472.14	20.03	4.01	1.871	50	0	468.67	20.04	4.01	1.855	
12/18/2013	WG1-7	452.7	19.86	3.98	1.831	30	0	449.98	19.88	3.98	1.821	
1/2/2014	WG1-8	456.55	20.05	3.98	1.832	150	0	450.72	20.05	3.97	1.814	
1/6/2014	WG1-9	465.68	20.01	3.99	1.866	300	0	456.19	20.01	3.98	1.831	
1/7/2014	WG1-10	467.68	19.99	3.99	1.869	15	0	465.65	19.99	3.99	1.862	
1/8/2014	WG1-11	465.53	20.05	3.98	1.867	30	0	463.01	20.05	3.98	1.858	
1/9/2014	WG1-12	464.35	20.04	3.98	1.860	15	0	462.4	20.04	3.98	1.853	
1/13/2014	WG1-13	469.68	19.98	4.00	1.869	50	0	466.11	19.97	4.00	1.859	
1/14/2014	WG1-14	472.23	20.04	4.01	1.862	150	0	465.88	20.04	4.01	1.842	
1/15/2014	WG1-15	465.1	20.04	3.99	1.856	300	0	456.8	20.04	3.98	1.833	
1/16/2014	WG1-16	469.56	19.99	4.01	1.862	100	0	465.96	19.98	4.00	1.856	H2O not constant
1/21/2014	AG3-1	438.68	20.00	3.99	1.753	50	0	434.8	20.01	3.98	1.748	
1/22/2014	AG3-2	462.65	20.06	4.00	1.839	30	0	459.87	20.06	3.98	1.841	
1/23/2014	AG3-3	465.83	20.09	3.99	1.851	15	0	464.25	20.09	3.98	1.854	
1/24/2014	AG3-4	470.17	20.02	4.00	1.869	100	0	465.59	20.02	4.00	1.852	
1/27/2014	AG3-5	454.19	20.01	3.99	1.812	300	0	442.98	20.00	3.98	1.777	
1/28/2014	AG3-6	464.52	20.06	4.00	1.844	150	0	458.65	20.06	3.99	1.830	
2/5/2014	AG3-7	464.52	20.08	3.99	1.855	300	0	456.02	20.08	3.98	1.825	
2/6/2014	AG3-8	463.04	19.91	3.98	1.872	150	0	456.39	19.93	3.97	1.847	
2/10/2014	AG3-9	455.72	19.90	3.98	1.840	15	0	452.73	19.91	3.97	1.836	He flow stopped
2/11/2014	AG3-10	463.36	19.97	3.98	1.869	30	0	460.81	19.97	3.98	1.855	
2/14/2014	AG3-11	464.43	20.02	3.99	1.856	50	0	460.31	20.03	3.98	1.847	
2/15/2014	AG3-12	457.97	20.00	3.99	1.836	100	0	452.59	20.00	3.98	1.822	

		Before test				Test Conditions		After test				
Test Date	Specimen ID	Weight mg	Average L mm	Average D mm	Density g/cm3	P H2O Pa	P H2 Pa	Weight mg	Average L mm	Average D mm	Density g/cm3	Notes
2/16/2014	AG3-13	442.65	20.03	4.00	1.756	0	0	441.12	20.03	4.01	1.748	
2/17/2014	AG3-14	465.53	20.05	4.00	1.848	0	0	464.2	20.05	3.99	1.848	
3/5/2014	AG3-15	463.73	20.09	3.99	1.846	15	30	462.79	20.09	3.99	1.842	
3/6/2014	AG3-16	471.69	19.96	4.02	1.866	30	30	470.47	19.96	4.02	1.859	
3/7/2014	AG3-17	467.5	19.95	3.99	1.871	50	30	465.71	19.95	3.99	1.870	
3/10/2014	AG3-18	464.33	19.99	3.99	1.860	100	30	463.49				He flow stopped
3/14/2014	AG3-19	460.88	19.97	3.99	1.849	100	30	457.88	19.95	3.99	1.837	
3/25/2014	AG3-20	453.58	20.09	3.98	1.814	150	30	448.41	20.09	3.98	1.797	
3/27/2014	AG3-21	467.18	19.99	4.02	1.842	300	30	457.54	19.99	4.02	1.808	
3/31/2014	AG3-22	456.19	19.83	3.98	1.846	15	0	454.09	19.83	3.98	1.844	H2O not constant
4/1/2014	WG1-17	468.16	19.98	4.00	1.862	100	30	464.68	19.99	4.00	1.850	
4/2/2014	WG1-18	468.16	20.01	3.99	1.868	50	30	462.35	20.01	3.99	1.847	
4/3/2014	WG1-19	464.23	20.04	3.99	1.856	30	30	462.7	20.04	3.98	1.852	
4/4/2014	WG1-20	465.3	20.03	3.98	1.865	150	30	460.74	20.04	3.98	1.846	
4/7/2014	WG1-21	466.16	20.03	3.99	1.861	300	30	459.19	20.01	3.99	1.839	
4/8/2014	WG1-22	457.51	19.80	3.99	1.844	15	30	456.71	19.81	3.99	1.845	H2O not constant
4/9/2014	WG1-23	470.38	20.01	4.00	1.871	3	100	469.74	20.02	4.01	1.863	H2 only
6/30/2014	WG1-24	465.29	20.07	3.99	1.853	500	0	442.02	20.07	3.98	1.774	
7/1/2014	WG1-25	465.38	20.05	3.98	1.868	1000	0	430.71	20.04	3.96	1.742	H2O not constant
7/3/2014	WG1-26	468.94	20.00	4.00	1.866	750	0	467.95	19.99	4.00	1.861	exp. Error
7/29/2014	WG1-27	467.87	20.02	3.99	1.865	100	30	465.72	20.01	3.99	1.861	H2 not constant
8/4/2014	WG1-28	466.22	20.01	3.99	1.863	100	30	464.77	20.02	3.98	1.864	H2 not constant
8/8/2014	WG1-29	466.01	20.03	3.98	1.868	100-200	variable	464.6	20.04	3.99	1.853	variable conditions
8/12/2014	WG1-30	466.83	20.04	4.00	1.859	30-50	variable	465.87	20.03	3.99	1.860	variable conditions
8/15/2014	WG1-31	470.25	19.99	4.01	1.868	vary	25	469.58	19.99	4.01	1.861	variable conditions
8/25/2014	WG1-32	456.9	20.02	4.00	1.818	15	26	456.34	20.03	4.00	1.816	T=800-850-900-950
9/3/2014	WG1-33	463.92	20.06	3.98	1.857	30	26	463.15	20.05	3.98	1.861	T=800-850-900-950
12/18/2014	WG1-34	468.30	20.01	3.99	1.869	30, 15, 3	0	464.8	20.02	4.00	1.850	T=800-850-900-950

ANNEX 4 LOG OF EXPERIMENTAL RESULTS - GRAPHITE NBG-17

Exp data			H2O Pressure		H2	Temperat	Weight		Time in the test			Weight loss %		Sample preparaton		Wt loss in	
number	Test Date	Specimen ID	target	actual [&]	Pressure	ure	before	after	before	after	Rate	before	after	duration	temperature	outgassing	Notes
			Pa	Pa	Pa	oC	mg	mg	hr	hr	s^{-1}	%	%	h	^{o}C	mg	
1	12/16/2013	WG1-5	100	100	0	800	465.07	465.04	4.60	7.36	5.84E-09	-0.03	-0.03	1	1200	0.18	
2	12/16/2013	WG1-5	100	101	0	850	464.99	464.91	7.70	10.46	1.71E-08	-0.01	0.00	1	1200	0.18	
3	12/16/2013	WG1-5	100	101	0	900	464.84	464.72	10.91	13.56	2.73E-08	0.02	0.04	1	1200	0.18	
4	12/16/2013	WG1-5	100	101	0	950	464.66	464.41	13.78	16.55	5.42E-08	0.06	0.11	1	1200	0.18	
5	12/16/2013	WG1-5	100	101	0	1000	464.30	463.68	16.94	19.68	1.35E-07	0.13	0.27	1	1200	0.18	
6	12/16/2013	WG1-5	100	100	0	1100	463.29	460.17	20.12	22.86	6.81E-07	0.35	1.02	1	1200	0.18	
7	12/17/2013	WG1-6	50	50	0	800	471.18	471.14	4.21	7.34	7.53E-09	0.17	0.18	1	1200	0.15	
8	12/17/2013	WG1-6	50	51	0	850	471.07	471.02	7.81	10.46	1.27E-08	0.19	0.21	1	1200	0.15	
9	12/17/2013	WG1-6	50	50	0	900	470.96	470.85	10.82	13.51	2.46E-08	0.22	0.24	1	1200	0.15	
10	12/17/2013	WG1-6	50	51	0	950	470.74	470.57	13.90	16.57	3.71E-08	0.27	0.30	1	1200	0.15	
11	12/17/2013	WG1-6	50	51	0	1000	470.46	470.05	17.02	19.68	9.21E-08	0.32	0.41	1	1200	0.15	
12	12/17/2013	WG1-6	50	51	0	1100	469.75	467.86	20.15	22.86	4.11E-07	0.47	0.87	1	1200	0.15	
13	12/18/2013	WG1-7	30	30	0	800	451.65	451.63	4.52	6.61	6.18E-09	0.20	0.20	2	1200	0.15	
14	12/18/2013	WG1-7	30	30	0	850	451.54	451.47	7.89	10.43	1.77E-08	0.22	0.24	2	1200	0.15	
15	12/18/2013	WG1-7	30	30	0	900	451.40	451.31	10.94	13.48	2.30E-08	0.25	0.27	2	1200	0.15	
16	12/18/2013	WG1-7	30	30	0	950	451.24	451.08	13.95	16.57	3.69E-08	0.29	0.32	2	1200	0.15	
17	12/18/2013	WG1-7	30	30	0	1000	450.99	450.67	17.02	19.70	7.33E-08	0.34	0.42	2	1200	0.15	
18	12/18/2013	WG1-7	30	30	0	1100	450.48	449.25	20.04	22.66	2.90E-07	0.46	0.73	2	1200	0.15	
19	1/2/2014	WG1-8	150	152	0	800	455.29	455.26	4.85	7.39	7.45E-09	0.23	0.23	2	1200	0.22	
20	1/2/2014	WG1-8	150	153	0	850	455.21	455.15	7.84	10.38	1.44E-08	0.25	0.26	2	1200	0.22	
21	1/2/2014	WG1-8	150	153	0	900	455.08	454.97	10.85	13.51	2.59E-08	0.27	0.30	2	1200	0.22	
22	1/2/2014	WG1-8	150	152	0	950	454.90	454.67	13.93	16.57	5.25E-08	0.31	0.36	2	1200	0.22	
23	1/2/2014	WG1-8	150	151	0	1000	454.57	453.93	16.94	19.73	1.40E-07	0.39	0.53	2	1200	0.22	
24	1/2/2014	WG1-8	150	150	0	1100	453.47	449.73	20.18	22.94	8.30E-07	0.63	1.45	2	1200	0.22	
25	1/6/2014	WG1-9	300	303	0	800	464.463	464.427	4.46	7.24	7.74E-09	0.21	0.22	2	1200	0.22	
26	1/6/2014	WG1-9	300	302	0	850	464.367	464.31	7.80	10.38	1.32E-08	0.24	0.25	2	1200	0.22	
27	1/6/2014	WG1-9	300	304	0	900	464.248	464.125	10.80	13.47	2.76E-08	0.26	0.29	2	1200	0.22	
28	1/6/2014	WG1-9	300	307	0	950	464.045	463.729	13.69	16.64	6.41E-08	0.30	0.37	2	1200	0.22	
29	1/6/2014	WG1-9	300	309	0	1000	463.582	462.677	17.03	19.70	2.03E-07	0.40	0.60	2	1200	0.22	
30	1/6/2014	WG1-9	300	314	0	1100	462.139	455.456	20.09	22.92	1.42E-06	0.71	2.15	2	1200	0.22	
31	1/7/2014	WG1-10	15	15	0	800	466.664	466.628	4.71	7.28	8.34E-09	0.18	0.19	2	1200	0.16	
32	1/7/2014	WG1-10	15	15	0	850	466.571	466.5	7.81	10.41	1.63E-08	0.20	0.22	2	1200	0.16	
33	1/7/2014	WG1-10	15	15	0	900	466.44	466.348	10.85	13.51	2.06E-08	0.23	0.25	2	1200	0.16	
34	1/7/2014	WG1-10	15	15	0	950	466.279	466.141	13.95	16.63	3.07E-08	0.27	0.29	2	1200	0.16	
35	1/7/2014	WG1-10	15	15	0	1000	466.07	465.81	16.91	19.70	5.55E-08	0.31	0.37	2	1200	0.16	

Exp data number	Test Date	Specimen ID	H2O Pressure target	H2O Pressure actual [&]	H2 Pressure	Temperature	Weight before	Weight after	Time in the test before	Time in the test after	Rate	Weight loss % before	Weight loss % after	Sample preparaton duration	Sample preparaton temperature	Wt loss in outgassing	Notes
			Pa	Pa	Pa	oC	mg	mg	hr	hr	s^{-1}	%	%	h	^{o}C	mg	
36	1/7/2014	WG1-10	15	15	0	1100	465.629	464.813	20.07	22.86	1.74E-07	0.40	0.58	2	1200	0.16	
37	1/8/2014	WG1-11	30	30	0	800	464.557	464.518	4.63	7.45	8.27E-09	0.18	0.19	2	1200	0.14	
38	1/8/2014	WG1-11	30	30	0	850	464.465	464.398	7.73	10.49	1.45E-08	0.20	0.21	2	1200	0.14	
39	1/8/2014	WG1-11	30	32	0	900	464.339	464.234	10.80	13.64	2.21E-08	0.23	0.25	2	1200	0.14	
40	1/8/2014	WG1-11	30	32	0	950	464.176	464.012	13.81	16.66	3.44E-08	0.26	0.30	2	1200	0.14	
41	1/8/2014	WG1-11	30	32	0	1000	463.939	463.613	16.88	19.73	6.85E-08	0.31	0.38	2	1200	0.14	
42	1/8/2014	WG1-11	30	32	0	1100	463.406	462.082	20.07	22.91	2.79E-07	0.43	0.71	2	1200	0.14	
44	1/9/2014	WG1-12	15	15	0	850	463.261	463.181	7.87	10.46	1.85E-08	0.20	0.22	2	1200	0.14	
45	1/9/2014	WG1-12	15	15	0	900	463.123	463.021	10.77	13.62	2.15E-08	0.23	0.26	2	1200	0.14	
46	1/9/2014	WG1-12	15	15	0	950	462.956	462.812	13.90	16.52	3.30E-08	0.27	0.30	2	1200	0.14	
47	1/9/2014	WG1-12	15	15	0	1000	462.727	462.455	16.94	19.70	5.92E-08	0.32	0.38	2	1200	0.14	
48	1/9/2014	WG1-12	15	16	0	1100	462.185	461.413	20.34	22.89	1.82E-07	0.44	0.60	2	1200	0.14	
49	1/13/2014	WG1-13	50	49	0	800	468.56	468.515	4.54	7.47	9.10E-09	0.20	0.21	2	1200	0.16	
50	1/13/2014	WG1-13	50	49	0	850	468.461	468.393	7.67	10.46	1.45E-08	0.22	0.24	2	1200	0.16	
51	1/13/2014	WG1-13	50	49	0	900	468.334	468.224	10.74	13.56	2.31E-08	0.25	0.28	2	1200	0.16	
52	1/13/2014	WG1-13	50	49	0	950	468.158	467.956	13.81	16.66	4.21E-08	0.29	0.33	2	1200	0.16	
53	1/13/2014	WG1-13	50	49	0	1000	467.881	467.458	16.86	19.76	8.66E-08	0.35	0.44	2	1200	0.16	
54	1/13/2014	WG1-13	50	49	0	1100	467.205	465.372	20.09	22.89	3.89E-07	0.49	0.88	2	1200	0.16	
55	1/14/2014	WG1-14	150	149	0	800	471.241	471.21	4.82	7.39	7.11E-09	0.18	0.19	2	1200	0.15	
56	1/14/2014	WG1-14	150	150	0	850	471.156	471.062	7.67	10.43	2.01E-08	0.20	0.22	2	1200	0.15	
57	1/14/2014	WG1-14	150	152	0	900	470.999	470.845	10.74	13.56	3.22E-08	0.23	0.26	2	1200	0.15	
58	1/14/2014	WG1-14	150	155	0	950	470.771	470.485	13.84	16.60	6.11E-08	0.28	0.34	2	1200	0.15	
59	1/14/2014	WG1-14	150	158	0	1000	470.358	469.646	16.99	19.73	1.53E-07	0.37	0.52	2	1200	0.15	
60	1/14/2014	WG1-14	150	160	0	1100	469.237	465.093	20.09	22.86	8.86E-07	0.60	1.48	2	1200	0.15	
61	1/15/2014	WG1-15	300	304	0	800	464.077	464.053	4.36	7.28	4.92E-09	0.19	0.19	2	1200	0.15	
62	1/15/2014	WG1-15	300	306	0	850	463.994	463.914	7.75	10.45	1.77E-08	0.21	0.22	2	1200	0.15	
63	1/15/2014	WG1-15	300	306	0	900	463.846	463.726	10.89	13.51	2.74E-08	0.24	0.26	2	1200	0.15	
64	1/15/2014	WG1-15	300	310	0	950	463.648	463.337	13.84	16.60	6.75E-08	0.28	0.35	2	1200	0.15	
65	1/15/2014	WG1-15	300	316	0	1000	463.207	462.319	16.96	19.77	1.90E-07	0.37	0.57	2	1200	0.15	
66	1/15/2014	WG1-15	300	327	0	1100	461.341	456.033	20.37	22.88	1.27E-06	0.78	1.92	2	1200	0.15	
67	1/16/2014	WG1-16	100	101	0	800	468.502	468.471	4.60	7.34	6.71E-09	0.19	0.20	2	1200	0.16	
68	1/16/2014	WG1-16	100	101	0	850	468.417	468.344	7.61	10.49	1.50E-08	0.21	0.22	2	1200	0.16	
69	1/16/2014	WG1-16	100	61	0	900	468.286	468.177	10.74	13.56	2.29E-08	0.24	0.26	2	1200	0.16	
70	1/16/2014	WG1-16	100	60	0	950	468.109	467.901	13.81	16.63	4.38E-08	0.28	0.32	2	1200	0.16	
71	1/16/2014	WG1-16	100	60	0	1000	467.825	467.375	16.86	19.73	9.31E-08	0.34	0.43	2	1200	0.16	
72	1/16/2014	WG1-16	100	60	0	1100	467.09	465.026	20.12	22.91	4.40E-07	0.49	0.93	2	1200	0.16	
73	1/21/2014	AG3-1	50	51	0	800	437.532	437.501	4.82	7.39	7.66E-09	0.22	0.23	2	1200	0.19	
74	1/21/2014	AG3-1	50	51	0	850	437.447	437.384	7.73	10.52	1.43E-08	0.24	0.25	2	1200	0.19	
75	1/21/2014	AG3-1	50	51	0	900	437.327	437.226	10.77	13.56	2.30E-08	0.27	0.29	2	1200	0.19	
76	1/21/2014	AG3-1	50	51	0	950	437.166	436.967	13.76	16.63	4.41E-08	0.30	0.35	2	1200	0.19	

Exp data number	Test Date	Specimen ID	H2O Pressure target	H2O Pressure actual [&]	H2 Pressure	Temperature	Weight before	Weight after	Time in the test before	Time in the test after	Rate	Weight loss % before	Weight loss % after	Sample preparaton duration	Sample preparaton temperature	Wt loss in outgassing	Notes
			Pa	Pa	Pa	oC	mg	mg	hr	hr	s^{-1}	%	%	h	^{o}C	mg	
77	1/21/2014	AG3-1	50	51	0	1000	436.877	436.445	16.94	19.70	9.95E-08	0.37	0.47	2	1200	0.19	
78	1/21/2014	AG3-1	50	50	0	1100	436.103	434.047	20.21	22.91	4.85E-07	0.54	1.01	2	1200	0.19	
79	1/22/2014	AG3-2	30	31	0	800	461.685	461.629	4.79	7.47	1.26E-08	0.18	0.19	2	1200	0.13	
80	1/22/2014	AG3-2	30	32	0	850	461.578	461.513	7.70	10.52	1.39E-08	0.20	0.22	2	1200	0.13	
81	1/22/2014	AG3-2	30	32	0	900	461.436	461.355	10.80	13.56	1.77E-08	0.23	0.25	2	1200	0.13	
82	1/22/2014	AG3-2	30	31	0	950	461.296	461.113	13.76	16.69	3.76E-08	0.26	0.30	2	1200	0.13	
83	1/22/2014	AG3-2	30	32	0	1000	461.038	460.649	16.91	19.76	8.22E-08	0.32	0.40	2	1200	0.13	
84	1/22/2014	AG3-2	30	32	0	1100	460.432	458.989	20.07	22.91	3.07E-07	0.45	0.76	2	1200	0.13	
85	1/23/2014	AG3-3	15	16	0	800	464.874	464.831	4.61	7.34	9.41E-09	0.18	0.19	2	1200	0.13	
86	1/23/2014	AG3-3	15	16	0	850	464.774	464.714	7.71	10.56	1.26E-08	0.20	0.21	2	1200	0.13	
87	1/23/2014	AG3-3	15	16	0	900	464.659	464.573	10.77	13.59	1.82E-08	0.22	0.24	2	1200	0.13	
88	1/23/2014	AG3-3	15	16	0	950	464.511	464.381	13.86	16.68	2.76E-08	0.26	0.28	2	1200	0.13	
89	1/23/2014	AG3-3	15	16	0	1000	464.311	464.053	16.91	19.70	5.53E-08	0.30	0.35	2	1200	0.13	
90	1/23/2014	AG3-3	15	16	0	1100	463.865	463.312	20.10	22.16	1.61E-07	0.39	0.51	2	1200	0.13	
91	1/24/2014	AG3-4	100	102	0	800	469.193	469.17	5.49	7.39	7.17E-09	0.18	0.19	2	1200	0.12	
92	1/24/2014	AG3-4	100	102	0	850	469.117	469.058	7.76	10.52	1.27E-08	0.20	0.21	2	1200	0.12	
93	1/24/2014	AG3-4	100	102	0	900	468.994	468.883	10.91	13.56	2.48E-08	0.23	0.25	2	1200	0.12	
94	1/24/2014	AG3-4	100	102	0	950	468.812	468.577	13.87	16.69	4.94E-08	0.26	0.31	2	1200	0.12	
95	1/24/2014	AG3-4	100	102	0	1000	468.489	467.919	16.91	19.76	1.19E-07	0.33	0.45	2	1200	0.12	
96	1/24/2014	AG3-4	100	101	0	1100	467.573	464.765	20.12	22.89	6.02E-07	0.53	1.12	2	1200	0.12	
97	1/27/2014	AG3-5	300	299	0	800	453.06	453.005	4.77	7.38	1.29E-08	0.20	0.22	2	1200	0.20	
98	1/27/2014	AG3-5	300	302	0	850	452.941	452.858	7.86	10.44	1.97E-08	0.23	0.25	2	1200	0.20	
99	1/27/2014	AG3-5	300	303	0	900	452.797	452.651	10.74	13.55	3.19E-08	0.26	0.29	2	1200	0.20	
100	1/27/2014	AG3-5	300	306	0	950	452.579	452.211	13.80	16.67	7.87E-08	0.31	0.39	2	1200	0.20	
101	1/27/2014	AG3-5	300	308	0	1000	452.083	450.983	16.94	19.78	2.38E-07	0.42	0.66	2	1200	0.20	
102	1/27/2014	AG3-5	300	310	0	1100	450.657	442.425	19.98	22.86	1.76E-06	0.73	2.55	2	1200	0.20	
103	1/28/2014	AG3-6	150	150	0	800	463.513	463.468	4.63	7.39	9.77E-09	0.19	0.20	2	1200	0.15	
104	1/28/2014	AG3-6	150	150	0	850	463.416	463.346	7.61	10.46	1.47E-08	0.21	0.22	2	1200	0.15	
105	1/28/2014	AG3-6	150	151	0	900	463.289	463.175	10.74	13.51	2.47E-08	0.23	0.26	2	1200	0.15	
106	1/28/2014	AG3-6	150	151	0	950	463.107	462.841	13.78	16.66	5.54E-08	0.27	0.33	2	1200	0.15	
107	1/28/2014	AG3-6	150	151	0	1000	462.763	462.042	16.83	19.81	1.45E-07	0.35	0.50	2	1200	0.15	
108	1/28/2014	AG3-6	150	151	0	1100	461.647	457.782	20.12	22.91	8.34E-07	0.59	1.42	2	1200	0.15	
109	2/5/2014	AG3-7	300	305	0	800	463.67	463.623	4.33	7.34	9.35E-09	0.20	0.21	2	1200	0.16	
110	2/5/2014	AG3-7	300	306	0	850	463.565	463.484	7.67	10.43	1.76E-08	0.22	0.24	2	1200	0.16	
111	2/5/2014	AG3-7	300	306	0	900	463.42	463.286	10.81	13.54	2.94E-08	0.25	0.28	2	1200	0.16	
112	2/5/2014	AG3-7	300	306	0	950	463.206	462.891	13.87	16.63	6.84E-08	0.30	0.36	2	1200	0.16	
113	2/5/2014	AG3-7	300	305	0	1000	462.783	461.878	16.90	19.79	1.88E-07	0.39	0.58	2	1200	0.16	
114	2/5/2014	AG3-7	300	307	0	1100	461.696	455.617	19.93	22.77	1.29E-06	0.62	1.93	2	1200	0.16	
115	2/6/2014	AG3-8	150	150	0	800	461.912	461.838	4.88	7.34	1.81E-08	0.20	0.22	2	1200	0.20	
116	2/6/2014	AG3-8	150	152	0	850	461.778	461.666	7.70	10.46	2.44E-08	0.23	0.25	2	1200	0.20	

Exp data number	Test Date	Specimen ID	H2O Pressure target	H2O Pressure actual [&]	H2 Pressure	Temperature	Weight before	Weight after	Time in the test before	Time in the test after	Rate	Weight loss % before	Weight loss % after	Sample preparaton duration	Sample preparaton temperature	Wt loss in outgassing	Notes
			Pa	Pa	Pa	oC	mg	mg	hr	hr	s^{-1}	%	%	h	^{o}C	mg	
117	2/6/2014	AG3-8	150	151	0	900	461.601	461.432	10.77	13.56	3.65E-08	0.27	0.30	2	1200	0.20	
118	2/6/2014	AG3-8	150	152	0	950	461.353	461.04	13.87	16.60	6.90E-08	0.32	0.39	2	1200	0.20	
119	2/6/2014	AG3-8	150	151	0	1000	460.937	460.182	16.88	19.68	1.62E-07	0.41	0.57	2	1200	0.20	
120	2/6/2014	AG3-8	150	152	0	1100	459.642	455.378	20.18	22.91	9.44E-07	0.69	1.61	2	1200	0.20	
121	2/10/2014	AG3-9	15	15	0	800	460.261	460.211	5.35	7.34	1.52E-08	0.25	0.26	2	1200	0.32	
122	2/10/2014	AG3-9	15	15	0	850	460.149	460.049	7.70	10.52	2.14E-08	0.27	0.29	2	1200	0.32	
123	2/10/2014	AG3-9	15	15	0	900	459.986	459.846	10.80	13.53	3.10E-08	0.31	0.34	2	1200	0.32	
124	2/10/2014	AG3-9	15	15	0	950	459.777	459.533	13.78	16.74	4.98E-08	0.35	0.40	2	1200	0.32	
125	2/10/2014	AG3-9	15	15	0	1000	459.462	459.092	16.97	19.73	8.10E-08	0.42	0.50	2	1200	0.32	
126	2/10/2014	AG3-9	15	15	0	1100	458.882	457.906	20.09	22.89	2.11E-07	0.55	0.76	2	1200	0.32	
127	2/11/2014	AG3-10	30	31	0	800	462.401	462.351	4.52	7.31	1.08E-08	0.18	0.19	2	1200	0.14	
128	2/11/2014	AG3-10	30	31	0	850	462.288	462.166	7.76	10.49	2.69E-08	0.20	0.23	2	1200	0.14	
129	2/11/2014	AG3-10	30	31	0	900	462.106	461.963	10.77	13.56	3.08E-08	0.24	0.27	2	1200	0.14	
130	2/11/2014	AG3-10	30	31	0	950	461.896	461.687	13.81	16.69	4.36E-08	0.29	0.33	2	1200	0.14	
131	2/11/2014	AG3-10	30	31	0	1000	461.613	461.259	16.88	19.76	7.40E-08	0.35	0.42	2	1200	0.14	
132	2/11/2014	AG3-10	30	31	0	1100	461.047	459.807	20.09	22.94	2.62E-07	0.47	0.74	2	1200	0.14	
133	2/14/2014	AG3-11	50	51	0	800	463.228	463.159	4.77	7.42	1.56E-08	0.22	0.23	2	1200	0.20	
134	2/14/2014	AG3-11	50	51	0	850	463.099	463.003	7.76	10.41	2.17E-08	0.24	0.26	2	1200	0.20	
135	2/14/2014	AG3-11	50	51	0	900	462.932	462.8	10.88	13.51	3.01E-08	0.28	0.31	2	1200	0.20	
136	2/14/2014	AG3-11	50	50	0	950	462.723	462.472	13.84	16.60	5.46E-08	0.33	0.38	2	1200	0.20	
137	2/14/2014	AG3-11	50	48	0	1000	462.379	461.866	16.88	19.68	1.10E-07	0.40	0.51	2	1200	0.20	
138	2/14/2014	AG3-11	50	50	0	1100	461.565	459.353	20.09	22.91	4.72E-07	0.57	1.05	2	1200	0.20	
139	2/15/2014	AG3-12	100	105	0	800	456.892	456.821	4.24	7.39	1.37E-08	0.19	0.21	2	1200	0.20	
140	2/15/2014	AG3-12	100	102	0	850	456.767	456.665	7.64	10.49	2.18E-08	0.22	0.24	2	1200	0.20	
141	2/15/2014	AG3-12	100	102	0	900	456.603	456.445	10.74	13.62	3.34E-08	0.26	0.29	2	1200	0.20	
142	2/15/2014	AG3-12	100	102	0	950	456.373	456.093	13.84	16.69	5.98E-08	0.31	0.37	2	1200	0.20	
143	2/15/2014	AG3-12	100	102	0	1000	455.999	455.387	16.91	19.68	1.35E-07	0.39	0.52	2	1200	0.20	
144	2/15/2014	AG3-12	100	101	0	1100	454.91	451.662	20.21	22.94	7.26E-07	0.63	1.34	2	1200	0.20	
145	2/16/2014	AG3-13	3	3	0	800	441.532	441.472	4.04	7.39	1.13E-08	0.22	0.23	2	1200	0.15	
146	2/16/2014	AG3-13	3	3	0	850	441.414	441.273	7.61	10.49	3.08E-08	0.25	0.28	2	1200	0.15	
147	2/16/2014	AG3-13	3	3	0	900	441.207	441.06	10.74	13.56	3.28E-08	0.29	0.33	2	1200	0.15	
148	2/16/2014	AG3-13	3	3	0	950	440.988	440.848	13.87	16.63	3.20E-08	0.34	0.37	2	1200	0.15	
149	2/16/2014	AG3-13	3	3	0	1000	440.774	440.6	16.94	19.76	3.89E-08	0.39	0.43	2	1200	0.15	
150	2/16/2014	AG3-13	3	3	0	1100	440.452	440.148	20.07	22.94	6.68E-08	0.46	0.53	2	1200	0.15	
151	2/17/2014	AG3-14	3	3	0	800	464.54	464.468	4.07	7.36	1.31E-08	0.18	0.20	2	1200	0.15	
152	2/17/2014	AG3-14	3	3	0	850	464.406	464.291	7.70	10.52	2.44E-08	0.21	0.24	2	1200	0.15	
153	2/17/2014	AG3-14	3	3	0	900	464.24	464.096	10.71	13.64	2.94E-08	0.25	0.28	2	1200	0.15	
154	2/17/2014	AG3-14	3	3	0	950	464.033	463.873	13.81	16.57	3.47E-08	0.29	0.32	2	1200	0.15	
155	2/17/2014	AG3-14	3	3	0	1000	463.795	463.636	16.91	19.65	3.48E-08	0.34	0.38	2	1200	0.15	
156	2/17/2014	AG3-14	3	3	0	1100	463.477	463.178	20.07	22.89	6.35E-08	0.41	0.47	2	1200	0.15	

Exp data number	Test Date	Specimen ID	H2O Pressure target	H2O Pressure actual [&]	H2 Pressure	Temperature	Weight before	Weight after	Time in the test before	Time in the test after	Rate	Weight loss % before	Weight loss % after	Sample preparaton duration	Sample preparaton temperature	Wt loss in outgassing	Notes
			Pa	Pa	Pa	oC	mg	mg	hr	hr	s^{-1}	%	%	h	^{o}C	mg	
157	3/31/2014	AG3-22	15	24	0	800	454.981	454.911	4.68	7.42	1.56E-08	0.22	0.23	2	1200	0.21	
158	3/31/2014	AG3-22	15	23	0	850	454.85	454.772	7.73	10.49	1.73E-08	0.25	0.27	2	1200	0.21	
159	3/31/2014	AG3-22	15	22	0	900	454.707	454.595	10.88	13.62	2.50E-08	0.28	0.30	2	1200	0.21	
160	3/31/2014	AG3-22	15	21	0	950	454.524	454.33	13.87	16.63	4.30E-08	0.32	0.36	2	1200	0.21	
161	3/31/2014	AG3-22	15	22	0	1000	454.249	453.891	16.88	19.76	7.60E-08	0.38	0.46	2	1200	0.21	
162	3/31/2014	AG3-22	15	8	0	1100	453.658	453.042	20.12	22.91	1.35E-07	0.51	0.64	2	1200	0.21	
164	3/5/2014	AG3-15	30	15	26	850	462.701	462.703	7.78	10.43	-4.53E-10	0.19	0.19	2	1200	0.16	
165	3/5/2014	AG3-15	30	15	26	900	462.652	462.639	10.85	13.56	2.88E-09	0.20	0.20	2	1200	0.16	
166	3/5/2014	AG3-15	30	15	26	950	462.584	462.555	13.87	16.60	6.38E-09	0.21	0.22	2	1200	0.16	
167	3/5/2014	AG3-15	30	15	26	1000	462.494	462.419	16.97	19.68	1.66E-08	0.23	0.25	2	1200	0.16	
168	3/5/2014	AG3-15	30	15	26	1100	462.271	461.95	20.12	22.83	7.12E-08	0.28	0.35	2	1200	0.16	
172	3/6/2014	AG3-16	30	29	26	950	470.614	470.576	13.98	16.63	8.46E-09	0.20	0.21	2	1200	0.12	
173	3/6/2014	AG3-16	30	29	26	1000	470.51	470.406	16.99	19.76	2.22E-08	0.22	0.25	2	1200	0.12	
174	3/6/2014	AG3-16	30	29	26	1100	470.222	469.564	20.07	22.94	1.35E-07	0.29	0.42	2	1200	0.12	
176	3/7/2014	AG3-17	50	52	26	850	466.444	466.438	7.70	10.55	1.25E-09	0.19	0.19	2	1200	0.15	
177	3/7/2014	AG3-17	50	51	26	900	466.385	466.35	10.77	13.51	7.61E-09	0.21	0.21	2	1200	0.15	
178	3/7/2014	AG3-17	50	51	26	950	466.29	466.215	13.84	16.69	1.57E-08	0.23	0.24	2	1200	0.15	
179	3/7/2014	AG3-17	50	51	26	1000	466.148	465.958	16.91	19.76	3.97E-08	0.26	0.30	2	1200	0.15	
180	3/7/2014	AG3-17	50	51	26	1100	465.767	464.757	20.09	22.84	2.19E-07	0.34	0.55	2	1200	0.15	
182	3/14/2014	AG3-19	100	100	26	850	459.711	459.703	7.87	10.52	1.82E-09	0.21	0.21	2	1200	0.22	
183	3/14/2014	AG3-19	100	100	26	900	459.652	459.639	10.77	13.51	2.87E-09	0.22	0.22	2	1200	0.22	
184	3/14/2014	AG3-19	100	99	26	950	459.575	459.478	13.95	16.66	2.16E-08	0.24	0.26	2	1200	0.22	
185	3/14/2014	AG3-19	100	99	26	1000	459.401	459.086	16.94	19.73	6.83E-08	0.27	0.34	2	1200	0.22	
186	3/14/2014	AG3-19	100	98	26	1100	458.788	458.109	20.18	21.24	3.88E-07	0.41	0.55	2	1200	0.22	
189	3/25/2014	AG3-20	150	152	26	900	452.222	452.195	10.74	13.51	5.99E-09	0.25	0.26	2	1200	0.22	
190	3/25/2014	AG3-20	150	151	26	950	452.137	451.999	13.78	16.69	2.91E-08	0.27	0.30	2	1200	0.22	
191	3/25/2014	AG3-20	150	151	26	1000	451.926	451.421	16.86	19.79	1.06E-07	0.32	0.43	2	1200	0.22	
192	3/25/2014	AG3-20	150	151	26	1100	451.018	447.52	20.15	23.00	7.56E-07	0.52	1.29	2	1200	0.22	
195	4/1/2014	WG1-17	100	103	26	900	466.935	466.924	10.80	13.58	2.35E-09	0.22	0.22	2	1200	0.17	
196	4/1/2014	WG1-17	100	102	26	950	466.865	466.77	13.78	16.63	1.98E-08	0.23	0.25	2	1200	0.17	
197	4/1/2014	WG1-17	100	103	26	1000	466.697	466.318	16.88	19.73	7.92E-08	0.27	0.35	2	1200	0.17	
198	4/1/2014	WG1-17	100	103	26	1100	466.064	463.773	20.07	22.97	4.71E-07	0.41	0.90	2	1200	0.17	
201	4/2/2014	WG1-18	50	51	26	900	463.309	463.301	10.71	13.59	1.67E-09	0.22	0.22	2	1200	0.18	
202	4/2/2014	WG1-18	50	52	26	950	463.244	463.173	13.84	16.69	1.49E-08	0.23	0.25	2	1200	0.18	
203	4/2/2014	WG1-18	50	52	26	1000	463.103	462.838	16.91	19.79	5.52E-08	0.27	0.32	2	1200	0.18	
204	4/2/2014	WG1-18	50	52	26	1100	462.635	461.385	20.07	22.91	2.64E-07	0.37	0.64	2	1200	0.18	
208	4/3/2014	WG1-19	30	30	26	950	463.009	462.969	13.82	16.64	8.51E-09	0.23	0.24	2	1200	0.17	
210	4/3/2014	WG1-19	30	30	26	1100	462.525	461.739	20.10	22.89	1.69E-07	0.33	0.50	2	1200	0.17	
213	4/4/2014	WG1-20	150	150	26	900	464.163	464.149	10.85	13.56	3.09E-09	0.21	0.21	2	1200	0.15	
214	4/4/2014	WG1-20	150	150	26	950	464.086	463.955	13.87	16.63	2.84E-08	0.23	0.26	2	1200	0.15	

Exp data number	Test Date	Specimen ID	H2O Pressure target	H2O Pressure actual [&]	H2 Pressure	Temperature	Weight before	Weight after	Time in the test before	Time in the test after	Rate	Weight loss % before	Weight loss % after	Sample preparaton duration	Sample preparaton temperature	Wt loss in outgassing	Notes
			Pa	Pa	Pa	oC	mg	mg	hr	hr	s^{-1}	%	%	h	^{o}C	mg	
215	4/4/2014	WG1-20	150	150	26	1000	463.875	463.425	16.88	19.59	9.94E-08	0.27	0.37	2	1200	0.15	
216	4/4/2014	WG1-20	150	149	26	1100	462.8	459.953	20.37	22.94	6.65E-07	0.50	1.12	2	1200	0.15	
217	4/7/2014	WG1-21	300	303	26	800	464.971	464.961	5.13	7.39	2.64E-09	0.21	0.22	2	1200	0.19	
218	4/7/2014	WG1-21	300	304	26	850	464.906	464.893	7.67	10.43	2.81E-09	0.23	0.23	2	1200	0.19	
220	4/7/2014	WG1-21	300	289	26	950	464.763	464.589	13.84	16.72	3.61E-08	0.26	0.30	2	1200	0.19	
221	4/7/2014	WG1-21	300	284	26	1000	464.502	463.907	16.91	19.73	1.26E-07	0.32	0.44	2	1200	0.19	
222	4/7/2014	WG1-21	300	309	26	1100	463.309	458.402	20.23	22.94	1.09E-06	0.57	1.62	2	1200	0.19	
225	4/8/2014	WG1-22	15	8	26	950	456.228	456.222	13.87	16.60	1.34E-09	0.24	0.24	2	1200	0.17	
226	4/8/2014	WG1-22	15	8	26	1000	456.161	456.086	16.97	19.81	1.61E-08	0.26	0.27	2	1200	0.17	
227	4/8/2014	WG1-22	15	8	25	1100	455.946	455.677	20.07	22.89	5.81E-08	0.30	0.36	2	1200	0.17	
234	6/30/2014	WG1-24	500	475	0	850	463.864	463.718	3.99	6.77	3.14E-08	0.25	0.28	2	1200	0.25	
235	6/30/2014	WG1-24	500	614	0	900	463.645	463.403	7.07	9.90	5.12E-08	0.30	0.35	2	1200	0.25	
236	6/30/2014	WG1-24	500	520	0	950	463.316	462.816	10.12	12.93	1.07E-07	0.37	0.48	2	1200	0.25	
237	6/30/2014	WG1-24	500	520	0	1000	462.648	461.181	13.25	16.01	3.19E-07	0.51	0.83	2	1200	0.25	
238	6/30/2014	WG1-24	500	519	0	1050	460.878	456.168	16.27	19.11	1.00E-06	0.89	1.91	2	1200	0.25	
240	7/1/2014	WG1-25	1000	988	0	850	464.032	463.951	4.46	6.31	2.62E-08	0.25	0.27	2	1200	0.18	
241	7/1/2014	WG1-25	1000	712	0	900	464.156	463.95	7.58	10.39	4.39E-08	0.22	0.27	2	1200	0.18	
242	7/1/2014	WG1-25	1000	738	0	950	463.683	463.353	11.44	13.43	9.93E-08	0.33	0.40	2	1200	0.18	
243	7/1/2014	WG1-25	1000	981	0	1000	463.183	461.502	13.76	16.41	3.80E-07	0.43	0.79	2	1200	0.18	
244	7/1/2014	WG1-25	1000	944	0	1050	460.798	454.859	16.99	19.61	1.37E-06	0.95	2.22	2	1200	0.18	
247	7/30/2014	WG1-27	100	95	0	850	466.431	466.355	4.17	8.00	1.18E-08	0.25	0.20	1	1200	0.26	
248	7/30/2014	WG1-27	100	98	26	850	465.3	465.263	10.39	20.73	2.14E-09	0.49	0.50	1	1200	0.26	
249	7/30/2014	WG1-27	100	96	22	850	465.253	465.137	21.64	26.02	1.58E-08	0.50	0.56	1	1200	0.26	
250	7/30/2014	WG1-27	100	96	25	850	465.093	465.033	28.92	37.39	4.23E-09	0.54	0.55	1	1200	0.26	
251	7/30/2014	WG1-27	100	93	0	850	465.014	464.769	38.64	48.00	1.56E-08	0.56	0.61	1	1200	0.26	
252	8/6/2014	WG1-28	100	100	0	850	464.83	464.582	3.22	10.97	1.91E-08	0.26	0.31	2	1200	0.17	
253	8/6/2014	WG1-28	100	100	25	850	464.511	464.435	12.35	21.41	5.02E-09	0.33	0.35	2	1200	0.17	
254	8/6/2014	WG1-28	100	100	0	850	464.428	464.312	21.88	25.35	2.00E-08	0.35	0.37	2	1200	0.17	
255	8/6/2014	WG1-28	100	99	26	850	464.3	464.229	25.78	33.22	5.71E-09	0.37	0.39	2	1200	0.17	
256	8/8/2014	WG1-29	100	102	0	850	466.76	466.582	3.26	10.19	1.53E-08	0.22	0.26	1	1200	0.07	
257	8/8/2014	WG1-29	100	102	13	850	466.544	466.454	12.07	22.56	5.11E-09	0.27	0.29	1	1200	0.07	
258	8/8/2014	WG1-29	100	102	25	850	466.444	466.414	24.44	28.09	4.89E-09	0.29	0.30	1	1200	0.07	
259	8/8/2014	WG1-29	100	102	42	850	466.407	466.368	28.93	35.49	3.54E-09	0.30	0.31	1	1200	0.07	
260	8/8/2014	WG1-29	100	102	0	850	466.351	466.078	36.90	46.27	1.74E-08	0.31	0.37	1	1200	0.07	
261	8/8/2014	WG1-29	200	215	0	850	466.024	465.787	47.49	55.17	1.84E-08	0.38	0.43	1	1200	0.07	
262	8/8/2014	WG1-29	200	213	44	850	465.753	465.682	56.95	68.10	3.80E-09	0.44	0.45	1	1200	0.07	
263	8/8/2014	WG1-29	200	212	21	850	465.661	465.59	70.72	78.78	5.25E-09	0.46	0.47	1	1200	0.07	
264	8/12/2014	WG1-30	100	31	0	850	465.485	465.392	3.15	7.24	1.36E-08	0.26	0.28	1	1200	0.144	
265	8/12/2014	WG1-30	100	31	13	850	465.377	465.368	8.70	11.20	2.15E-09	0.28	0.28	1	1200	0.144	
266	8/12/2014	WG1-30	100	31	25	850	465.365	465.339	11.74	20.03	1.87E-09	0.28	0.29	1	1200	0.144	

Exp data number	Test Date	Specimen ID	H2O Pressure target	H2O Pressure actual [&]	H2 Pressure	Temperature	Weight before	Weight after	Time in the test before	Time in the test after	Rate	Weight loss % before	Weight loss % after	Sample preparaton duration	Sample preparaton temperature	Wt loss in outgassing	Notes
			Pa	Pa	Pa	oC	mg	mg	hr	hr	s^{-1}	%	%	h	^{o}C	mg	
267	8/12/2014	WG1-30	100	31	39	850	465.338	465.326	20.52	24.36	1.87E-09	0.29	0.29	1	1200	0.144	
268	8/12/2014	WG1-30	100	31	0	850	465.305	465.22	26.12	28.80	1.89E-08	0.30	0.31	1	1200	0.144	
269	8/12/2014	WG1-30	100	52	0	850	465.202	465.118	29.36	31.91	1.97E-08	0.32	0.34	1	1200	0.144	
270	8/12/2014	WG1-30	100	52	39	850	465.105	465.094	33.01	35.56	2.58E-09	0.34	0.34	1	1200	0.144	
271	8/12/2014	WG1-30	100	52	25	850	465.09	465.036	36.42	45.13	3.70E-09	0.34	0.35	1	1200	0.144	
272	8/12/2014	WG1-30	100	52	13	850	465.027	464.985	46.60	51.04	5.65E-09	0.36	0.36	1	1200	0.144	
275	8/15/2014	WG1-31	15	14	25	850	469.05	469.042	12.39	18.33	7.98E-10	0.23	0.24	1	1200	0.097	
277	8/15/2014	WG1-31	50	52	25	850	469.037	469.019	22.48	27.74	2.03E-09	0.24	0.24	1	1200	0.097	
278	8/15/2014	WG1-31	100	105	26	850	469.01	468.938	28.50	35.88	5.78E-09	0.24	0.26	1	1200	0.097	
279	8/15/2014	WG1-31	30	30	25	850	468.937	468.911	36.89	46.14	1.67E-09	0.26	0.26	1	1200	0.097	
280	8/15/2014	WG1-31	150	150	28	850	468.881	468.786	46.99	51.82	1.17E-08	0.27	0.29	1	1200	0.097	
281	8/15/2014	WG1-31	150	154	28	850	468.786	468.703	51.82	58.44	7.43E-09	0.29	0.31	1	1200	0.097	
282	8/15/2014	WG1-31	3	5	25	850	468.721	468.706	59.62	70.73	8.00E-10	0.30	0.31	1	1200	0.097	
283	8/25/2014	WG1-32	15	15	26	800	455.577	455.569	5.83	14.08	5.91E-10	0.26	0.26	2	1200	0.15	
284	8/25/2014	WG1-32	15	15	26	850	455.496	455.472	14.89	24.11	1.59E-09	0.27	0.28	2	1200	0.15	
285	8/25/2014	WG1-32	15	15	26	900	455.393	455.365	25.13	34.36	1.85E-09	0.30	0.30	2	1200	0.15	
286	8/25/2014	WG1-32	15	15	26	950	455.285	455.207	34.99	44.46	5.03E-09	0.32	0.34	2	1200	0.15	
287	9/3/2014	WG1-33	30	30	25	800	462.61	462.59	6.36	14.26	1.44E-09	0.239	0.243	2	1200	0.207	
288	9/3/2014	WG1-33	30	30	25	850	462.53	462.49	15.17	24.17	2.74E-09	0.256	0.265	2	1200	0.207	
289	9/3/2014	WG1-33	30	30	25	900	462.42	462.35	25.08	34.45	4.36E-09	0.279	0.294	2	1200	0.207	
290	9/3/2014	WG1-33	30	30	25	950	462.28	462.10	35.04	44.59	1.16E-08	0.309	0.349	2	1200	0.207	
291	12/30/2014	WG1-34	30	30	0	800	468.207	468.247	10.34	15.33	6.30E-09	0.020	0.01	1	1200	0.063	
292	12/30/2014	WG1-34	30	30	0	850	468.235	468.143	15.82	25.31	9.81E-09	0.014	0.03	1	1200	0.063	
293	12/30/2014	WG1-34	30	30	0	900	468.226	468.067	26.13	35.55	1.47E-08	0.016	0.05	1	1200	0.063	
294	12/30/2014	WG1-34	30	30	0	950	468.225	467.903	35.88	45.69	2.40E-08	0.016	0.08	1	1200	0.063	
295	1/1/2015	WG1-34	12	12	0	850	468.307	468.226	9.69	14.45	9.22E-09	0.00	0.02	1	1200	0.06	
296	1/1/2015	WG1-34	12	12	0	900	468.233	468.191	14.78	19.51	1.37E-08	0.01	0.02	1	1200	0.06	
297	1/5/2015	WG1-34	3	3	0	800	468.273	468.253	4.42	9.45	5.54E-09	0.01	0.02	1	1200	0.092	
298	1/5/2015	WG1-34	3	3	0	850	468.237	468.22	9.81	14.48	1.02E-08	0.01	0.02	1	1200	0.092	
299	1/5/2015	WG1-34	3	3	0	900	468.233	468.197	14.81	19.63	1.27E-08	0.01	0.02	1	1200	0.092	
300	1/5/2015	WG1-34	3	3	0	950	468.229	468.181	19.93	24.60	1.51E-08	0.01	0.02	1	1200	0.092	
301	1/7/2016	WG1-34	3	3	0	800	468.686	468.276	5.33	9.94	3.09E-09	0.01	0.02	1	1200	0.081	
302	1/7/2016	WG1-34	3	3	0	850	468.239	468.228	10.25	14.95	9.09E-09	0.01	0.02	1	1200	0.081	
303	1/7/2016	WG1-34	3	3	0	900	468.234	468.188	15.26	20.05	1.39E-08	0.01	0.02	1	1200	0.081	
304	1/7/2016	WG1-34	3	3	0	950	468.229	468.165	20.32	25.18	1.65E-08	0.01	0.02	1	1200	0.081	
DATA REJECTED																	
239	6/30/2014	WG1-24	500	530	0	1100	455.242	441.4	19.41	22.27	2.95E-06	2.11	5.08	2	1200	0.25	
245	7/1/2014	WG1-25	1000	702	0	1100	453.542	442.934	19.95	21.74	3.63E-06	2.51	4.79	2	1200	0.18	
246	7/1/2014	WG1-25	1000	1447	0	1100	442.934	430.093	21.74	22.84	7.32E-06	4.79	7.55	2	1200	0.18	

Exp data number	Test Date	Specimen ID	H2O Pressure target	H2O Pressure actual [&]	H2 Pressure	Temperature	Weight before	Weight after	Time in the test before	Time in the test after	Rate	Weight loss % before	Weight loss % after	Sample preparaton duration	Sample preparaton temperature	Wt loss in outgassing	Notes
			Pa	Pa	Pa	oC	mg	mg	hr	hr	s^{-1}	%	%	h	°C	mg	
163	3/5/2014	AG3-15	30	15	26	800	462.756	462.756	4.82	7.36	0.00E+00	0.18	0.18	2	1200	0.16	negative rate
169	3/6/2014	AG3-16	30	30	26	800	470.752	470.749	4.68	7.34	6.65E-10	0.17	0.17	2	1200	0.12	exp. Errors
170	3/6/2014	AG3-16	30	15	25	850	470.696	470.7	7.73	10.41	-8.81E-10	0.18	0.18	2	1200	0.12	negative rate
175	3/7/2014	AG3-17	50	52	26	800	466.475	466.491	4.60	7.36	-3.45E-09	0.19	0.18	2	1200	0.15	negative rate
188	3/25/2014	AG3-20	150	151	26	850	452.259	452.272	7.67	10.43	-2.89E-09	0.24	0.24	2	1200	0.22	negative rate
193	4/1/2014	WG1-17	100	102	26	800	467.009	466.98	5.13	7.39	7.63E-09	0.20	0.21	2	1200	0.17	exp. Errors
194	4/1/2014	WG1-17	100	101	25	850	466.953	466.985	7.70	10.46	-6.90E-09	0.22	0.21	2	1200	0.17	negative rate
199	4/2/2014	WG1-18	50	51	26	800	463.408	463.386	5.51	7.42	6.90E-09	0.20	0.20	2	1200	0.18	exp. Errors
200	4/2/2014	WG1-18	50	51	26	850	463.34	463.361	7.70	10.55	-4.42E-09	0.21	0.21	2	1200	0.18	negative rate
205	4/3/2014	WG1-19	30	30	26	800	463.123	463.123	5.53	7.38	0.00E+00	0.20	0.20	2	1200	0.17	negative rate
206	4/3/2014	WG1-19	30	30	26	850	463.075	463.114	7.68	10.47	-8.39E-09	0.21	0.20	2	1200	0.17	negative rate
207	4/3/2014	WG1-19	30	30	26	900	463.063	463.066	10.75	13.55	-6.43E-10	0.21	0.21	2	1200	0.17	negative rate
209	4/3/2014	WG1-19	30	30	26	1000	465.219	462.71	16.95	19.80	5.26E-07	-0.25	0.29	2	1200	0.17	exp. Errors
211	4/4/2014	WG1-20	150	152	26	800	464.249	464.24	4.88	7.39	2.15E-09	0.19	0.19	2	1200	0.15	exp. Errors
212	4/4/2014	WG1-20	150	150	26	850	464.191	464.215	7.81	10.49	-5.36E-09	0.21	0.20	2	1200	0.15	negative rate
223	4/8/2014	WG1-22	15	22	26	850	456.287	456.317	7.67	10.43	-6.62E-09	0.23	0.22	2	1200	0.17	negative rate
224	4/8/2014	WG1-22	15	8	26	900	456.266	456.283	10.74	13.59	-3.63E-09	0.23	0.23	2	1200	0.17	negative rate
229	4/9/2014	WG1-23	30	4	96	850	469.615	469.638	7.69	10.45	-4.93E-09	0.11	0.10	2	1200	0.26	negative rate
230	4/9/2014	WG1-23	30	4	96	900	469.638	469.655	10.79	13.46	-3.77E-09	0.10	0.10	2	1200	0.26	negative rate
231	4/9/2014	WG1-23	30	4	96	950	469.634	469.655	13.89	16.62	-4.55E-09	0.10	0.10	2	1200	0.26	negative rate
273	8/15/2014	WG1-31	3	4	85	850	469.07	469.062	3.49	9.17	5.21E-10	0.23	0.23	1	1200	0.097	exp. Errors
274	8/15/2014	WG1-31	3	4	85	850	469.062	469.064	9.17	11.04	-6.33E-10	0.23	0.23	1	1200	0.097	negative rate
187	3/25/2014	AG3-20	150	152	26	800	452.311	452.31	5.38	7.39	3.06E-10	0.23	0.23	2	1200	0.22	exp. Errors
219	4/7/2014	WG1-21	300	296	26	900	464.84	464.828	10.74	13.56	2.54E-09	0.24	0.25	2	1200	0.19	unstable
276	8/15/2014	WG1-31	15	8	25	850	469.042	469.041	18.33	21.72	1.75E-10	0.24	0.24	1	1200	0.097	exp. Errors
171	3/6/2014	AG3-16	30	29	26	900	470.671	470.67	12.67	13.59	6.41E-10	0.19	0.19	2	1200	0.12	unstable
228	4/9/2014	WG1-23	30	4	96	800	469.592	469.613	4.56	7.26	-4.60E-09	0.11	0.11	2	1200	0.26	exp. Errors
232	4/9/2014	WG1-23	30	4	96	1000	469.65	469.601	16.96	19.63	1.09E-08	0.10	0.11	2	1200	0.26	exp. Errors
233	4/9/2014	WG1-23	30	4	96	1100	469.581	469.517	20.15	22.85	1.40E-08	0.12	0.13	2	1200	0.26	exp. Errors
181	3/14/2014	AG3-19	100	101	26	800	459.769	459.772	5.30	7.25	-9.29E-10	0.19	0.19	2	1200	0.22	negative rate
43	1/9/2014	WG1-12	15	15	0	800	463.377	463.249	4.13	6.72	2.96E-08	0.18	0.21	2	1200	0.14	unstable

ANNEX 5 PHYSICAL MEASUREMENTS ON GRAPHITE PCEA SPECIMENS BEFORE AND AFTER TESTS

Experimental data number	Date of test	Specimen ID	Before Oxidation Weight (mg)	Average L (mm)	Average D (mm)	Density (g/cm^3)	After Oxidation Weight (mg)	Average L (mm)	Average D (mm)	Density (g/cm^3)	P_{H2O} (Pa)	P_{H2} (Pa)	Weight loss	Notes
2; 3; 4; 5; 6	2/21/2012	#1--1	447.6				446.8				100	0		
7; 8; 9; 10; 11	2/22/2012	#1--2	445.3				447.1				70	0		
12; 13; 14; 15; 16	2/23/2012	#1--3	445.1				443.3				150	0		
17; 18; 19; 20; 21	2/24/2012	#1--4	443.5				441.7				250	0		
22; 23; 24; 25; 26	3/1/2012	#2--1	451.1				450.4				100	0		
27; 28; 29; 30; 31	3/5/2012	#2--2	445.8				444.9				70	0		
32; 33; 34; 35; 36	3/6/2012	#2--3	449.7				449.0				100	0		
37; 38; 39; 40; 41	3/7/2012	#2--4									150	0		
42; 43; 44; 45; 46	3/8/2012	#3--1	446.4				444.0				250	0		
47; 48; 49; 50; 51	3/19/2012	#3--2	446.9				445.6				70	0		
52; 53; 54; 55; 56	3/20/2012	#3--4	448.5				447.2				65	0		
57; 58; 59; 60; 61	3/26/2012	#3--3	445.0				443.8				150	0		
62; 63; 64; 65; 66	4/19/2012	DB1-1	444.9				443.8				250	0		
67; 68; 69; 70; 71	4/23/2012	DB1-2	443.7				441.6				70	0		
72; 73; 74; 75; 76	4/24/2012	DB1-3	445.2				444.3				70	0		
77; 78; 79; 80; 81	4/26/2012	DB1-4	446.2				444.9				50	0		
82; 83; 84; 85; 86;	5/1/2012	DB1-5	447.8				446.5				30	0		
87; 88; 89; 90; 91	5/2/2012	DB2-1	450.9				448.1				200	0		
92; 93; 94; 95; 96	5/11/2012	DB2-2	444.0				442.9				100	0		
97; 98; 99; 100; 101	5/14/2012	DB2-3	443.7				442.4				150	0		
102; 103; 104; 105; 106	5/16/2012	DB2-5	448.5				446.6				100	0		
107; 108; 109; 110; 111	5/17/2012	DB2-6	444.2				442.7				150	0		
112; 113; 114; 115; 116	5/21/2012	DB2-7	445.3				444.0				500	0		
117; 118; 119; 120; 121	5/22/2012	DB2-8	447.8				444.5				750	0		
122; 123; 124; 125; 126	5/23/2012	DB3-1	444.9				444.1				3	0		
127;	5/30/2012	DB3-2	443.9				442.8				150	0		
128; 129	5/31/2012	DB3-3	444.2				443.7				150	0		
130;131	6/27/2012	DB3-4									75	150		
133; 132	6/28/2012	DB3-5									75	100		
134; 135	7/3/2012	DB3-6									75	100		

Experimental data number	Date of test	Specimen ID	Before Oxidation Weight (mg)	Average L (mm)	Average D (mm)	Density (g/cm^3)	After Oxidation Weight (mg)	Average L (mm)	Average D (mm)	Density (g/cm^3)	P_{H2O} (Pa)	P_{H2} (Pa)	Weight loss	Notes
136;137	7/5/2012	DB3-7	442.5	20.01	3.95	1.804	437.5	19.98	3.96	1.777	30	0	1.13%	
138; 139	7/9/2012	DB3-8	443.3	20.01	3.96	1.798	425.2	19.99	3.91	1.771	300	0	4.08%	
140; 141	7/10/2012	DB4-1	440.2	19.98	3.97	1.776	434.2	19.95	3.96	1.767	300	100	1.36%	
142; 143	7/11/2012	DB4-2	438.5	20.04	3.94	1.792	423.9	20.01	3.92	1.755	300	0	3.33%	
144; 145	7/12/2012	DB4-3	443.4	20.01	3.98	1.785	440.0	19.99	3.96	1.790	30	0	0.77%	
146; 147	7/16/2012	DB4-4	444.4	19.97	3.98	1.786	440.9	19.95	3.97	1.787	30	100	0.79%	
148; 149	7/17/2012	DB4-5	442.4	19.82	3.98	1.792	418.1	19.78	3.94	1.738	300	0	5.49%	
150; 151	7/18/2012	DB4-6	446.8	20.00	3.97	1.805	437.3	19.98	3.96	1.782	30	0	2.13%	
152; 153	7/19/2012	DB4-7	443.7	20.00	3.97	1.790	433.4	19.98	3.95	1.771	300	100	2.32%	
154; 155	7/20/2012	DB4-8	439.9	20.06	3.94	1.797	423.1	20.02	3.91	1.758	300	0	3.82%	
156; 157	7/23/2012	#10-1	442.1	19.94	3.97	1.788	420.2	19.92	3.95	1.726	30	0	4.95%	
158; 159	7/24/2012	#10-2	440.7	20.07	3.98	1.767	436.1	20.03	3.96	1.768	30	100	1.04%	
	7/25/2012	#10-3	445.9	20.01	3.99	1.783	328.2	19.97	3.96	1.336	300	0	26.40%	high wt loss
160; 161	7/26/2012	#11-1	452.4	20.00	3.99	1.811	440.2	19.98	3.97	1.783	300	0	2.70%	
162; 163	7/30/2012	#0-1	443.1	20.03	3.95	1.808	437.5	20.01	3.95	1.788	30	0	1.26%	
164; 165	8/1/2013	#0-2	447.5	19.98	3.99	1.788	440.0	19.94	3.98	1.778	300	100	1.68%	
	8/2/2012	#0-3	447.3	20.11	3.98	1.793	380.0	20.02	3.98	1.528	300	0	15.05%	high wt loss
166; 167	8/6/2012	#0-4	443.2	20.07	3.96	1.797	431.8	20.01	3.91	1.797	300	0	2.57%	
168; 169	8/7/2012	#0-5	444.4	19.96	3.98	1.792	438.9	19.94	3.97	1.780	30	0	1.24%	
170; 171	8/8/2012	#0-6	454.4	19.96	3.99	1.826	453.3	19.95	3.99	1.818	30	100	0.24%	
172; 173	8/9/2012	#0-7	447.7	19.99	3.97	1.814	416.6	19.99	3.96	1.695	300	0	6.95%	
174; 175	8/13/2012	#0-8	442.7				434.6	20.00	3.97	1.756	30	0	1.83%	
176; 177	8/15/2012	#0-10	455.0				445.5	20.00	3.97	1.801	300	100	2.09%	
181; 182	8/16/2012	#0-11	442.0				438.6	20.06	3.97	1.771	30	0	0.77%	
153; 184; 185	10/18/2012	#0-12	443.4	20.01	3.99	1.772	417.8	20.05	3.97	1.686	300	0	5.76%	
186; 187; 188	10/22/2012	#0-13	445.9	20.03	3.95	1.814	443.2	20.03	3.97	1.788	30	100	0.60%	
189; 190; 191	10/25/2012	#0-14	449.9	19.96	4.02	1.779	444.5	19.95	4.01	1.761	30	0	1.22%	
192; 196; 194	10/30/2012	#0-15	441.6	20.01	3.96	1.789	436.7	20.00	3.95	1.786	300	100	1.11%	
195; 196; 197	11/5/2012	#0-16	441.9	20.02	3.95	1.803	439.8	20.03	3.97	1.770	30	100	0.47%	
	2/15/2013	#0-17	441.3	20.00	3.97	1.779	406.1	20.00	3.98	1.636	300	0	7.98%	high wt loss
	2/18/2013	#0-18	446.0	19.99	3.99	1.786	364.2	19.97	3.98	1.468	300	0	18.33%	significant pits
198; 199; 200	2/20/2013	#0-19	450.1	19.99	4.00	1.791	419.2	19.98	3.99	1.680	300	0	6.87%	
	2/25/2013	#0-20	451.2	20.01	4.00	1.792	238.8	19.91	3.86	1.027	30	100	47.07%	high wt loss
	3/1/2013	#0-21	441.1	20.04	3.95	1.793	431.6	20.03	3.94	1.765	300	0	2.16%	BO fntc 50 hr
201; 202; 203	3/5/2013	#0-22	446.4	20.03	3.99	1.780	444.9	20.02	3.98	1.783	30	100	0.34%	
178; 179; 180	3/7/2013	#0-23	446.7	19.98	3.99	1.789	421.2	19.97	3.98	1.697	300	0	5.69%	
204; 205; 206	3/11/2013	#0-24	448.5	19.95	3.99	1.800	436.1	19.95	3.99	1.748	300	100	2.76%	

Experimental data number	Date of test	Specimen ID	Before Oxidation Weight (mg)	Average L (mm)	Average D (mm)	Density (g/cm^3)	After Oxidation Weight (mg)	Average L (mm)	Average D (mm)	Density (g/cm^3)	P_{H2O} (Pa)	P_{H2} (Pa)	Weight loss	Notes
207; 208; 209	3/12/2013	#0-25	455.1	19.99	4.00	1.815	448.5	19.97	4.00	1.790	30	100	1.45%	
210; 211; 212	3/14/2013	#0-26	454.1	20.00	3.98	1.824	449.9	19.99	3.97	1.819	300	100	0.92%	
	3/18/2013	#0-27	447.2	20.01	3.96	1.811	384.3	20.00	3.97	1.549	300	0	14.06%	significant pits
213; 214; 215	3/19/2013	#0-28	428.0	20.10	3.91	1.774	414.4	20.07	3.90	1.733	300	0	3.17%	
216; 217; 218; 219; 220	3/26/2013	DB8-1	438.7	19.74	3.99	1.776	429.8	19.73	3.98	1.753	300	100	2.03%	
221; 222; 223	4/2/2013	DB8-2	450.5	20.05	3.98	1.803	438.5	20.03	3.98	1.765	100	0	2.66%	
224; 225; 226; 227	4/3/2013	DB8-3	446.0	20.02	3.98	1.794	440.5	20.02	3.97	1.774	100	100	1.24%	
228; 229; 230; 231	4/5/2013	DB8-4	446.4	20.01	3.99	1.785	434.7	19.93	3.98	1.751	100	50	2.62%	
	4/16/2013	DB9-1	437.7	20.02	3.96	1.779	425.9	19.92	3.94	1.757	30	50	2.70%	noise in the data
	4/25/2013	DB9-2	439.3	19.99	3.95	1.793	431.7	19.97	3.94	1.772			1.72%	noise in the data
232; 233; 234; 235	5/24/2013	DB9-3	440.9	19.99	3.96	1.792	430.8	19.96	3.96	1.751	100	50	2.30%	
	5/28/2013	DB9-4	444.0	20.02	3.97	1.795	437.4						1.48%	test operation
	5/29/2013	DB9-5	437.5	20.02	3.95	1.786								lost in the furnace
236; 237; 238; 239	5/31/2013	DB9-6	438.3	20.01	3.94	1.801	433.8	19.96	3.94	1.783	30	50	1.03%	lost parameters file
240; 241; 242; 243	6/3/2013	DB10-1	446.9	20.02	3.98	1.799	437.9	19.97	3.97	1.769	30	150	2.02%	
244; 245; 246; 247	6/4/2013	DB10-2	444.9	20.00	3.98	1.791	421.5	19.75	3.98	1.719	100	150	5.25%	
248; 249; 250; 251	6/6/2013	DB10-3	448.5	20.09	3.98	1.798	439.6	20.03	3.97	1.771	15	0	1.99%	
252; 253; 254; 255	6/7/2013	DB10-4	441.0	20.08	3.95	1.796	433.8	20.00	3.95	1.774	15	0	1.63%	
256; 257; 258; 259	6/18/2013	DB10-5	444.9	20.01	3.97	1.797	436.1	19.97	3.97	1.767	15	0	1.97%	
260; 261; 262; 263	6/20/2013	DB10-6	445.8	20.00	3.98	1.795	443.1	19.97	3.98	1.787	0	0	0.61%	
264; 265; 266; 267	6/21/2013	DB10-7	447.3	20.04	3.98	1.791	444.8	20.13	3.98	1.778	0	0	0.56%	
268; 269; 270	7/15/2013	#12--1	454.3	20.04	4.00	1.800	452.7	20.05	4.01	1.790	0	0	0.36%	
271; 272; 273; 274; 275; 276	7/25/2013	#12--2	448.6	20.00	4.01	1.778	444.1	19.99	4.00	1.769	15	0	1.00%	
277; 278; 279; 280; 281; 282	7/26/2013	#12--3	449.2	20.07	4.00	1.785	447.5	20.07	4.00	1.776	15	15	0.39%	
283; 284; 285; 286; 287; 288	7/27/2013	#12--4	448.5	20.03	4.00	1.786	446.1	20.02	4.00	1.777	30	0	0.53%	
289; 290; 291; 292; 293; 294	7/29/2013	#17-1	453.4	19.97	4.02	1.794	447.0	19.97	4.01	1.770	30	30	1.41%	
295; 296; 297; 298; 299; 300	7/30/2013	#17-2	452.5	20.00	4.00	1.798	447.8	20.01	4.00	1.783	100	0	1.03%	
301; 302; 303; 304; 305; 306	7/31/2013	#17-3	450.6	20.01	3.99	1.800	447.5	20.00	3.99	1.792	15	0	0.70%	
307; 308; 309; 310; 311; 312	8/2/2013	#17-4	453.8	19.96	4.01	1.803	444.2	19.96	4.01	1.761	100	30	2.13%	
313; 314; 315; 316; 317; 318	8/3/2013	#16-1	452.2	20.01	4.00	1.796	434.5	20.01	4.00	1.727	150	0	3.91%	
319; 320; 321; 322; 323; 324	8/4/2013	#16-2	449.4	20.03	3.99	1.796	429.8	20.03	3.99	1.717	100	100	4.35%	significant pits
325; 236; 327; 328; 329; 330	8/5/2013	#16-3	447.8	20.03	3.99	1.793	441.5	20.02	3.98	1.771	100	150	1.41%	
331; 332; 333; 334; 335; 336	8/6/2013	#16-4	454.4	19.98	4.02	1.796	453.9	19.97	4.02	1.796	30	150	0.12%	
337; 338; 339; 340; 341; 342	8/7/2013	#14-01	442.5	20.02	3.98	1.782	440.7	20.01	3.97	1.776	30	100	0.42%	
343; 344; 345; 346; 347; 348	8/8/2013	#14-02	448.3	20.01	4.00	1.782	446.2	19.99	4.00	1.775	15	100	0.46%	
349; 350	8/12/2013	#14-03	449.9	19.98	4.01	1.785	449.4	19.97	4.01	1.779	0	100	0.11%	
351; 352; 353; 354; 355	8/21/2013	#14-04	451.9	19.97	4.01	1.794	435.1	19.97	4.01	1.730	100	100	3.71%	

ANNEX 6 LOG OF EXPERIMENTAL RESULTS - GRAPHITE PCEA

Exp data number	Test Date	Specimen ID	H2O Pressure target	H2O Pressure actual [&]	H2 Pressure	Temperature	Weight before	Weight after	Time in the test before	Time in the test after	Rate	Weight loss % before	Weight loss % after	Sample preparaton duration	Sample preparaton temperature	Wt loss in outgassing
			Pa	Pa	Pa	oC	mg	mg	hr	hr	s^{-1}	%	%	h	^{o}C	mg
2	2/21/12	#1-1	100	105	0	900	446.79	446.65	6.97	9.97	2.86E-08	0.00%	0.03%	4	1100	0.352
3	2/21/12	#1-1	100	104	0	925	446.64	446.45	10.01	13.01	3.97E-08	0.03%	0.08%	4	1100	0.352
4	2/21/12	#1-1	100	102	0	950	446.43	446.15	13.05	16.05	5.93E-08	0.08%	0.14%	4	1100	0.352
5	2/21/12	#1-1	100	101	0	975	446.13	445.68	16.09	19.09	9.50E-08	0.15%	0.25%	4	1100	0.352
6	2/21/12	#1-1	100	103	0	1000	445.66	444.91	19.13	22.13	1.56E-07	0.25%	0.42%	4	1100	0.352
7	2/22/12	#1-2	50	69	0	**900**	444.90	444.79	6.97	9.97	2.17E-08	0.00%	0.02%	4	1100	0.242
8	2/22/12	#1-2	50	68	0	**925**	444.78	444.65	10.01	13.01	2.89E-08	0.03%	0.06%	4	1100	0.242
9	2/22/12	#1-2	50	65	0	**950**	444.64	444.44	13.05	16.05	4.17E-08	0.06%	0.10%	4	1100	0.242
10	2/22/12	#1-2	50	66	0	**975**	444.42	444.11	16.09	19.09	6.55E-08	0.11%	0.18%	4	1100	0.242
11	2/22/12	#1-2	50	68	0	**1000**	444.09	443.53	19.13	22.13	1.19E-07	0.18%	0.31%	4	1100	0.242
12	2/23/12	#1-3	150	145	0	**900**	444.37	444.19	6.97	9.97	3.59E-08	0.00%	0.04%	4	1100	0.726
13	2/23/12	#1-3	150	140	0	**925**	444.18	443.97	10.01	13.01	4.56E-08	0.04%	0.09%	4	1100	0.726
14	2/23/12	#1-3	150	142	0	**950**	443.95	443.61	13.05	16.05	7.19E-08	0.09%	0.17%	4	1100	0.726
15	2/23/12	#1-3	150	145	0	**975**	443.59	443.02	16.09	19.09	1.30E-07	0.17%	0.30%	4	1100	0.726
16	2/23/12	#1-3	150	145	0	**1000**	443.00	442.11	19.13	22.13	2.24E-07	0.31%	0.51%	4	1100	0.726
17	2/24/13	#1-4	250	255	0	900	445.62	445.41	6.97	9.97	2.95E-08	0.00%	0.05%	4	1100	0.945
18	2/24/13	#1-4	250	258	0	925	445.39	445.09	10.01	13.01	4.04E-08	0.05%	0.12%	4	1100	0.945
19	2/24/13	#1-4	250	259	0	950	445.07	444.67	13.05	16.05	5.35E-08	0.12%	0.21%	4	1100	0.945
20	2/24/13	#1-4	250	261	0	975	444.65	444.01	16.09	19.09	8.57E-08	0.22%	0.36%	4	1100	0.945
21	2/24/13	#1-4	250	261	0	1000	443.98	442.77	19.13	22.13	1.67E-07	0.37%	0.64%	4	1100	0.945
22	3/1/12	#2-1	100	104	0	900	446.25	446.18	23.47	26.47	1.48E-08	0.00%	0.02%	20	1100	2.451
23	3/1/12	#2-1	100	99	0	925	446.17	446.07	26.51	29.51	2.04E-08	0.02%	0.04%	20	1100	2.451
24	3/1/12	#2-1	100	99	0	950	446.06	445.90	29.55	32.55	3.37E-08	0.04%	0.08%	20	1100	2.451
25	3/1/12	#2-1	100	99	0	975	445.89	445.64	32.59	35.59	5.07E-08	0.08%	0.14%	20	1100	2.451
26	3/1/12	#2-1	100	97	0	1000	445.63	445.23	35.63	38.63	8.40E-08	0.14%	0.23%	20	1100	2.451
27	3/5/12	#2-2	70	65	0	900	445.72	445.44	6.80	9.80	5.82E-08	0.00%	0.06%	4	1100	0.368
28	3/5/12	#2-2	70	70	0	925	445.44	445.23	9.84	12.84	4.43E-08	0.06%	0.11%	4	1100	0.368
29	3/5/12	#2-2	70	70	0	950	445.23	445.08	12.88	15.88	3.14E-08	0.11%	0.14%	4	1100	0.368
30	3/5/12	#2-2	70	73	0	975	445.09	444.95	15.93	18.93	2.79E-08	0.14%	0.17%	4	1100	0.368
31	3/5/12	#2-2	70	68	0	1000	444.96	444.87	18.97	21.97	1.86E-08	0.17%	0.19%	4	1100	0.368
32	3/6/12	#2-3	100	107	0	900	449.74	449.48	6.80	9.80	5.39E-08	0.00%	0.06%	4	1100	0.228
33	3/6/12	#2-3	100	106	0	925	449.49	449.30	9.84	12.84	3.84E-08	0.06%	0.10%	4	1100	0.228
34	3/6/12	#2-3	100	105	0	950	449.30	449.16	12.88	15.88	3.01E-08	0.10%	0.13%	4	1100	0.228
35	3/6/12	#2-3	100	104	0	975	449.16	449.04	15.93	18.93	2.41E-08	0.13%	0.15%	4	1100	0.228
36	3/6/12	#2-3	100	104	0	1000	449.05	448.95	18.97	21.97	2.11E-08	0.15%	0.18%	4	1100	0.228

Exp data number	Test Date	Specimen ID	H2O Pressure target	H2O Pressure actual [&]	H2 Pressure	Temperature	Weight before	Weight after	Time in the test before	Time in the test after	Rate	Weight loss % before	Weight loss % after	Sample preparaton duration	Sample preparaton temperature	Wt loss in outgassing
			Pa	Pa	Pa	oC	mg	mg	hr	hr	s^{-1}	%	%	h	^{o}C	mg
37	3/7/12	#2-4	150	176	0	900	451.08	450.68	6.80	9.80	5.37E-08	0.00%	0.09%	4	1100	0.280
38	3/7/12	#2-4	150	174	0	925	450.68	450.37	9.84	12.84	3.83E-08	0.09%	0.16%	4	1100	0.280
39	3/7/12	#2-4	150	174	0	950	450.38	450.15	12.88	15.88	3.00E-08	0.16%	0.21%	4	1100	0.280
40	3/7/12	#2-4	150	173	0	975	450.15	449.98	15.93	18.93	2.40E-08	0.21%	0.24%	4	1100	0.280
41	3/7/12	#2-4	150	174	0	1000	449.99	449.85	18.97	21.97	2.11E-08	0.24%	0.27%	4	1100	0.280
42	3/8/12	#3-1	250	264	0	900	446.36	445.46	6.80	9.80	1.88E-07	0.00%	0.20%	4	1100	0.263
43	3/8/12	#3-1	250	261	0	925	445.45	444.78	9.84	12.84	1.39E-07	0.20%	0.35%	4	1100	0.263
44	3/8/12	#3-1	250	258	0	950	444.78	444.30	12.88	15.88	9.94E-08	0.35%	0.46%	4	1100	0.263
45	3/8/12	#3-1	250	247	0	975	444.30	443.99	15.93	18.93	6.41E-08	0.46%	0.53%	4	1100	0.263
46	3/8/12	#3-1	250	238	0	1000	444.00	443.83	18.97	21.97	3.47E-08	0.53%	0.57%	4	1100	0.263
47	3/19/12	#3-2	70	64	0	900	446.91	446.50	6.80	9.80	2.15E-08	0.00%	0.09%	4	1100	0.263
48	3/19/12	#3-2	70	64	0	925	446.50	446.19	9.84	12.84	2.87E-08	0.09%	0.16%	4	1100	0.263
49	3/19/12	#3-2	70	65	0	950	446.19	445.97	12.88	15.88	4.14E-08	0.16%	0.21%	4	1100	0.263
50	3/19/12	#3-2	70	72	0	975	445.98	445.79	15.93	18.93	6.51E-08	0.21%	0.25%	4	1100	0.263
51	3/19/12	#3-2	70	72	0	1000	445.80	445.66	18.97	21.97	1.18E-07	0.25%	0.28%	4	1100	0.263
52	3/20/12	#3-4	65	65	0	900	446.91	446.50	6.80	9.80	2.16E-08	0.00%	0.09%	4	1100	0.263
53	3/20/12	#3-4	65	63	0	925	446.50	446.19	9.84	12.84	2.88E-08	0.09%	0.16%	4	1100	0.263
54	3/20/12	#3-4	65	65	0	950	446.19	445.97	12.88	15.88	4.16E-08	0.16%	0.21%	4	1100	0.263
55	3/20/12	#3-4	65	71	0	975	445.98	445.79	15.93	18.93	6.53E-08	0.21%	0.25%	4	1100	0.263
56	3/20/12	#3-4	65	74	0	1000	445.80	445.66	18.97	21.97	1.18E-07	0.25%	0.28%	4	1100	0.263
57	3/26/12	#3-3	150	148	0	900	444.62	444.53	6.97	9.97	1.76E-08	0.00%	0.02%	4	1100	0.575
58	3/26/12	#3-3	150	136	0	925	444.52	444.39	10.01	13.01	2.74E-08	0.02%	0.05%	4	1100	0.575
59	3/26/12	#3-3	150	134	0	950	444.38	444.18	13.05	16.05	4.21E-08	0.05%	0.10%	4	1100	0.575
60	3/26/12	#3-3	150	133	0	975	444.17	443.87	16.09	19.09	6.28E-08	0.10%	0.17%	4	1100	0.575
61	3/26/12	#3-3	150	154	0	1000	443.85	443.32	19.13	22.13	1.12E-07	0.17%	0.29%	4	1100	0.575
62	4/19/12	DB1-1	250	247	0	900	444.87	444.75	6.97	9.97	2.57E-08	0.00%	0.03%	4	1100	0.415
63	4/19/12	DB1-1	250	244	0	925	444.74	444.56	10.01	13.01	3.66E-08	0.03%	0.07%	4	1100	0.415
64	4/19/12	DB1-1	250	233	0	950	444.55	444.31	13.05	16.05	5.17E-08	0.07%	0.13%	4	1100	0.415
65	4/19/12	DB1-1	250	256	0	975	444.29	443.88	16.09	19.09	8.57E-08	0.13%	0.22%	4	1100	0.415
66	4/19/12	DB1-1	250	260	0	1000	443.86	443.17	19.13	22.13	1.44E-07	0.23%	0.38%	4	1100	0.415
67	4/23/12	DB1-2	70	68	0	900	442.62	442.43	6.97	9.97	3.71E-08	0.00%	0.04%	4	1100	0.743
68	4/23/12	DB1-2	70	63	0	925	442.42	442.23	10.01	13.01	3.98E-08	0.04%	0.09%	4	1100	0.743
69	4/23/12	DB1-2	70	62	0	950	442.22	441.99	13.05	16.05	4.82E-08	0.09%	0.14%	4	1100	0.743
70	4/23/12	DB1-2	70	66	0	975	441.97	441.68	16.09	19.09	6.24E-08	0.15%	0.21%	4	1100	0.743
71	4/23/12	DB1-2	70	71	0	1000	441.66	441.22	19.13	22.13	9.22E-08	0.22%	0.32%	4	1100	0.743
72	4/24/12	DB1-3	70	62	0	900	445.21	445.07	6.97	9.97	3.02E-08	0.00%	0.03%	4	1100	0.357
73	4/24/12	DB1-3	70	64	0	925	445.06	444.89	10.01	13.01	3.54E-08	0.03%	0.07%	4	1100	0.357
74	4/24/12	DB1-3	70	63	0	950	444.88	444.67	13.05	16.05	4.38E-08	0.07%	0.12%	4	1100	0.357
75	4/24/12	DB1-3	70	67	0	975	444.65	444.38	16.09	19.09	5.76E-08	0.12%	0.19%	4	1100	0.357
76	4/24/12	DB1-3	70	70	0	1000	444.36	444.02	19.13	22.13	7.20E-08	0.19%	0.27%	4	1100	0.357

Exp data number	Test Date	Specimen ID	H2O Pressure target	H2O Pressure actual [&]	H2 Pressure	Temperature	Weight before	Weight after	Time in the test before	Time in the test after	Rate	Weight loss % before	Weight loss % after	Sample preparaton duration	Sample preparaton temperature	Wt loss in outgassing
			Pa	Pa	Pa	oC	mg	mg	hr	hr	s^{-1}	%	%	h	^{o}C	mg
77	4/26/12	DB1-4	50	49	0	900	445.89	445.71	6.97	9.97	3.83E-08	0.00%	0.04%	4	1100	0.455
78	4/26/12	DB1-4	50	47	0	925	445.69	445.47	10.01	13.01	4.59E-08	0.04%	0.09%	4	1100	0.455
79	4/26/12	DB1-4	50	47	0	950	445.46	445.23	13.05	16.05	4.91E-08	0.10%	0.15%	4	1100	0.455
80	4/26/12	DB1-4	50	48	0	975	445.21	444.92	16.09	19.09	6.06E-08	0.15%	0.22%	4	1100	0.455
81	4/26/12	DB1-4	50	56	0	1000	444.90	444.50	19.13	22.13	8.45E-08	0.22%	0.31%	4	1100	0.455
82	5/1/12	DB1-5	30	31	0	900	447.44	447.21	6.97	9.97	3.85E-08	0.00%	0.05%	4	1100	0.648
83	5/1/12	DB1-5	30	31	0	925	447.20	447.01	10.01	13.01	3.88E-08	0.05%	0.09%	4	1100	0.648
84	5/1/12	DB1-5	30	30	0	950	447.00	446.79	13.05	16.05	4.38E-08	0.10%	0.15%	4	1100	0.648
85	5/1/12	DB1-5	30	31	0	975	446.78	446.51	16.09	19.09	5.51E-08	0.15%	0.21%	4	1100	0.648
86	5/1/12	DB1-5	30	35	0	1000	446.49	446.13	19.13	22.13	7.73E-08	0.21%	0.29%	4	1100	0.648
87	5/2/12	DB2-1	200	216	0	900	450.49	450.30	6.97	9.97	4.10E-08	0.00%	0.04%	4	1100	0.436
88	5/2/12	DB2-1	200	207	0	925	450.28	450.03	10.01	13.01	5.34E-08	0.05%	0.10%	4	1100	0.436
89	5/2/12	DB2-1	200	204	0	950	450.01	449.66	13.05	16.05	7.31E-08	0.11%	0.18%	4	1100	0.436
90	5/2/12	DB2-1	200	207	0	975	449.64	449.10	16.09	19.09	1.12E-07	0.19%	0.31%	4	1100	0.436
91	5/2/12	DB2-1	200	236	0	1000	449.08	448.11	19.13	22.13	2.02E-07	0.31%	0.53%	4	1100	0.436
92	5/11/12	DB2-2	100	96	0	900	443.97	443.80	6.97	9.97	3.46E-08	0.00%	0.04%	4	1100	0.403
93	5/11/12	DB2-2	100	95	0	925	443.79	443.58	10.01	13.01	4.46E-08	0.04%	0.09%	4	1100	0.403
94	5/11/12	DB2-2	100	98	0	950	443.57	443.32	13.05	16.05	5.31E-08	0.09%	0.15%	4	1100	0.403
95	5/11/12	DB2-2	100	99	0	975	443.30	442.96	16.09	19.09	7.24E-08	0.15%	0.23%	4	1100	0.403
96	5/11/12	DB2-2	100	98	0	1000	442.94	442.46	19.13	22.13	1.13E-07	0.23%	0.34%	4	1100	0.403
97	5/14/12	DB2-3	150	140	0	900	443.70	443.52	6.97	9.97	3.77E-08	0.00%	0.04%	4	1100	0.464
98	5/14/12	DB2-3	150	157	0	925	443.50	443.26	10.01	13.01	5.06E-08	0.04%	0.10%	4	1100	0.464
99	5/14/12	DB2-3	150	153	0	950	443.25	442.94	13.05	16.05	6.59E-08	0.10%	0.17%	4	1100	0.464
100	5/14/12	DB2-3	150	153	0	975	442.92	442.47	16.09	19.09	9.49E-08	0.18%	0.28%	4	1100	0.464
101	5/14/12	DB2-3	150	159	0	1000	442.45	441.71	19.13	22.13	1.56E-07	0.28%	0.45%	4	1100	0.464
102	5/16/12	DB2-5	100	103	0	900	448.47	448.20	6.97	9.97	5.57E-08	0.00%	0.06%	4	1100	0.399
103	5/16/12	DB2-5	100	96	0	925	448.18	447.80	10.01	13.01	7.91E-08	0.06%	0.15%	4	1100	0.399
104	5/16/12	DB2-5	100	97	0	950	447.78	447.28	13.05	16.05	1.05E-07	0.15%	0.27%	4	1100	0.399
105	5/16/12	DB2-5	100	97	0	975	447.26	446.63	16.09	19.09	1.31E-07	0.27%	0.41%	4	1100	0.399
106	5/16/12	DB2-5	100	110	0	1000	446.61	445.73	19.13	22.13	1.84E-07	0.41%	0.61%	4	1100	0.399
107	5/17/12	DB2-6	150	156	0	900	444.23	444.03	6.97	9.97	4.11E-08	0.00%	0.04%	4	1100	0.442
108	5/17/12	DB2-6	150	156	0	925	444.02	443.73	10.01	13.01	6.10E-08	0.05%	0.11%	4	1100	0.442
109	5/17/12	DB2-6	150	157	0	950	443.71	443.30	13.05	16.05	8.54E-08	0.12%	0.21%	4	1100	0.442
110	5/17/12	DB2-6	150	161	0	975	443.29	442.72	16.09	19.09	1.19E-07	0.21%	0.34%	4	1100	0.442
111	5/17/12	DB2-6	150	159	0	1000	442.70	441.91	19.13	22.13	1.66E-07	0.34%	0.52%	4	1100	0.442
112	5/21/12	DB2-7	500	514	0	900	445.30	445.07	6.97	9.97	3.84E-08	0.00%	0.05%	4	1100	0.547
113	5/21/12	DB2-7	500	493	0	925	445.06	444.60	10.01	13.01	4.60E-08	0.06%	0.16%	4	1100	0.547
114	5/21/12	DB2-7	500	498	0	950	444.58	443.89	13.05	16.05	4.92E-08	0.16%	0.32%	4	1100	0.547
115	5/21/12	DB2-7	500	494	0	975	443.87	442.80	16.09	19.09	6.07E-08	0.32%	0.56%	4	1100	0.547
116	5/21/12	DB2-7	500	577	0	1000	442.77	440.75	19.13	22.13	8.47E-08	0.57%	1.02%	4	1100	0.547

Exp data number	Test Date	Specimen ID	H2O Pressure target	H2O Pressure actual [&]	H2 Pressure	Temperature	Weight before	Weight after	Time in the test before	Time in the test after	Rate	Weight loss % before	Weight loss % after	Sample preparaton duration	Sample preparaton temperature	Wt loss in outgassing
			Pa	Pa	Pa	oC	mg	mg	hr	hr	s^{-1}	%	%	h	^{o}C	mg
117	5/22/12	DB2-8	750	801	0	900	447.67	447.39	6.97	9.97	5.75E-08	0.00%	0.06%	4	1100	0.781
118	5/22/12	DB2-8	750	778	0	925	447.38	447.00	10.01	13.01	7.89E-08	0.07%	0.15%	4	1100	0.781
119	5/22/12	DB2-8	750	774	0	950	446.98	446.31	13.05	16.05	1.38E-07	0.15%	0.30%	4	1100	0.781
120	5/22/12	DB2-8	750	777	0	975	446.29	444.97	16.09	19.09	2.73E-07	0.31%	0.60%	4	1100	0.781
121	5/22/12	DB2-8	750	846	0	1000	444.93	442.08	19.13	22.13	5.94E-07	0.61%	1.25%	4	1100	0.781
122	5/23/12	DB3-1	3	3	0	900	444.87	444.74	6.97	9.97	2.66E-08	0.00%	0.03%	4	1100	0.423
123	5/23/12	DB3-1	3	3	0	925	444.73	444.56	10.01	13.01	3.57E-08	0.03%	0.07%	4	1100	0.423
124	5/23/12	DB3-1	3	3	0	950	444.55	444.37	13.05	16.05	3.83E-08	0.07%	0.11%	4	1100	0.423
125	5/23/12	DB3-1	3	3	0	975	444.36	444.15	16.09	19.09	4.37E-08	0.12%	0.16%	4	1100	0.423
126	5/23/12	DB3-1	3	3	0	1000	444.14	443.90	19.13	22.13	4.99E-08	0.17%	0.22%	4	1100	0.423
127	6/1/12	DB3-3	150	150	0	1200	443.07	420.32	2.50	6.70	4.81E-06	0.00%	0.02%	4	1100	0.453
128	5/31/12	DB3-3	150	132	0	750	444.23	444.13	7.40	17.40	3.85E-08	0.03%	0.08%	4	1100	0.453
129	5/31/12	DB3-3	150	154	0	850	444.11	443.89	17.48	24.48	4.61E-08	0.26%	5.38%	4	1100	0.453
130	6/27/12	DB3-4	75	66	0	900	410.97	410.62	4.36	8.13	6.13E-08	8.38%	8.45%	2	1000	0.148
132	6/28/12	DB3-5	75	62	0	900	444.24	443.96	4.97	10.97	4.15E-08	0.00%	0.07%	2	1000	0.144
134	7/3/12	DB3-6	75	68	0	900	445.85	445.31	4.97	10.97	9.00E-08	0.40%	0.52%	2	1000	0.342
131	6/27/12	DB3-4	75	65	100	900	372.68	372.34	8.49	23.21	1.70E-08	9.24%	9.32%	2	1000	0.148
133	6/28/12	DB3-5	75	66	100	900	443.66	443.52	10.31	24.29	5.60E-09	0.07%	0.10%	2	1000	0.144
135	7/3/12	DB3-6	75	68	100	900	442.86	440.82	10.31	24.29	3.72E-08	0.55%	1.01%	2	1000	0.342
136	7/5/12	DB3-7	30	27	0	900	442.15	441.81	4.97	10.97	3.67E-08	0.01%	0.08%	2	1200	0.326
137	7/5/12	DB3-7	30	28	0	1100	441.64	437.85	11.30	17.30	4.11E-07	0.12%	0.98%	2	1200	0.326
138	7/9/12	DB3-8	300	252	0	900	442.10	441.46	4.97	10.97	6.94E-08	0.15%	0.30%	2	1200	0.516
139	7/9/12	DB3-8	300	242	0	1100	441.10	425.95	11.30	17.30	1.64E-06	0.38%	3.80%	2	1200	0.516
140	7/10/12	DB4-1	300	260	100	900	439.88	439.79	4.97	10.97	1.02E-08	0.01%	0.03%	2	1200	0.293
141	7/10/12	DB4-1	300	260	100	1100	439.63	434.19	11.30	17.30	5.89E-07	0.06%	1.30%	2	1200	0.293
142	7/11/12	DB4-2	300	245	0	900	438.18	437.84	4.97	10.97	3.78E-08	0.01%	0.09%	2	1200	0.286
143	7/11/12	DB4-2	300	247	0	1100	437.60	424.88	11.30	17.30	1.39E-06	0.14%	3.04%	2	1200	0.286
144	7/12/12	DB4-3	30	28	0	900	443.09	442.79	4.97	10.97	3.33E-08	0.00%	0.07%	2	1200	0.287
145	7/12/12	DB4-3	30	29	0	1100	442.63	439.29	11.30	17.30	3.60E-07	0.11%	0.86%	2	1200	0.287
146	7/16/12	DB4-4	30	30	100	900	443.34	443.18	4.97	10.97	1.70E-08	0.10%	0.13%	2	1200	0.638
147	7/16/12	DB4-4	30	30	100	1100	443.06	441.63	11.30	17.30	1.56E-07	0.16%	0.48%	2	1200	0.638
148	7/17/12	DB4-5	300	241	0	900	440.93	440.51	4.97	10.97	4.99E-08	0.21%	0.30%	2	1200	0.553
149	7/17/12	DB4-5	300	244	0	1100	439.92	419.12	11.30	17.30	2.27E-06	0.44%	5.14%	2	1200	0.553
150	7/18/12	DB4-6	30	35	0	900	446.42	446.08	4.97	10.97	3.64E-08	0.01%	0.08%	2	1200	0.553
151	7/18/12	DB4-6	30	38	0	1100	445.91	442.11	11.30	17.30	4.07E-07	0.12%	0.97%	2	1200	0.553
152	7/19/12	DB4-7	300	264	100	900	442.05	441.46	4.97	10.97	6.38E-08	0.02%	0.15%	2	1200	1.566
153	7/19/12	DB4-7	300	244	100	1100	441.23	433.90	11.30	17.30	7.91E-07	0.20%	1.86%	2	1200	1.566
154	7/20/12	DB4-8	300	241	0	900	439.51	438.61	4.97	10.97	9.83E-08	0.01%	0.22%	2	1200	0.325
155	7/20/12	DB4-8	300	239	0	1100	438.26	423.76	11.30	17.30	1.60E-06	0.30%	3.60%	2	1200	0.325
156	7/23/12	#10-1	30	41	0	900	430.35	429.71	4.97	10.97	7.32E-08	2.66%	2.80%	2	1200	11.618

Exp data number	Test Date	Specimen ID	H2O Pressure target	H2O Pressure actual [&]	H2 Pressure	Temperature	Weight before	Weight after	Time in the test before	Time in the test after	Rate	Weight loss % before	Weight loss % after	Sample preparaton duration	Sample preparaton temperature	Wt loss in outgassing
			Pa	Pa	Pa	oC	mg	mg	hr	hr	s^{-1}	%	%	h	^{o}C	mg
157	7/23/12	#10-1	30	36	0	1100	429.39	422.36	11.30	17.30	7.91E-07	2.87%	4.46%	2	1200	11.618
158	7/24/12	#10-2	30	30	100	900	440.35	439.90	4.97	10.97	4.88E-08	0.01%	0.11%	2	1200	0.327
159	7/24/12	#10-2	30	31	100	1100	439.74	436.65	11.30	17.30	3.37E-07	0.14%	0.85%	2	1200	0.327
160	7/26/12	#11-1	300	258	0	900	451.98	451.60	4.97	10.97	4.00E-08	0.01%	0.09%	2	1200	0.389
161	7/26/12	#11-1	300	255	0	1100	451.30	440.01	11.30	17.30	1.20E-06	0.16%	2.65%	2	1200	0.389
162	7/31/12	#11-2	30	31	0	900	442.12	441.62	4.97	10.97	5.44E-08	0.10%	0.22%	2	1200	0.514
163	7/31/12	#11-2	30	28	0	1100	441.46	438.10	11.30	17.30	3.63E-07	0.25%	1.01%	2	1200	0.514
164	8/1/12	#0-2	300	246	100	900	445.43	445.09	4.97	10.97	3.57E-08	0.00%	0.08%	2	1200	0.263
165	8/1/12	#0-2	300	241	100	1100	444.92	440.22	11.30	17.30	5.03E-07	0.12%	1.17%	2	1200	0.263
166	8/6/12	#0-4	300	245	0	900	442.27	442.00	4.97	10.97	2.88E-08	0.08%	0.14%	2	1200	0.556
167	8/6/12	#0-4	300	245	0	1100	441.75	432.24	11.30	17.30	1.04E-06	0.20%	2.35%	2	1200	0.556
168	8/7/12	#0-5	30	29	0	900	443.94	443.39	4.97	10.97	5.92E-08	0.01%	0.13%	2	1200	0.428
169	8/7/12	#0-5	30	28	0	1100	443.21	439.65	11.30	17.30	3.82E-07	0.17%	0.97%	2	1200	0.428
170	8/8/12	#0-6	30	29	100	900	454.04	453.89	4.97	10.97	1.63E-08	0.00%	0.04%	2	1200	0.339
171	8/8/12	#0-6	30	28	100	1100	453.80	453.00	11.30	17.30	8.45E-08	0.06%	0.23%	2	1200	0.339
172	8/9/12	#0-7	300	236	0	900	447.28	446.36	4.97	10.97	9.85E-08	0.01%	0.21%	2	1200	0.382
173	8/9/12	#0-7	300	245	0	1100	445.81	417.73	11.30	17.30	3.01E-06	0.34%	6.61%	2	1200	0.382
174	8/13/12	#0-8	30	25	0	900	442.12	441.32	4.97	10.97	8.70E-08	0.01%	0.19%	2	1200	0.531
175	8/13/12	#0-8	30	27	0	1100	441.10	435.42	11.30	17.30	6.15E-07	0.24%	1.53%	2	1200	0.531
176	8/15/12	#0-10	300	234	100	900	454.52	454.16	4.97	10.97	3.81E-08	0.04%	0.11%	2	1200	0.320
177	8/15/12	#0-10	300	242	100	1100	453.93	446.57	11.30	17.30	7.79E-07	0.17%	1.78%	2	1200	0.320
181	8/16/12	#0-11	30	29	0	900	441.63	441.45	4.97	10.97	1.98E-08	0.00%	0.04%	2	1200	0.353
182	8/16/12	#0-11	30	29	0	1100	441.33	438.70	11.30	17.30	2.83E-07	0.07%	0.67%	2	1200	0.353
183	10/18/12	#0-12	300	242	0	900	441.30	439.61	5.05	11.05	1.79E-07	0.26%	0.64%	2	1200	0.956
184	10/18/12	#0-12	300	228	0	1100	422.84	303.58	11.38	17.38	1.38E-05	4.43%	31.38%	2	1200	0.956
185	10/18/12	#0-12	300	271	0	900	415.90	414.37	17.72	23.72	1.73E-07	6.00%	6.34%	2	1200	0.956
186	10/23/12	#0-13	30	30	100	900	445.12	444.82	0.30	5.96	3.25E-08	0.17%	0.23%	2	1200	0.778
188	10/23/12	#0-13	30	31	100	900	443.25	442.97	12.79	18.14	3.23E-08	0.59%	0.65%	2	1200	0.778
187	10/23/12	#0-13	30	28	100	1100	444.63	443.19	6.36	12.24	1.53E-07	0.28%	0.60%	2	1200	0.778
189	10/25/12	#0-14	30	30	100	900	449.71	449.08	4.97	10.97	6.64E-08	0.02%	0.16%	2	1200	0.125
191	10/25/12	#0-14	30	31	100	900	445.88	445.27	17.63	23.63	7.06E-08	0.87%	1.01%	2	1200	0.125
190	10/25/12	#0-14	30	28	100	1100	448.83	445.91	11.30	17.30	3.10E-07	0.22%	0.87%	2	1200	0.125
192	10/30/12	DB-26	300	270	100	900	441.36	441.12	4.97	10.97	2.54E-08	0.00%	0.05%	2	1200	0.201
194	10/30/12	DB-26	300	261	100	900	437.10	436.81	17.63	23.63	3.33E-08	0.96%	1.03%	2	1200	0.201
193	10/30/12	DB-26	300	219	100	1100	441.07	437.15	11.30	17.30	4.01E-07	0.06%	0.95%	2	1200	0.201
195	11/5/12	#0-16	30	26	100	900	442.00	441.47	4.97	10.97	5.84E-08	-0.07%	0.05%	2	1200	0.209
197	11/5/12	#0-16	30	30	100	900	440.40	440.09	17.63	23.63	3.55E-08	0.30%	0.37%	2	1200	0.209
196	11/5/12	#0-16	30	25	100	1100	441.29	440.35	11.30	17.30	1.01E-07	0.10%	0.31%	2	1200	0.209
198	2/21/13	#0-19	300	298	0	900	449.92	449.16	5.16	11.06	5.95E-08	0.01%	0.18%	2	1200	0.141
199	2/21/13	#0-19	300	308	0	1100	448.79	420.35	11.38	17.38	2.09E-06	0.26%	6.58%	2	1200	0.141

Exp data number	Test Date	Specimen ID	H2O Pressure target	H2O Pressure actual [&]	H2 Pressure	Temperature	Weight before	Weight after	Time in the test before	Time in the test after	Rate	Weight loss % before	Weight loss % after	Sample preparaton duration	Sample preparaton temperature	Wt loss in outgassing
			Pa	Pa	Pa	oC	mg	mg	hr	hr	s^{-1}	%	%	h	^{o}C	mg
200	2/21/13	#0-19	300	313	0	900	420.35	419.70	19.18	19.38	5.52E-08	6.58%	6.73%	2	1200	0.141
201	3/5/13	#0-22	30	30	100	900	445.95	445.75	5.05	11.05	2.08E-08	0.06%	0.10%	2	1200	0.219
203	3/5/13	#0-22	30	28	100	900	445.05	444.93	17.72	23.72	1.24E-08	0.26%	0.29%	2	1200	0.219
202	3/5/13	#0-22	30	28	100	1100	445.63	444.98	11.38	17.38	6.79E-08	0.13%	0.28%	2	1200	0.219
178	3/7/13	#0-23	300	306	0	900	446.44	445.75	4.97	11.30	7.18E-08	0.01%	0.17%	2	1200	0.125
179	3/7/13	#0-23	300	304	0	1100	445.40	423.14	11.51	17.38	2.31E-06	0.25%	5.23%	2	1200	0.125
180	3/7/13	#0-23	300	307	0	900	422.41	421.58	17.71	23.71	9.14E-08	5.40%	5.58%	2	1200	0.125
204	3/11/13	#0-24	300	299	100	900	448.28	447.94	5.20	11.05	3.43E-08	0.01%	0.09%	2	1200	0.165
206	3/11/13	#0-24	300	304	100	900	436.77	436.28	17.72	23.72	5.28E-08	2.58%	2.69%	2	1200	0.165
205	3/11/13	#0-24	300	289	100	1100	447.67	437.27	11.38	17.38	1.09E-06	0.15%	2.47%	2	1200	0.165
207	3/12/13	#0-25	30	33	100	900	454.48	454.06	7.14	11.05	6.95E-08	0.08%	0.17%	2	1200	0.227
209	3/12/13	#0-25	30	30	100	900	450.43	448.89	17.63	23.63	1.60E-07	0.97%	1.31%	2	1200	0.227
208	3/12/13	#0-25	30	29	100	1100	453.91	450.49	11.30	17.30	3.41E-07	0.21%	0.96%	2	1200	0.227
210	3/14/13	#0-26	300	301	100	900	453.93	453.72	4.97	10.97	2.11E-08	0.00%	0.05%	2	1200	0.145
212	3/14/13	#0-26	300	307	100	900	445.73	445.28	17.63	23.63	4.80E-08	1.81%	1.91%	2	1200	0.145
211	3/14/13	#0-26	300	309	100	1100	453.48	446.15	11.30	17.30	7.73E-07	0.10%	1.72%	2	1200	0.145
213	3/20/13	#0-28	300	311	0	900	427.49	427.25	7.35	10.97	4.35E-08	0.04%	0.10%	2	1200	0.331
214	3/20/13	#0-28	300	331	0	1100	427.08	415.75	11.30	17.30	1.25E-06	0.14%	2.79%	2	1200	0.331
215	3/20/13	#0-28	300	346	0	900	415.68	415.25	17.63	23.63	5.32E-08	2.80%	2.90%	2	1200	0.331
220	3/26/13	DB8-1	300	307	30	900	430.15	430.12	21.63	23.63	7.69E-09	1.91%	1.92%	2	1200	0.217
219	3/26/13	DB8-1	300	305	50	900	430.17	430.15	19.63	21.63	8.01E-09	1.91%	1.91%	2	1200	0.217
216	3/26/13	DB8-1	300	312	100	900	438.37	438.10	5.20	10.86	3.10E-08	0.03%	0.10%	2	1200	0.217
218	3/26/13	DB8-1	300	304	100	900	430.18	430.17	17.63	19.63	4.85E-09	1.90%	1.91%	2	1200	0.217
217	3/26/13	DB8-1	300	328	100	1100	437.59	430.32	11.30	17.30	7.95E-07	0.21%	1.87%	2	1200	0.217
221	4/2/13	DB8-2	100	101	0	900	450.27	449.88	2.01	7.85	4.11E-08	0.01%	0.09%	2	1200	0.217
222	4/2/13	DB8-2	100	101	0	1000	449.76	448.04	8.35	13.96	1.90E-07	0.12%	0.50%	2	1200	0.217
223	4/2/13	DB8-2	100	106	0	1100	447.69	439.64	14.49	20.37	8.50E-07	0.58%	2.37%	2	1200	0.217
224	4/3/13	DB8-3	100	108	100	900	445.87	445.65	5.03	10.81	2.37E-08	-0.01%	0.04%	2	1200	0.202
225	4/3/13	DB8-3	100	101	100	1000	445.55	444.17	11.18	16.79	1.54E-07	0.06%	0.37%	2	1200	0.202
226	4/3/13	DB8-3	100	107	100	1100	443.98	442.33	17.19	19.81	3.94E-07	0.42%	0.79%	2	1200	0.202
227	4/3/13	DB8-3	100	97	100	1100	442.33	440.86	19.81	23.02	2.86E-07	0.79%	1.11%	2	1200	0.202
228	4/15/13	DB8-4	100	95	50	900	445.30	444.61	4.74	10.58	7.30E-08	0.18%	0.34%	2	1200	0.283
229	4/15/13	DB8-4	100	94	50	1000	444.47	443.12	11.18	14.50	2.42E-07	0.37%	0.67%	2	1200	0.283
230	4/15/13	DB8-4	100	115	50	1000	443.12	441.84	14.50	16.71	3.62E-07	0.67%	0.96%	2	1200	0.283
231	4/15/13	DB8-4	100	123	50	1100	441.42	435.28	17.25	23.09	6.61E-07	1.05%	2.43%	2	1200	0.283
232	5/24/13	DB9-3	100	102	50	900	439.93	439.21	4.94	10.82	7.77E-08	0.12%	0.28%	2	1200	0.467
233	5/24/13	DB9-3	100	83	50	1000	439.11	437.04	11.05	16.93	2.22E-07	0.30%	0.77%	2	1200	0.467
234	5/24/13	DB9-3	100	78	50	1100	436.85	434.32	17.21	19.48	7.11E-07	0.82%	1.39%	2	1200	0.467
235	5/24/13	DB9-3	100	80	50	1100	433.55	431.14	20.25	23.08	5.44E-07	1.57%	2.11%	2	1200	0.467
236	5/31/13	DB9-6	30	32	50	900	437.96	437.63	5.46	10.72	3.98E-08	0.00%	0.07%	2	1200	0.312

Exp data number	Test Date	Specimen ID	H2O Pressure target	H2O Pressure actual [&]	H2 Pressure	Temperature	Weight before	Weight after	Time in the test before	Time in the test after	Rate	Weight loss % before	Weight loss % after	Sample preparaton duration	Sample preparaton temperature	Wt loss in outgassing
			Pa	Pa	Pa	oC	mg	mg	hr	hr	s^{-1}	%	%	h	^{o}C	mg
237	5/31/13	DB9-6	30	28	50	1000	437.50	436.69	11.35	16.70	9.67E-08	0.10%	0.29%	2	1200	0.312
238	5/31/13	DB9-6	30	27	50	1100	436.27	435.56	18.02	19.81	2.53E-07	0.38%	0.54%	2	1200	0.312
239	5/31/13	DB9-6	30	23	50	1100	435.55	434.14	19.81	23.11	2.73E-07	0.55%	0.87%	2	1200	0.312
240	6/3/13	DB10-1	30	33	150	900	445.76	445.38	5.49	10.65	4.57E-08	-0.05%	0.03%	2	1200	1.329
241	6/3/13	DB10-1	30	32	150	1000	445.19	443.56	11.13	16.81	1.79E-07	0.08%	0.44%	2	1200	1.329
242	6/3/13	DB10-1	30	33	150	1100	443.29	441.45	17.21	19.45	5.12E-07	0.50%	0.92%	2	1200	1.329
243	6/3/13	DB10-1	30	34	150	1100	441.45	437.70	19.45	23.06	6.54E-07	0.92%	1.76%	2	1200	1.329
244	6/4/13	DB10-2	100	99	150	900	444.77	443.83	5.46	10.64	1.13E-07	-0.04%	0.17%	2	1200	0.255
245	6/4/13	DB10-2	100	100	150	1000	441.97	437.97	12.96	16.77	6.59E-07	0.59%	1.49%	2	1200	0.255
246	6/4/13	DB10-2	100	100	150	1100	437.20	433.75	17.28	18.97	1.30E-06	1.67%	2.44%	2	1200	0.255
247	6/4/13	DB10-2	100	99	150	1100	433.75	422.42	18.97	21.14	1.75E-06	2.44%	4.99%	2	1200	0.255
248	6/6/13	DB10-3	15	16	0	900	448.25	447.70	5.97	10.79	7.10E-08	-0.01%	0.11%	2	1200	0.307
249	6/6/13	DB10-3	15	16	0	1000	446.98	445.71	12.89	16.56	2.16E-07	0.27%	0.56%	2	1200	0.307
250	6/6/13	DB10-3	15	16	0	1100	445.29	443.78	17.27	19.28	4.71E-07	0.65%	0.99%	2	1200	0.307
251	6/6/13	DB10-3	15	16	0	1100	443.78	440.32	19.28	23.08	5.70E-07	0.99%	1.76%	2	1200	0.307
252	6/7/13	DB10-4	15	15	0	900	440.88	440.37	6.09	10.83	6.85E-08	-0.03%	0.09%	2	1200	0.220
253	6/7/13	DB10-4	15	15	0	1000	439.86	438.79	12.70	16.81	1.64E-07	0.21%	0.45%	2	1200	0.220
254	6/7/13	DB10-4	15	15	0	1100	438.38	437.08	17.53	19.60	3.96E-07	0.54%	0.83%	2	1200	0.220
255	6/7/13	DB10-4	15	15	0	1100	437.08	434.45	19.60	23.14	4.72E-07	0.83%	1.43%	2	1200	0.220
256	6/18/13	DB10-5	15	15	0	900	444.29	443.58	6.03	10.81	9.34E-08	0.03%	0.19%	2	1200	0.449
257	6/18/13	DB10-5	15	15	0	1000	443.39	441.50	11.15	16.79	2.10E-07	0.23%	0.65%	2	1200	0.449
258	6/18/13	DB10-5	15	15	0	1100	441.11	440.14	17.36	18.74	4.42E-07	0.74%	0.96%	2	1200	0.449
259	6/18/13	DB10-5	15	16	0	1100	440.14	436.81	18.74	23.02	4.91E-07	0.96%	1.71%	2	1200	0.449
260	6/20/13	DB10-6	0	3	0	900	445.71	445.37	4.88	10.81	3.67E-08	-0.06%	0.01%	2	1200	0.400
261	6/20/13	DB10-6	0	3	0	1000	445.23	444.73	11.12	16.81	5.50E-08	0.05%	0.16%	2	1200	0.400
262	6/20/13	DB10-6	0	3	0	1100	444.55	443.70	17.30	23.05	9.17E-08	0.20%	0.39%	2	1200	0.400
264	6/21/13	DB10-7	0	3	0	900	447.26	446.96	5.11	10.66	3.31E-08	-0.07%	0.00%	2	1200	0.335
265	6/21/13	DB10-7	0	3	0	1000	446.82	446.30	11.09	16.81	5.61E-08	0.03%	0.15%	2	1200	0.335
266	6/21/13	DB10-7	0	3	0	1100	446.11	445.34	17.36	23.00	8.46E-08	0.19%	0.36%	2	1200	0.335
268	7/15/13	#12--1	0	3	0	900	454.27	454.12	4.93	10.81	1.50E-08	-0.07%	-0.04%	2	1200	0.378
269	7/15/13	#12--1	0	3	0	1000	454.00	452.74	11.07	16.98	1.30E-07	-0.02%	0.26%	2	1200	0.378
270	7/15/13	#12--1	0	3	0	1100	453.60	453.10	17.20	23.03	5.27E-08	0.07%	0.18%	2	1200	0.378
271	7/25/13	#12--2	15	15	0	800	448.61	448.47	4.32	7.39	2.72E-08	-0.04%	-0.01%	1	1200	0.210
272	7/25/13	#12--2	15	15	0	850	448.39	448.08	7.70	10.49	6.93E-08	0.01%	0.08%	1	1200	0.210
273	7/25/13	#12--2	15	14	0	900	447.96	447.51	10.90	13.53	1.08E-07	0.10%	0.20%	1	1200	0.210
274	7/25/13	#12--2	15	14	0	950	447.38	446.66	13.84	16.66	1.58E-07	0.23%	0.39%	1	1200	0.210
275	7/25/13	#12--2	15	14	0	1000	446.54	445.62	16.68	19.75	1.88E-07	0.42%	0.63%	1	1200	0.210
276	7/25/13	#12--2	15	15	0	1100	445.37	444.57	20.03	21.57	3.22E-07	0.68%	0.86%	1	1200	0.210

Exp data number	Test Date	Specimen ID	H2O Pressure target	H2O Pressure actual [&]	H2 Pressure	Temperature	Weight before	Weight after	Time in the test before	Time in the test after	Rate	Weight loss % before	Weight loss % after	Sample preparaton duration	Sample preparaton temperature	Wt loss in outgassing
			Pa	Pa	Pa	oC	mg	mg	hr	hr	s^{-1}	%	%	h	^{o}C	mg
277	7/26/13	#12--3	15	14	30	800	448.82	448.82	4.41	7.45	8.14E-10	-0.07%	-0.07%	1	1200	0.132
278	7/26/13	#12--3	15	15	30	850	448.76	448.73	7.59	10.52	5.49E-09	-0.06%	-0.05%	1	1200	0.132
279	7/26/13	#12--3	15	14	30	900	448.67	448.59	10.74	13.62	1.83E-08	-0.04%	-0.02%	1	1200	0.132
280	7/26/13	#12--3	15	14	30	950	448.52	448.37	13.76	16.57	3.26E-08	-0.01%	0.03%	1	1200	0.132
281	7/26/13	#12--3	15	14	30	1000	448.29	448.04	16.97	19.70	5.61E-08	0.05%	0.10%	1	1200	0.132
282	7/26/13	#12--3	15	14	30	1100	447.82	447.28	20.26	22.83	1.31E-07	0.15%	0.27%	1	1200	0.132
283	7/27/13	#12-04	30	31	0	800	448.82	448.81	4.46	7.42	2.30E-09	-0.10%	-0.10%	1	1200	0.117
284	7/27/13	#12-04	30	31	0	850	448.75	448.71	7.73	10.43	9.63E-09	-0.09%	-0.08%	1	1200	0.117
285	7/27/13	#12-04	30	31	0	900	448.64	448.53	10.77	13.56	2.53E-08	-0.06%	-0.04%	1	1200	0.117
286	7/27/13	#12-04	30	31	0	950	448.45	448.27	13.87	16.60	4.06E-08	-0.02%	0.02%	1	1200	0.117
287	7/27/13	#12-04	30	31	0	1000	448.19	447.90	16.88	19.70	6.37E-08	0.04%	0.10%	1	1200	0.117
288	7/27/13	#12-04	30	31	0	1100	447.69	446.57	20.07	22.77	2.58E-07	0.15%	0.40%	1	1200	0.117
289	7/29/13	#17-01	30	31	30	800	453.60	453.59	4.10	7.39	3.16E-09	-0.08%	-0.07%	1	1200	0.108
290	7/29/13	#17-01	30	32	30	850	453.52	453.29	7.67	10.49	4.97E-08	-0.06%	-0.01%	1	1200	0.108
291	7/29/13	#17-01	30	32	30	900	453.21	452.70	10.74	13.62	1.07E-07	0.01%	0.12%	1	1200	0.108
292	7/29/13	#17-01	30	32	30	950	452.61	451.76	13.81	16.66	1.82E-07	0.14%	0.33%	1	1200	0.108
293	7/29/13	#17-01	30	32	30	1000	451.61	450.30	16.91	19.76	2.83E-07	0.36%	0.65%	1	1200	0.108
294	7/29/13	#17-01	30	33	30	1100	449.98	447.38	20.09	22.94	5.62E-07	0.72%	1.30%	1	1200	0.108
295	7/30/13	#17-02	100	104	0	800	452.73	452.72	4.10	7.42	1.85E-09	-0.10%	-0.10%	1	1200	0.212
296	7/30/13	#17-02	100	100	0	850	452.65	452.63	7.70	10.49	6.38E-09	-0.09%	-0.08%	1	1200	0.212
297	7/30/13	#17-02	100	101	0	900	452.56	452.42	10.74	13.62	2.90E-08	-0.07%	-0.04%	1	1200	0.212
298	7/30/13	#17-02	100	103	0	950	452.34	452.05	13.81	16.66	6.33E-08	-0.02%	0.05%	1	1200	0.212
299	7/30/13	#17-02	100	102	0	1000	451.92	451.36	17.08	19.76	1.27E-07	0.08%	0.20%	1	1200	0.212
300	7/30/13	#17-02	100	103	0	1100	450.90	448.34	20.29	22.80	6.27E-07	0.30%	0.87%	1	1200	0.212
301	7/31/13	#17-03	15	17	0	800	450.62	450.61	5.52	7.39	3.63E-09	-0.07%	-0.07%	1	1200	0.333
302	7/31/13	#17-03	15	14	0	850	450.54	450.43	7.73	10.43	2.56E-08	-0.06%	-0.03%	1	1200	0.333
303	7/31/13	#17-03	15	13	0	900	450.35	450.17	10.80	13.53	4.04E-08	-0.01%	0.03%	1	1200	0.333
304	7/31/13	#17-03	15	13	0	950	450.09	449.81	13.84	16.69	6.00E-08	0.04%	0.11%	1	1200	0.333
305	7/31/13	#17-03	15	14	0	1000	449.74	449.27	16.91	19.81	9.95E-08	0.12%	0.23%	1	1200	0.333
306	7/31/13	#17-03	15	14	0	1100	449.07	448.12	20.07	22.89	2.08E-07	0.27%	0.48%	1	1200	0.333
307	8/2/13	#17-04	100	104	30	800	454.13	454.13	6.14	7.11	-8.83E-11	-0.10%	-0.10%	1	1200	0.152
308	8/2/13	#17-04	100	101	30	850	454.07	454.07	7.78	10.43	1.41E-10	-0.08%	-0.08%	1	1200	0.152
309	8/2/13	#17-04	100	100	30	900	454.00	453.70	10.95	13.48	7.18E-08	-0.07%	0.00%	1	1200	0.152
310	8/2/13	#17-04	100	100	30	950	453.54	452.73	13.95	16.60	1.87E-07	0.03%	0.21%	1	1200	0.152
311	8/2/13	#17-04	100	122	30	1000	452.08	450.75	17.73	19.66	4.24E-07	0.35%	0.65%	1	1200	0.152
312	8/2/13	#17-04	100	102	30	1100	449.19	444.96	20.76	22.86	1.25E-06	0.99%	1.92%	1	1200	0.152
313	8/3/13	#16-01	150	153	0	800	452.46	452.44	4.66	7.36	3.18E-09	-0.09%	-0.09%	1	1200	0.095
314	8/3/13	#16-01	150	155	0	850	452.38	452.36	7.76	10.49	5.85E-09	-0.07%	-0.07%	1	1200	0.095
315	8/3/13	#16-01	150	158	0	900	452.22	451.91	11.38	13.56	8.71E-08	-0.04%	0.03%	1	1200	0.095
316	8/3/13	#16-01	150	162	0	950	451.46	450.53	14.68	16.52	3.11E-07	0.13%	0.34%	1	1200	0.095

Exp data number	Test Date	Specimen ID	H2O Pressure target	H2O Pressure actual [&]	H2 Pressure	Temperature	Weight before	Weight after	Time in the test before	Time in the test after	Rate	Weight loss % before	Weight loss % after	Sample preparaton duration	Sample preparaton temperature	Wt loss in outgassing
			Pa	Pa	Pa	oC	mg	mg	hr	hr	s^{-1}	%	%	h	^{o}C	mg
317	8/3/13	#16-01	150	165	0	1000	449.72	446.51	17.33	19.70	8.38E-07	0.52%	1.23%	1	1200	0.095
318	8/3/13	#16-01	150	165	0	1100	443.52	435.22	20.75	22.89	2.43E-06	1.89%	3.72%	1	1200	0.095
319	8/4/13	#16-02	100	110	100	800	449.81	449.80	4.66	7.22	1.69E-09	-0.11%	-0.11%	1	1200	0.092
320	8/4/13	#16-02	100	106	100	850	449.73	449.68	7.87	10.38	1.28E-08	-0.09%	-0.08%	1	1200	0.092
321	8/4/13	#16-02	100	108	100	900	449.47	448.81	11.38	13.51	1.94E-07	-0.04%	0.11%	1	1200	0.092
322	8/4/13	#16-02	100	117	100	950	448.00	446.12	14.53	16.39	6.26E-07	0.29%	0.71%	1	1200	0.092
323	8/4/13	#16-02	100	107	100	1000	445.46	441.15	16.92	19.59	1.00E-06	0.86%	1.82%	1	1200	0.092
324	8/4/13	#16-02	100	112	100	1100	438.33	432.62	20.70	22.92	1.63E-06	2.44%	3.71%	1	1200	0.092
325	8/5/13	#16-03	100	105	150	800	0.44	0.44	4.77	7.45	-1.16E-09	-0.10%	-0.10%	1	1200	0.097
326	8/5/13	#16-03	100	108	150	850	0.38	0.38	7.76	10.43	1.16E-09	-0.09%	-0.08%	1	1200	0.097
327	8/5/13	#16-03	100	111	150	900	0.26	0.03	11.36	13.48	6.67E-08	-0.06%	-0.01%	1	1200	0.097
328	8/5/13	#16-03	100	115	150	950	-0.15	-0.80	14.09	16.41	1.72E-07	0.03%	0.18%	1	1200	0.097
329	8/5/13	#16-03	100	122	150	1000	-1.30	-2.36	17.50	19.56	3.21E-07	0.29%	0.53%	1	1200	0.097
330	8/5/13	#16-03	100	110	150	1100	-3.45	-5.61	20.85	22.86	6.71E-07	0.77%	1.25%	1	1200	0.097
331	8/6/13	#16-04	30	31	150	800	454.72	454.72	4.91	7.42	-7.30E-10	-0.09%	-0.09%	1	1200	0.096
332	8/6/13	#16-04	30	32	150	850	454.67	454.67	7.67	10.49	0.00E+00	-0.08%	-0.08%	1	1200	0.096
333	8/6/13	#16-04	30	34	150	900	454.61	454.59	10.88	13.51	4.41E-09	-0.07%	-0.07%	1	1200	0.096
334	8/6/13	#16-04	30	36	150	950	454.53	454.48	13.93	16.57	1.13E-08	-0.05%	-0.04%	1	1200	0.096
335	8/6/13	#16-04	30	40	150	1000	454.41	454.32	16.97	19.79	1.91E-08	-0.03%	-0.01%	1	1200	0.096
336	8/6/13	#16-04	30	33	150	1100	454.19	454.04	20.09	22.83	3.19E-08	0.02%	0.06%	1	1200	0.096
337	8/7/13	#14-01	30	31	100	800	442.91	442.91	4.74	7.34	-1.45E-09	-0.10%	-0.10%	1	1200	0.081
338	8/7/13	#14-01	30	31	100	850	442.86	442.83	7.70	10.46	5.91E-09	-0.09%	-0.08%	1	1200	0.081
339	8/7/13	#14-01	30	32	100	900	442.77	442.65	10.80	13.59	2.74E-08	-0.07%	-0.04%	1	1200	0.081
340	8/7/13	#14-01	30	33	100	950	442.57	442.31	13.64	16.69	5.35E-08	-0.03%	0.03%	1	1200	0.081
341	8/7/13	#14-01	30	34	100	1000	442.23	441.87	16.91	19.76	8.00E-08	0.05%	0.13%	1	1200	0.081
342	8/7/13	#14-01	30	34	100	1100	441.70	441.10	20.81	22.89	1.83E-07	0.17%	0.31%	1	1200	0.081
343	8/8/13	#14-02	15	15	100	800	442.87	442.86	4.59	7.34	9.12E-10	-0.09%	-0.09%	1	1200	0.092
344	8/8/13	#14-02	15	16	100	850	442.81	442.74	7.86	10.37	1.67E-08	-0.08%	-0.07%	1	1200	0.092
345	8/8/13	#14-02	15	17	100	900	442.66	442.51	10.94	13.51	3.66E-08	-0.05%	-0.01%	1	1200	0.092
346	8/8/13	#14-02	15	14	100	950	442.42	442.13	13.97	16.56	7.13E-08	0.01%	0.07%	1	1200	0.092
347	8/8/13	#14-02	15	22	100	1000	442.02	441.62	16.94	19.64	9.31E-08	0.10%	0.19%	1	1200	0.092
348	8/8/13	#14-02	15	22	100	1100	441.43	440.85	20.08	22.94	1.28E-07	0.23%	0.36%	1	1200	0.092
349	8/12/13	#14-03	0	4	0	950	453.54	453.44	3.84	8.36	1.44E-08	-0.06%	-0.04%	1	1200	0.108
350	8/12/13	#14-03	0	4	0	950	453.42	453.36	8.86	18.54	3.86E-09	-0.04%	-0.02%	1	1200	0.108
351	8/21/13	#14-04	3	3	0	950	451.96	451.86	2.79	5.13	2.60E-08	-0.06%	-0.03%	1	1200	0.190
352	8/21/13	#14-04	100	106	0	950	450.95	448.69	5.37	7.98	5.33E-07	0.17%	0.67%	1	1200	0.190
353	8/21/13	#14-04	100	101	100	950	448.18	445.56	8.64	12.07	4.73E-07	0.78%	1.36%	1	1200	0.190
354	8/21/13	#14-04	100	103	100	950	445.56	441.13	12.07	16.93	5.68E-07	1.36%	2.34%	1	1200	0.190
355	8/21/13	#14-04	100	108	100	950	441.13	435.57	16.93	22.59	6.19E-07	2.34%	3.57%	1	1200	0.190

DISTRIBUTION LIST

Oak Ridge National Laboratory

Cristian Contescu	contescuci@ornl.gov
Timothy Burchell	burchelltd@ornl.gov
Anne Campbell	campbellaa@ornl.gov
Yutai Katoh	katohy@ornl.gov
Nidia Gallego	gallegonc@ornl.gov
John Hunn	hunnjd@ornl.gov
Weiju Ren	renw@ornl.gov
Mark Vance	vancemc@ornl.gov

University of Tennessee

Robert Mee	rmee@utk.edu

Idaho National Laboratory

Mark Caroll	Mark.Caroll@inl.gov
Diane Crosson	Diane.Crosson@inl.gov
Michael Davenport	Michael.Davenport@inl.gov
Hans Gougar	Hans.Gougar@inl.gov
Laurence Hull	Laurence.Hull@inl.gov
David Jensen	David.Jensen@inl.gov
Joshua Kane	Joshua.Kane@inl.gov
Travis Mitchell	Travis.Mitchell@inl.gov
David Petti	David.Petti@inl.gov
Rebecca Smith	Rebecca.Smith@inl.gov
David Swank	w.swank@inl.gov
William Windes	William.Windes@inl.gov

Argonne National Laboratory

Sam Shan	ssham@anl.gov

Department of Energy

William Corwin	William.Corwin@Nuclear.Energy.gov
Thomas O'Connor	Tom.OConnor@Nuclear.Energy.gov
Carl Sink	Carl.Sink@Nuclear.Energy.gov